



Ministry of Higher Education and Scientific Research

Kasdi Merbah University- Ouargla

Faculty of Mathematics and Matter Sciences

Chemistry Department



Thesis Submitted in Fulfillment of the requirements for the

L.M.D Doctor in Chemistry

Specialty :Analytical chemistry

Prepared by: MECHERI Razika

Title:

Removal of cationic / anionic textile dyes by natural and modified algerian clay minerals: kinetic, isotherm and thermodynamic studies

Publicly submitted on:

In front of the jury

Pr. DOUADI Ali	University of Ouargla	President
Dr. ATIA Djamal	University of El Oued	Examiner
Dr. MANSOURI Khaled	University of Ghardaia	Examiner
Dr. BENMENINE Abdelkader	University of Ouargla	Examiner
Pr. ZOBEIDI Ammar	University of El Oued	Supervisor
Pr. ATIA Salem	University of Ouargla	Co- Supervisor

Academic Year : 2023/2024

Acknowledgements

We would first like to express our gratitude to God for leading us and providing us with the fortitude, bravery, and endurance necessary to complete this work to the best of our abilities. Without His direction, I have no doubt that this work would never have been completed.

*My thesis allowed me to learn about several people whom I sincerely thank for helping me complete this work under ideal conditions. I want to thank my supervisors **ZOBEIDI Ammar, ATIA Salem** from the bottom of my heart for their patience, wise advice, and presence while writing this thesis.*

*I thank **Pr. DOUADI Ali** for having accepted to chair the jury. I thank Gentlemen: **Dr. ATIA Djamal, and Dr. MANSOURI Khaled, Dr. BENMENINE Abdelkader** for having done me the honor to examine this work,*

*I express all my gratitude **Pr. DOUADI Ali**, director of laboratory the Pollution & Waste Treatment Laboratory (PWTL) Ouargla, for allowing us to carry out this work within their structure.*

*I would like to thank **Dr. ATIA Djamal, Dr. BENKHALFA Hakim** and all **CRAPC Ouargla team** for having welcomed me in the scientific and technical research center in physico-chemical analysis (CRAPC) at university of Ouargla. I am very grateful for all the facilities he has made available to me as well as all the equipment.*

*Thank you very much to everyone we could not mention. I would like to thank the members of Department of Environmental Engineering Mersin University, Turkey Especially **Pr. DIZGE Nadir** for his valuable guidance and advice and allows me to work with them on different subjects and all members of the team **ESKIKAYA Ozan, ISIK Zelah, ELTERKAOUI Aya, Pinar....***

Thank you very much to everyone we could not mention.

Dedication

For all of the times I never said thank you because I thought you knew, I thank you now more than ever, thank your mom for always being here for me to love me and care for me when I felt like no one else did. No one can ever take your place ever.

*To the soul of my dear father, who is always present despite the absence, I dedicate this research. Dear Father **AHMED**.*

*To my dear brothers: **Khaled, Mohamed El ghazel, Salah Eddine, Djamel Eddine**.*

To my dear sister.

*To all the **MECHERI** family and the **MENASSRIA** family.*

To my dear friends who accompanied me throughout this university journey

To all my teachers from primary to higher education.

And to everyone who is dear to me.

RAZIKA

Abstract

This work aims to manufacture an environmentally friendly adsorbent from kaolinite clay (Kaol), Kaolinite was combined with cellulose (Cel) extracted from red bean peels, where (Kaol) was used to remove the color of eight different cationic and anionic dyes (Basic Red 18, Safranin O, Rhodamine B, Reactive Orange 16 Reactive Red 180, Acid Red18, Crystal Violet, Methyl Orange), to conduct the rest of the experiments, both dyes (positive: crystal violet, negative: methyl orange) were chosen for their high efficiency to complete the rest of the study, where many analytical methods were used, X-ray diffraction, Fourier transform infrared spectroscopy, scanning electron microscopy, energy dispersive X-ray spectroscopy, and pHpzc surface charge test (to obtain the physical and chemical properties). Box-Behnken Design was applied to determine the factors affecting the adsorption performance. These factors included cellulose loading by 25%, adsorbent dosage of 0.035 g for CV and 0.05 g for MO dye, solution pH of 10 for CV and 7 for MO, contact time of 5 min for CV and 17.5 min for MO dye, temperature of 45°C for CV and 30°C for MO dye. The results also showed agreement with the Langmuir model, and the Langmuir model estimated the capacity of 294.12 mg/g for CV and 113.64 mg/g for MO. These results indicate that Kaol/Cel can be a promising raw material for developing a high-efficiency adsorbent for treating wastewater contaminated with organic dyes.

Keywords:

Kaolinite, red bean peels, kaolinite/cellulose composite, dye adsorption, response surface methodology.

الملخص

يستهدف هذا العمل تصنيع مادة مازة صديقة للبيئة من طين الكاولينيت (Kaol)، تم دمج الكاولينيت مع السليلوز (Cel) المستخلص من قشور الفاصوليا الحمراء، حيث تم استخدام (Kaol) لإزالة لون ثمانية أصباغ مختلفة كاتيونية و أيونية (Reactive Red 180, Basic Red 18, Safranin O, Rhodamine B, Reactive Orange 16) لإجراء بقية التجارب تم اختيار كل من الصبغتين (الموجبة : البنفسج البلوري، السالبة : الميثيل البرتقالي) لكفاءتهما العالية لإتمام بقية الدراسة حيث تم استخدام العديد من الطرق التحليلية ، حيود الأشعة السينية ومطياف الأشعة تحت الحمراء لتحويل فورييه والمجهر الإلكتروني الماسح، ومطياف الأشعة السينية المشتتة من الطاقة ، وإختبار pH_{pzc} الشحنة السطحية (للحصول على الخصائص الفيزيائية والكيميائية). تم تطبيق تصميم Box-Behnken Design لتحديد العوامل التي تؤثر على أداء الامتزاز. وشملت هذه العوامل تحميل السليلوز بنسبة 25٪، وجرعة ماصة قدرها 0.035 g CV و 0.05 g MO، ودرجة حموضة المحلول عند 10 ل CV و 7 ل MO، وزمن تلامس 5 min ل CV و 17.5 min لصبغة MO، ودرجة حرارة 45° C ل CV و 30°C لصبغة MO. كما أظهرت النتائج التوافق مع نموذج لانجمير، وقدر نموذج لانجمير بسعة 294.12 mg/g ل CV و 113.64 mg/g ل MO تشير هذه النتائج إلى أن Kaol/Cel يمكن أن يكون مادة أولية واعدة لتطوير مادة مازة عالية الكفاءة لمعالجة مياه الصرف الصحي الملوثة بالأصباغ العضوية.

الكلمات المفتاحية:

الكاولينيت، قشور الفاصوليا الحمراء، مركب الكاولينيت / السليلوز، امتزاز الأصباغ، منهجية استجابة السطح.

Résumé

Ce travail vise à fabriquer un matériau adsorbant respectueux de l'environnement à partir d'argile kaolinite. La kaolinite a été combinée à de la cellulose (Cel) extraite des écorces de haricots rouges. Le Kaol a été utilisé pour éliminer la couleur de huit colorants cationiques et ioniques différents (Basic Red 18, Safranin O), Rhodamine B, Reactive Orange 16, Reactive Red 180, Acid Red18, Crystal Violet, Methyl Orange), pour réaliser la suite des expériences, les deux colorants ont été choisis (positif : crystal violet, négatif : methyl orange) pour leur grande efficacité. Pour compléter la suite de l'étude, plusieurs colorants ont été utilisés. Méthodes analytiques : diffraction des rayons X, spectroscopie infrarouge à transformée de Fourier, microscope électronique à balayage, dispersion d'énergie.

Une conception Box-Behnken a été appliquée pour déterminer les facteurs affectant les performances d'adsorption. Ces facteurs comprenaient une charge de cellulose de 25 %, une dose absorbante de 0,035 g pour CV et 0,05 g pour MO, un pH de solution de 10 pour CV et 7 pour MO, un temps de contact de 5 min pour CV et 17,5 min pour le colorant MO, et une température de 45°C pour le colorant CV et de 30°C pour le colorant MO. Les résultats ont également montré un accord avec le modèle de Langmuir, et le modèle de Langmuir a estimé une capacité de 294,12 mg/g pour le CV et de 113,64 mg/g pour le MO. Ces résultats indiquent que Kaol/Cel pourrait être une matière première prometteuse pour développer une matière première hautement efficace. adsorbant pour traiter les eaux usées contaminées par des colorants organiques.

Les mots clés :

Kaolinite, coquilles de haricots rouges, complexe kaolinite/cellulose, adsorption de colorant, méthodologie de réponse de surface.

List of tables

CHAPTER I: Review of literature		
Table I .1	Lethal dose for 50 % of the population	11
Table I .2	Clay mineral classification	24
Table I .3	Some lignocellulosic fibers' chemical makeup	31
CHAPTER II: Methodology		
Table II.1	Percentage of dye removal by pre-treated clay.	56
Table II.2	CV, MO independent factor experimental levels using Box-Behnken design codes.	58
CHAPTER III: Results and Discussion		
Table III.1	Surface Area of three different samples of clay minerals.	65
Table III.2	Results of experiments for the crystal violet and the box-Behnken design matrix with five factors	71
Table III.3	Results of experiments for the methyl orange, the box-Behnken design matrix with five factors	72
Table III.4	Analysis of variance of the crystal violet dye removal response surface quadratic model	74
Table III.5	Analysis of variance of the MO dye removal response surface quadratic model.	76
Table III.6	The optimal conditions for the CV sorption onto Kaol/Cel composite in terms of the pseudo-first-order and pseudo-second-order kinetic parameters.	89
Table III.7	The optimal conditions for the MO sorption onto Kaol/Cel composite in terms of the pseudo-first-order and pseudo-second-order kinetic parameters.	90
Table III.8	Langmuir, Freundlich, and Temkin constants of CV dye adsorption onto Kaol/Cel composite are presented	92
Table III.9	Comparison of the q_{\max} (mg/g) values for CV dye adsorption to that of various adsorbents	93

Table III.10	Langmuir, Freundlich, and Temkin constants of MO dye adsorption onto Kaol/Cel composite are presented	94
Table III.11	Comparison of the q_{\max} (mg/g) values for MO dye adsorption to that of various adsorbents	94
Table III.12	Parameters thermodynamic of crystal violet dye adsorption onto Kaol/Cel-25	97
Table III.13	Parameters thermodynamic of methyl orange dye adsorption onto Kaol/Cel-25	98

List of figures

CHAPTER I: Review of literature		
Figure I.1	A timeline of the invention, use, and interesting information regarding dyes	7
Figure I.2	Dyes classification	10
Figure I.3	Dye removal techniques (benefits and drawbacks)	12
Figure I.4	Diagrammatic illustration of desorption and adsorption mechanisms	13
Figure I.5	Adsorption nature and types of adsorption bonding	14
Figure I.6	Adsorption Isotherm types based on IUPAC classification	15
Figure I.7	Factors affecting adsorption process	16
Figure I.8	Representation of tetrahedrons (a) and octahedra Sheet	22
Figure I.9	Clay Mineral Types, (a, b, c)	25
Figure I.10	Lignocellulose fiber components	32
Figure I.11	Cellulose structure	35
Figure I.12	Hemicellulose structure	36
Figure I.13	Lignin structure	37
Figure I.14	Response surface model plot	41
Figure I.15	Central composite design augmented with hybrid points	42
Figure I.16	Composite design provided by (Design-Expert 13)	43
Figure I.17	Box-Behnken design for three variables by (Design-Expert 13)	44
Figure I.18	Box-Behnken design for three variables by (Design-Expert 13).	45
CHAPTER II: Methodology		
Figure II.1	Diagrammatic demonstration of preparation and analysis utilizing a clay sample	51
Figure II.2	Sample of raw clay	52
Figure II.3	Diagram showing the steps involved in extracting cellulose from red bean peels	52

Figure II.4	Percentage of dye removal by pre-treated clay	57
CHAPTER III: Results and Discussion		
Figure III.1	SEM and EDX a) brown clay minerals, b) green clay minerals, c) red clay minerals	65
Figure III.2	Patterns of X-ray diffraction for a) Kaol, b) Cel, and c) Kaol/Cel-25	66
Figure III.3	FT-IR Fourier-transform spectra of the following: (a) Kaol/Cel-25 and (b) Kaol/Cel-25 following CV dye adsorption	68
Figure III.4	Energy-dispersive X-ray spectra and scanning electron microscopy (SEM) of (a) Kaol, (b) Kaol/Cel-25, and (c) Kaol/Cel-25 following CV dye adsorption	69
Figure III.5	The natural dyes decantation after adsorption onto Kaol/Cel for(a-MO and b-CV).	70
Figure III.6	Linear correlation between predicted values vs. the observed values of CV adsorption on Kaol/Cel-25	75
Figure III.7	Linear correlation between predicted values vs. the observed values of MO adsorption on Kaol/Cel-25	78
Figure III.8	3D surface plot of the influence of adsorbent dose and solution pH of CV adsorption on Kaol/Cel-25	80
Figure III.9	2D contour plot of the influence of adsorbent dose and solution pH of CV adsorption on Kaol/Cel-25	80
Figure III.10	The zero-point of charge (pH_{pzc}) of CV adsorption on Kaol/Cel-25	80

3D surfaceplot of the influence of adsorbent dose and temperature on Kaol/Cel-25 CV adsorption		
Figure III.12	2D contour plot of the influence of adsorbent dose and temperature on Kaol/Cel-25 CV adsorption	82
Figure III.13	3D surface plot of the influence of adsorbent dose and solution pH of MO adsorption on Kaol/Cel-25	84
Figure III.14	2D contour plot of the influence of adsorbent dose and solution pH of MO adsorption on Kaol/Cel-25	85
Figure III.15	Influence of initial concentrations versus CV adsorption contact time on Kaol/Cel-25	87
Figure III.16	Effect of MO adsorption contact time on Kaol/Cel-25 versus initial concentrations	87
Figure III.17	Plot of Van't Hoff equation for CV adsorption onto Kaol/Cel-25	96
Figure III.18	Plot of Van't Hoff equation for MO adsorption onto Kaol/Cel-25	96
Figure III.19	Possible mechanism between Kaol/Cel-25 surface and dyes (Crystal Violet and Methyl Orange)	99

List of abbreviations

<i>Abbreviation</i>	<i>Synonym</i>
AR 18	Acid Red 18
BBD	Box Behnken design
BR18	Basic Red 18
CCD	Central Composite Design
CEC	Cation-Exchange Capacity
<i>Cel</i>	Cellulose
CV	Crystal Violet
<i>Df</i>	Degree of Freedom
EDX	Energy- Dispersive X-ray spectroscopy
FTIR	Fourier Transform Infrared
<i>Kaol</i>	Kaolinite
MO	Methyl Orange
PFO	Pseudo-First-Order
PSO	Pseudo-Second-Order
q_e	Adsorption Capacity at Equilibrium (mg/g)
q_{max}	Maximum Capacity for Adsorption (mg/g)
RhB	Rhodamine B
RSM	Response Surface Methodology
SEM	Scanning Electron Microscope
SO	Safranin O

RR180	Reactive Red 180
RBP_s	Red Bean Peels
XRD	X-Ray Diffraction

Table of contents

Acknowledgment	i
Dedication	ii
Abstract	iii
List of tables	vi
List of figures	viii
List of Abbreviations	xi
Table of contents	Xiii
General Introduction	2
ChapterI. Review of literature	4
I.1.Dye	5
I .1.1.Definition of dyes	5
I.1.2 .An overview of the use of dye	6
I.1.3 .Classification of synthetic dyes	8
I.1.4 .Toxicity of dyes	10
I.1.5.Toxicity measurement	11
I.1.6.Current dye removal treatment techniques	11
I.2 .Sorption	13
I.2.1 .Sorption– definition and types	13
I.2.2 .Models for isotherms of adsorption	14
I.2.3.Factors affecting adsorption of dye	15
I.2.4.Equilibrium of adsorption	16

I.2.5.Different models of adsorption isotherms applicability to adsorption of dyes	17
I.2.6.Dye adsorption kinetic-study	18
I.2.7.Adsorption thermodynamics	19
I.2.8. Adsorption mechanism	19
I.3 .Clay and clay minerals	20
I.3.1.Clay definition	20
I.3.2 .Composition and clay mineral structure	21
I.3.3.Clay mineral classification	22
I.3.3.1 .Classification based on structure	23
I.3.3.2. Categorization based on color	26
I.3.4 .Methods of modification of clay minerals	26
I.3.4.1 .Pillared clays	27
I.3.4.2 .Organo clays	27
I.3.4.3 .Thermal Activation	27
I.3.4.4 .Acid activation	28
I.3.5.Clay with polymer modification	29
I.4 .Cellulose (Biopolymers)	29
I.4.1 .Lignocellulosic material	30
I.4.1.1 .Structure and characteristics of lignin and lignocellulosic fibers	31
I.4.1.2. Some lignocellulosic fibers' chemical makeup	31
I.4.2 .Cellulose	32

I.4.2.1. Structure of cellulose	33
I.4.2.2 .Properties of cellulose	35
I.4.3 Hemicellulose	35
I.4.4. Lignin	36
I.5 .Methods of optimization	37
I.5.1. Experimental design	38
I.5.2. Response Surface Methodology	39
I.5.2.1 .Principle of RSM	39
I.5.2.2. Phases of modeling with the RSM	40
I.5.3 .Types of designs	42
I.5.3.1 .Creating a Central Composite	42
I.5.3.2. Box-Behnken Design (BBD):	44
Chapter II. Methodology	48
II.1. Introduction	49
II.2. Chemical Solvents and Materials Used	49
II.3. Sampling of Raw Clay	50
II.4 .Pre-treatment of red clay's (PTRC) production	50
II.5 .Extracting Cellulose from Red Bean Peels (RBPs)	51
II.6. Making the Kaol/Cel Composite	52
II.7. Instrumentation	53
II.7.1 .Infrared spectroscopy using the Fourier Transform	53
II.7.2 .Scanning Electron Microscopy	53
II.7.3 .X-Ray Diffraction	53

II.7.4. Isotherm for the adsorption/desorption of nitrogen (BET)	54
II.8 .Zero-point charge	54
II.9 .Preliminary Gexperiments of dyes with PTRC	55
II.10.Design Experiments Pre-treatment red clay's (PTRC), Kaol/Cel Composite	57
II.11 .Adsorption Studies in Batch	59
II.12 .Isotherms of Adsorption	60
II.12.1 .The Isotherm of Langmuir	60
II.12.2 .The Isotherm of Freundlich	61
II.12.3 .The Isotherm of Temkin	61
II.13 .Kinetics of Adsorption	61
II.13.1. Model of pseudo-first order	62
II.13.2. Model of pseudo-second order	62
Chapter III. Results and Discussion	64
III. Results and Discussion	64
III.1.Characterization of kaolinite clay.	64
III.1.1. Surface Morphology	64
III.1.2. Surface Area	65
III.2. Characterization of kaolinite mixed with cellulose (Kaol/Cel)	66
III.2.1.XRD analysis	66
III.2.2. FT-IR analysis	67
III.2.3.SEM-EDX analysis	68

III.2.3.SEM-EDX analysis	70
III.2.4.Adsorbent Characterization of Kaol/Cel Composite after CV and MO dye adsorption	70
III.3. Results and Discussion of BBD model analysis for MO dye	74
III.3. 1. Fitting the Process Models Kaol/Cel Composite following the adsorption of CV dye	74
III.3. 2. Fitting the Process Models Kaol/Cel Composite following the adsorption of MO dye	76
III.3.3.Interactions Significant for Crystal Violet (CV) Dye Removal	78
III.3.4.Interactions Significant for Methyl orange (MO) Dye Removal	83
III.4. Result of adsorption experiments with Kaol/Cel Composite after CV and MO adsorption	85
III.5. Kinetic Modeling of adsorption experiments with Kaol/Cel Composite after CV and MO adsorption after CV and MO adsorption	88
III.6. Isotherms of adsorption experiments with Kaol/Cel Composite after CV and MO adsorption	90

General Conclusion	103

GENERAL INTRODUCTION

GENERAL INTRODUCTION

The planet is currently dealing with severe pollution problems, which are a global threat to the natural eco-system. A significant amount of wastewater containing dyes from human activity is released into the environment untreated, which has a negative impact on the quality of drinking water[1]. Dyes can be classified as nonionic (disperse), (Methyl Orange, Reactive Orange 16, Reactive Red 180, Acid Red 18) and cationic (basic) [2]. Dyes that are organic and cationic, like Crystal Violet, Basic Red 18, Safranin O, and Rhodamine B. Dyes can be eliminated from wastewater using a variety of methods, such as ion exchange, membrane filtering, irradiation, [3]. However, the adsorption method is still the method of choice for dye removal because it has several advantages over other methods other forms do not have. Recently, clays and their composites have shown promise as dye-containing water adsorbents. This is because of the clays' high cation-exchange capacity (CEC), high stability, high micro porosity, outstanding swelling ability, and environmental safety [4-6]. Among the numerous kinds of biopolymers (which includes chitosan, alginate, and starch); cellulose is ubiquitous and renewable and has ample herbal availability. In general, there are methods that can be used to improve the properties of clay such as chemical modified, and synthesis of composite in a matrix of cellulose. Thus, the main objectives of the current study are:

- ✓ To purify three clay varieties by describing the mineralogical and physicochemical properties of clays from Aougrout (Timimoun), Algeria.
- ✓ To Use eight cationic and anionic dyes (Basic Red 18, Safranin O, Rhodamine B, Reactive Orange 16, Reactive Red 180, Acid Red18, Crystal Violet, and Methyl Orange) to select high-performance dyes for the remaining study using kaolinite clay.
- ✓ To extract cellulose-based compounds from red bean peels (RBPs), which gives this study its innovative quality, to prepare new kaolinite /cellulose (Kaol/Cel) composite sorption materials that could remove the cationic dye methylene blue (MB) and the anionic dye methyl orange (MO) from water.
- ✓ To characterize the adsorbents, the usage of scanning electron microscopy (SEM), Fourier transform, infrared (FTIR) spectroscopy, and energy-dispersive x-ray (EDX) spectroscopic techniques, to evaluate the composites for dye removal from aqueous solution by using response surface methodology (RSM) in a Box-Behnken design (BBD), to assess the adsorption process through the use of kinetic studies and isotherm models applied to experimental data.

GENERAL INTRODUCTION

This thesis is divided into three chapters

Chapter 1: Discusses the literature associated with the contemporary work along with reassets of wastewater. Inside the surface medium. In addition, the approach has been used for cleansing technology of dyes. Additionally, the definition, composition, and structure of clay minerals. After the technique modification of clay minerals, and ultimately the cellulose and the techniques of optimization.

Chapter 2: In this chapter, we mentioned Chemical Solvents and Materials Used and the method used on this observe additionally the Instrumentation and experiments in the end Adsorption Studies in Batch on Kaol/Cel Composite and Kaolinite clay.

Chapter 3: This chapter is for results and discussion. At the cease of this work became general end which summarizing the primary of acquired consequences and supplying a few tips for future paintings.

CHAPTER I

REVIEW OF LITERATURE

I.1 Dye

I.1.1 Definition of Dyes

The Middle English word "dye" comes from "deie" also from the older English language "dag", "dah". The terms "dye" predates the 12th century in its initial use, according to records. Dyes can dissolve in water or oil, Compounds of organic color that are soluble in the water in addition attached in surfaces as well textiles to add color to textiles. Most dyes are made of intricate chemical compounds that are intended to form a strong bond with the molecules of polymers that comprise the fibers of textiles fiber, and need to be resilient to a variety of outside influences[7].

Within his work "*Synthetic dyes*", R. Gurdeep Chatwal [8] describes dyes as organic chemicals or mixes that are colored and used to color papers, leather, plastics, and fabric. Washability and light stability are requirements for the dye substrates. Not every material that has color is a dye; in order to give a material a lasting color, a dye needs to be fastened to the material [9].

In accordance with the widely recognized Color Index International convention, Dye is an organic compound with a strong hue or fluorescence that adds color to a substrate by selectively absorbing light. These materials undergo a process that disintegrates them or dissolves them, The crystal structure through ionic or chemical interaction, mechanical action, adsorption, or otherwise [10].

Most dyes are made up of complicated organic compounds. In addition, are composed of two parts:

- ✓ Chromophores (the component of a molecule that gives it color), such as carbonyl, azo, carbon-nitrogen, carbon, nitro, nitroso, sulphur and additional carbon sulfur groups.
- ✓ auxochromes (A collection of functions that alters the light absorption) ,can be sulfonic acid, aldehydes, hydroxyl, carboxyl groups, amine [11, 12].

1.1.2. An Overview of the Use of Dye

The term in English "dye" as well as the ancient English language words "dag" also "dah" is the term's original "dye". Earlier than the twelfth century, the word "Dye" was first recorded. More than one million different hues are visible to human sight, all of which are present in our natural surroundings. These stunning and distinctive hues draw people's attention away from their surroundings, and commonplace objects have been designed to imitate them. Archaeological research demonstrates that the practice of dying has existed from the dawn of human society. Figure .I.1 depicts a chronology with some significant historical turning points pertaining to dyestuffs that is based on Susan C. Druding's thorough historical analysis (sadly, the data from the literature was destroyed, thus there are no references in it) [13].

While a comprehensive list can be found in the literature, we would like to offer a few noteworthy facts without trying to be exhaustive. These findings show that colored clothing and madder dye remnants were discovered in the Indus Valley Civilization's ruins, which were built between 2600 and 1900 BC. Additionally, it was at this time that the earliest documented account of the use of dyestuffs was discovered in China. Another fascinating examination revealed that the "El Castillo" cave paintings were formed around 40,000 years before in Spanish. Another fascinating examination revealed that the "El Castillo" cave paintings in Spain were created around 40,000 years ago. At a historic cave situated in the Georgian Republic, colorful flax fiber that dates to roughly 34,000 BC is perhaps the earliest ever discovered[14]. Between 715 and 55 BC, there are numerous references from the Roman Empire, when purple was used to dye their garments, including robes, and wool dyeing first emerged as a craft. Alexander the Great reports discovering 541 BC purple textiles in the royal treasury following the invasion of Susa (the capital of Persia) in 333 BC [15]. The current market value of the five thousand purple talents fabric dyed accompanied by mucous (a yellow substance produced by a small gland on the neck of a sea snail) is almost \$68 million.

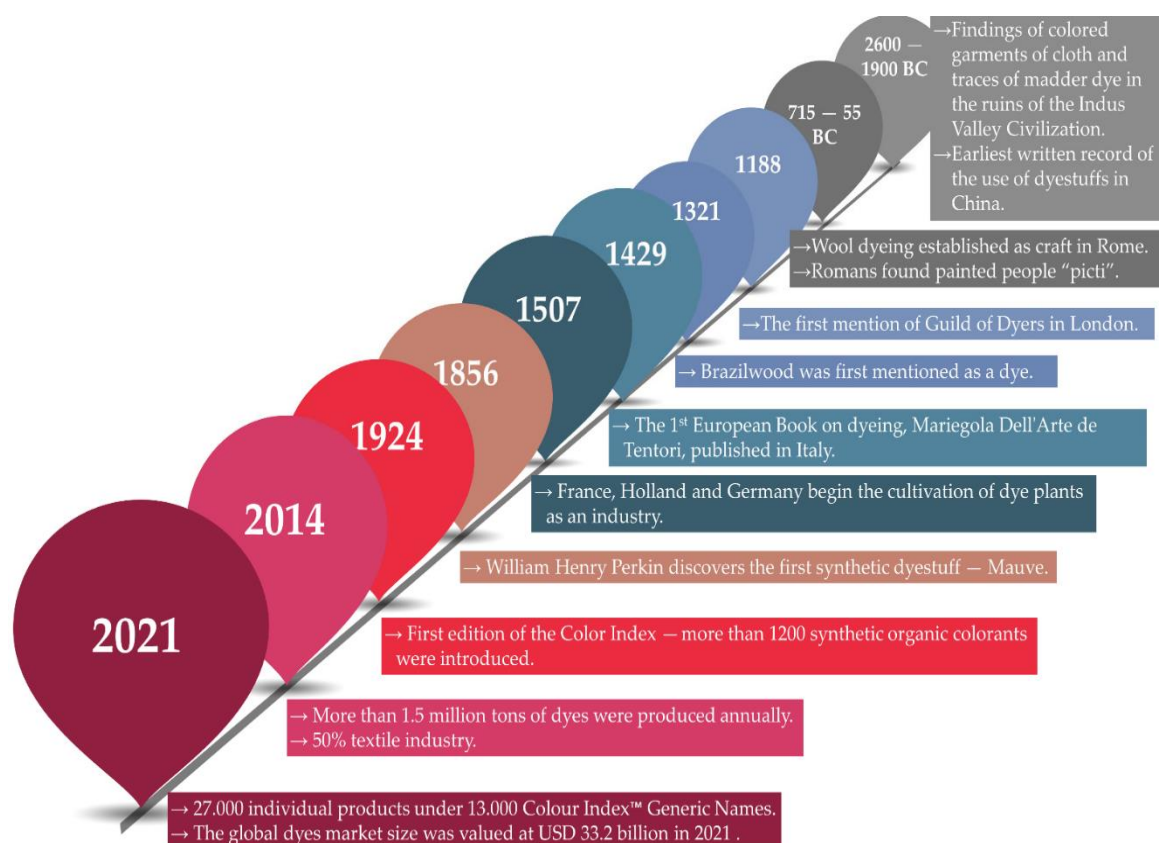


Figure. I .1. A timeline of the invention, use, and interesting information regarding dyes.

By way of example, London in 1188, various painters' guilds were established in Europe's main towns during the 12th century. More than two hundred tailors, clothiers, and painters were officially registered at Florence during the mid-century. Several kings took action to safeguard traders and good[16].As a result, The development of chemistry as well as the industry, social, and economic demands of the nineteenth century are directly concerning the discoveries and advancement of artificial dyes. Many attempts were made to create synthetic dyes, but they failed because of their weak lightfastness. William Henry Perkin is credited as the inventor and the forerunner of synthetic colors. He separated a little quantity of violet dye at the time of Easter in 1856 since studying how to make synthetically produced quinine (oxidized dichromate) in order to treat malaria. He gave the dye the name "mauve,"

which quickly gained popularity among the family of royals and led to the creation of a new sector [17].

The dye business thrived up to the turn of the twentieth century, producing a wide variety of dyes, necessitating their classification, recording, and cataloging. The first version of the Color Index, which included a list of more than Twelve hundred dyes, both synthetic and organic, was published at 1924. According to reports, more than One half of a million tonnes of pigments were generated globally in 2014, with the textile industry using half of them [18, 19]. A 2016 article said that each year, more than 50 thousand tons in several There were invented synthetic dyes, it may reach ten percent of those colours were combined featuring bodies of water [20]. In light of current data, the size of the global market for dyes was estimated to reach \$33.2 billion USD in the year 2021.27,000 unique goods are listed in The Colour Index TM fewer than 13,000 common names and traits. (According to projections, the money made via the production of pigments and dyes On 2023, the amount at Romania is around \$65.1 a million [21].

1.1.3 Classification of Synthetic Dyes:

Different characteristics, such as their chemical structure, use, and dye procedure, can be used to classify synthetic dyes in several ways. Synthetic dyes are often categorized as follows:

- ✓ **Chemical structure:**Chemical structure can be used to categorize synthetic dyes, including azo, anthraquinone, phthalocyanine, and indigo colors.
- ✓ **Dyeing process:**They can be divided into groups according on the kind of dyeing method that was employed, including vat, disperse, reactive, acid, and direct dyes.
- ✓ **Application:** categorized by use, including inkjet dyes, textile dyes, leather dyes, paper dyes, food dyes, and cosmetic dyes.

- ✓ **Colorfastness:** Additionally, they are categorized according to colorfastness attributes such as heat stability, washability, and lightfastness.
- ✓ **Toxicity:** These dyes can be classified based on their toxicity level, such as eco-friendly dyes, low-toxicity dyes, and high-toxicity dyes [22].

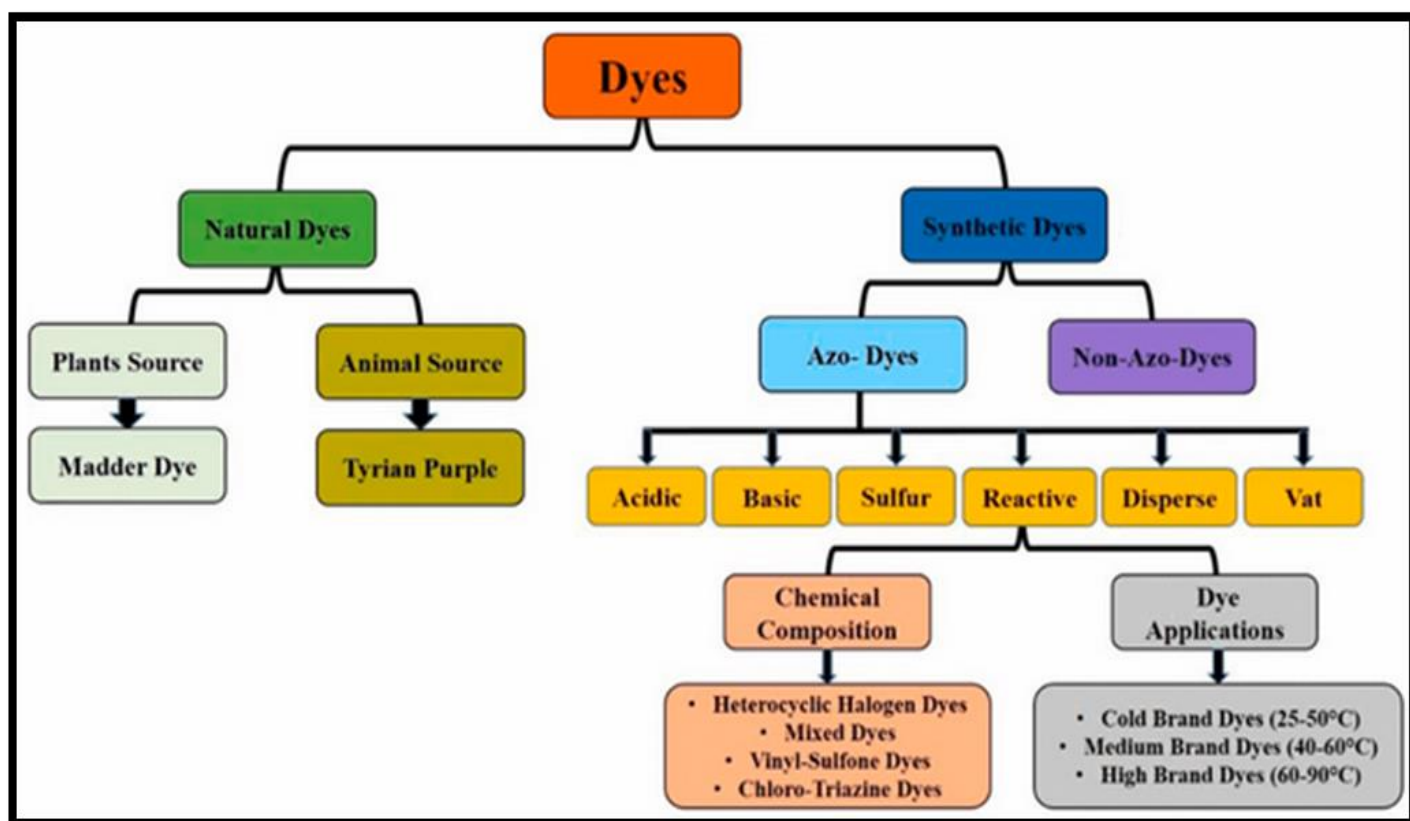


Figure. I .2. Dyes classification.

I.1.4 Toxicity of Dyes:

The toxicity of dyes can vary significantly depending on the specific chemical composition of the dye. Some dyes are considered safe for use in food, cosmetics, and textiles, while others may pose health risks. Here are a few key points :

- ✓ **Food Dyes:** health authorities in most countries regulate Dyes used in food. They undergo rigorous testing to ensure they are safe for human consumption. However, some studies suggest that certain artificial food dyes may cause allergic reactions or hyperactivity in sensitive individuals.
- ✓ **Textile Dyes:** Dyes used in textiles can contain heavy metals or other harmful chemicals if not properly regulated. Workers in textile industries may face health risks from exposure to these dyes during manufacturing processes.
- ✓ **Cosmetic Dyes:** Dyes used in cosmetics and personal care products are regulated to ensure they do not pose health risks when used as intended. However, allergic reactions to certain dyes can occur, especially in individuals with sensitive skin.
- ✓ **Environmental Impact:** Improper disposal of dye-containing wastewater from manufacturing processes can lead to environmental pollution. Some dyes are persistent in the environment and can have long-term ecological impacts.

To determine the safety of specific dyes, it's essential to look at regulatory approvals, safety data sheets, and studies on their potential health effects [23].

I.1.5 Toxicity measurement

LD50, or "lethal dose, 50%," is a standard measure used in toxicology to indicate the dose of a substance that is required to kill 50% of a test population. It is commonly used to assess the acute toxicity of substances. The lower the LD50 value, the more toxic the substance. LD50 is typically expressed in milligrams of substance per kilogram of body weight (mg/kg). This measure helps in understanding the potential risk and safety levels of chemicals and medications [24].

Table.I.1. Lethal Dose for 50 % of the Population [25].

Dye	Lethal dose for 50 % of the population (LD50) (mg/Kg)
Methyl Orange	60
Reactive Orange 16	3000
Reactive Red 180	2000
Acid Red 18	7200
Crystal Violet	96
Basic Red 18	3800
Safranin O	3800
Rhodamine B	500

I.1.6. Current dye removal treatment techniques

Different methods to managing effluents that contain dyes contaminants. Although the presence with a number of strategies for getting rid of dye impurities from wastewater, as chemical oxidation, membrane separation, coagulation, and electrochemical techniques anaerobic and aerobic the breakdown of microbes, each of these methods has its intrinsic constraints. These Technologies have the potential to categorized divided into 3 main groups: biological , chemical, physical [26, 27]. Even though over the last thirty years,

Many dye elimination methods are currently researching. Due to the limitations of the majority of the methods, Currently, the relevant industries are only implementing a small number of these [28]. Each of these approaches has its unique

strengths and weaknesses. Figure.I.3. provides an overview of the pros and cons associated with different methods for removing dyes.

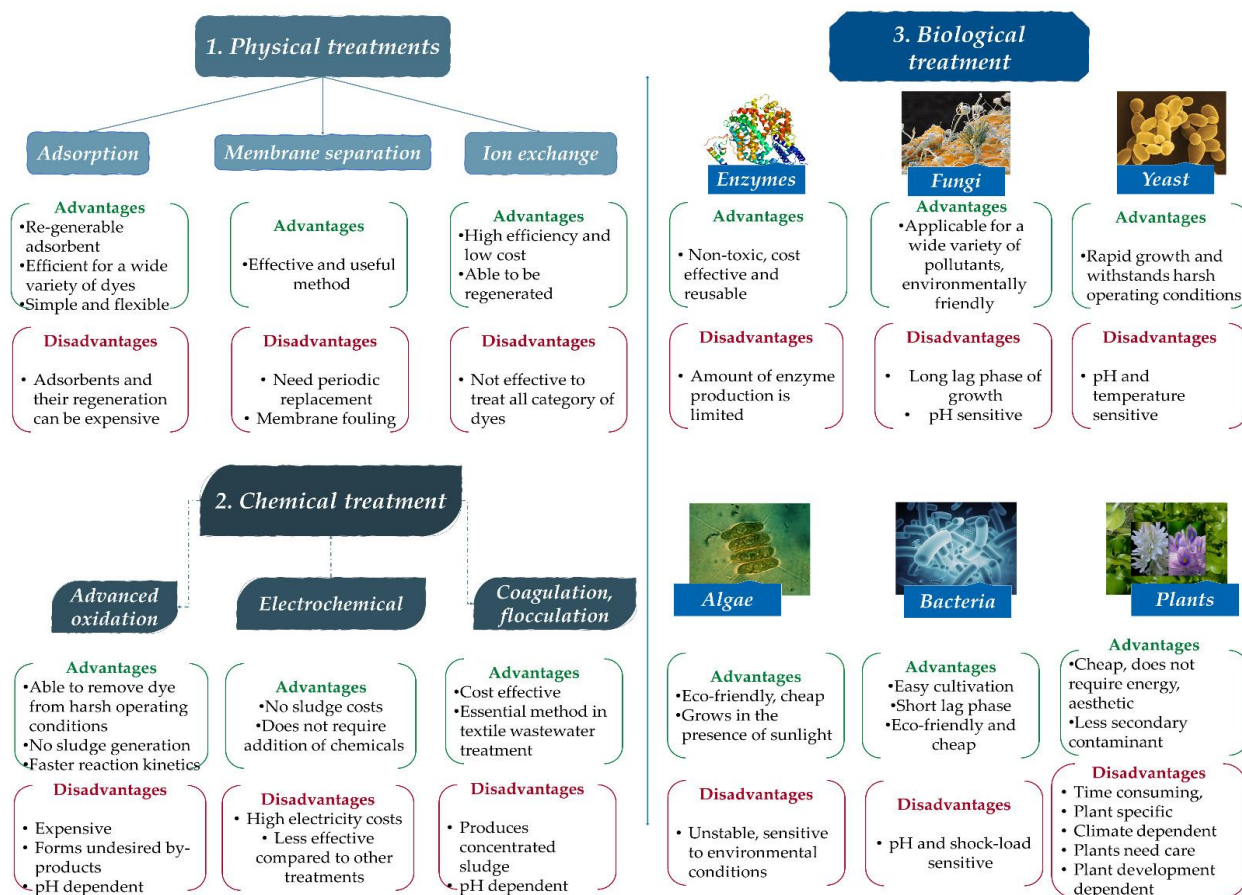


Figure. I. 3. Dye removal techniques(benefits and drawbacks) [29].

I.2 Sorption

I.2.1. Sorption– definition and types

First recorded in 1881, the term "adsorption" by Heinrich Kayser, a German scientist [30]. Adsorption represents a technique for mass transfer. Where a material (the adsorbate) goes from liquid or a gas to create monolayer surface in either a liquid

or a solid phase (the adsorbent). Typically, molecules are involved, atoms, or dissolved ions adhering to the surface [31]. Conversely, though, the adsorbed molecules' release is known as the process of desorption. from the adsorbent's surface, and these contrasts with adsorption [32]. This procedure is shown in schematic form in (Figure.I.4).

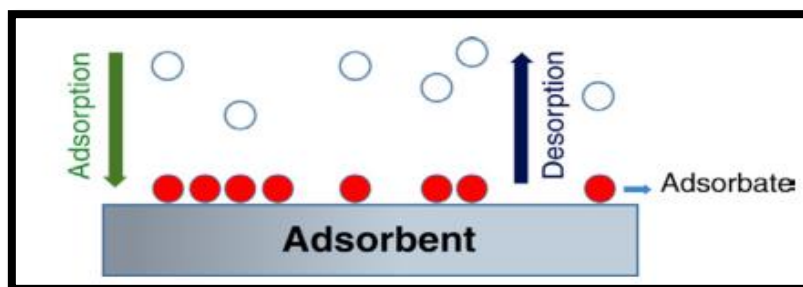


Figure.I.4. Diagrammatic Illustration of Desorption and Adsorption Mechanisms [33].

There are two possible methods that Adsorbent surfaces are capable of attracting molecules: «physical adsorption,” additionally called as “physisorption,” and “chemical sorption,” additionally called as “chemisorption.” It is reliant on upon how the molecules utilize in surface interaction [34]. Adsorption can be categorized in a number of ways, **Figure.I.5.** gives a classification according to the type of bond (chemical or physical bonds) developed between the contaminant and the adsorbent, defining its features [35, 36].

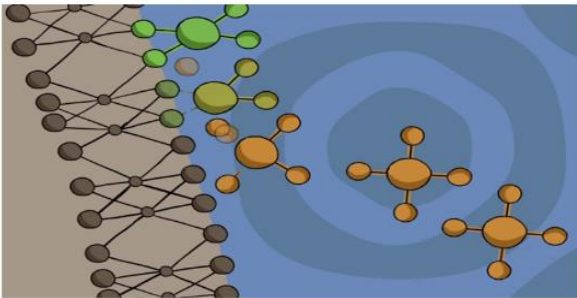
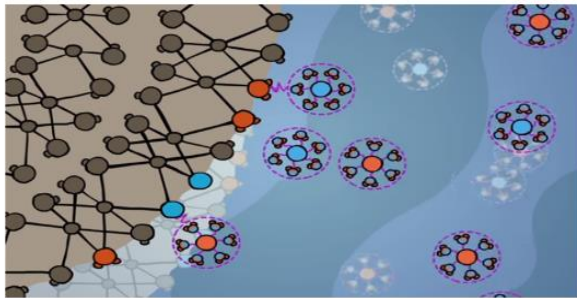
The interactions between the molecules of each phase (liquid, solid, gas) can form different bonds:

Primary bonds

- Specific, **chemical adsorption**, chemisorption,
- electron transfer, covalent bonding,
- single layer, slow,
- can act at short distances,
- changes the structure of the molecule,
- irreversible.

Secondary bonds

- **Physical adsorption**, physisorption, van der Waals interactions are long-range but weak,
- no chemical bonding or Coulomb interaction,
- multilayered, fast,
- occurring on almost any solid surface, reversible process,
- the bond energy generated depends on the polarizability.

Figures from: <https://www.youtube.com/watch?v=Az1h5qMfQOM>

Figure.I.5 .Adsorption nature and types of adsorption bonding [37].

1.2.2. Models for Isotherms of Adsorption

As per the IUPAC, the general categories of adsorption isotherms are six. [38] As indicated in (**Figure.I.6.**) Type I isotherms of adsorption explain how gas molecules bind to adsorbents with micropores, like activated carbon, and create a single layer of molecules adsorbed on the surface of the adsorbent. Gas molecules' adsorption to macroporous adsorbents is described by the type II sorption isotherm. After monolayer adsorbed molecules have covered the adsorbent surface, a layer upon layer of molecules adsorbed forms; the isotherm of Type II adsorption does not display a point of saturation much as that of the Type I does[39]. Adsorption type III, the term "isotherm" describes low-energy, weak interactions leading to multilayer adsorption between the adsorbent that contains macropores and the adsorbed molecules. The Types V and IV models of sorption represent the combination of capillary

condensation and multilayer adsorption with respect to adsorbents mesoporous. A multilayer's gradual development on an adsorbent's nonporous surface is described by the Type VI adsorption isotherm[40].

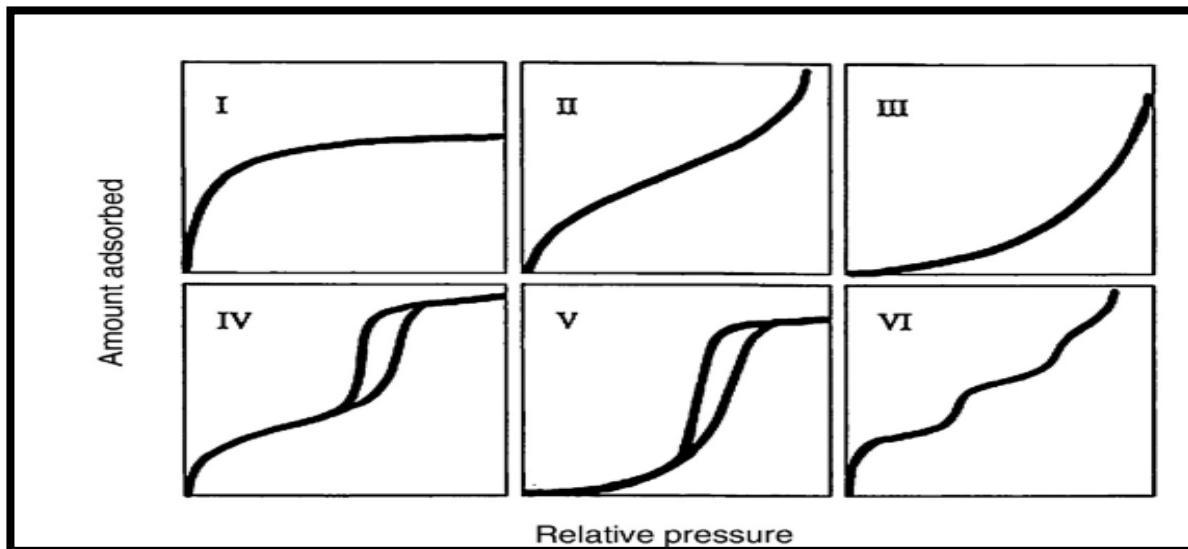


Figure.I.6. Adsorption Isotherm Types Based on IUPAC Classification [41].

I.2.3. Factors affecting adsorption of dye

The liquid phase adsorption's efficiency, and consequently the water purification process's ideal functioning, depending on a number of factors. As shown in the sorption efficiency, a number of physico-chemical parameters affect **Figure.I.7**, the category of pollution followed by the composition of its molecules, characteristics of the employed adsorbent. Among these physicochemical factors is the relationship between the adsorbent and adsorptive materials, the pore structure of the adsorbent and surface chemistry, Particles size, adsorbent type, pH, temperature, pressure, additional ions present in the solution's aqueous phase, and duration of the interaction. It's also important to consider the adsorbate's characteristics, including its polarity, molecular weight, molecular structure, and molecular size [42, 43].

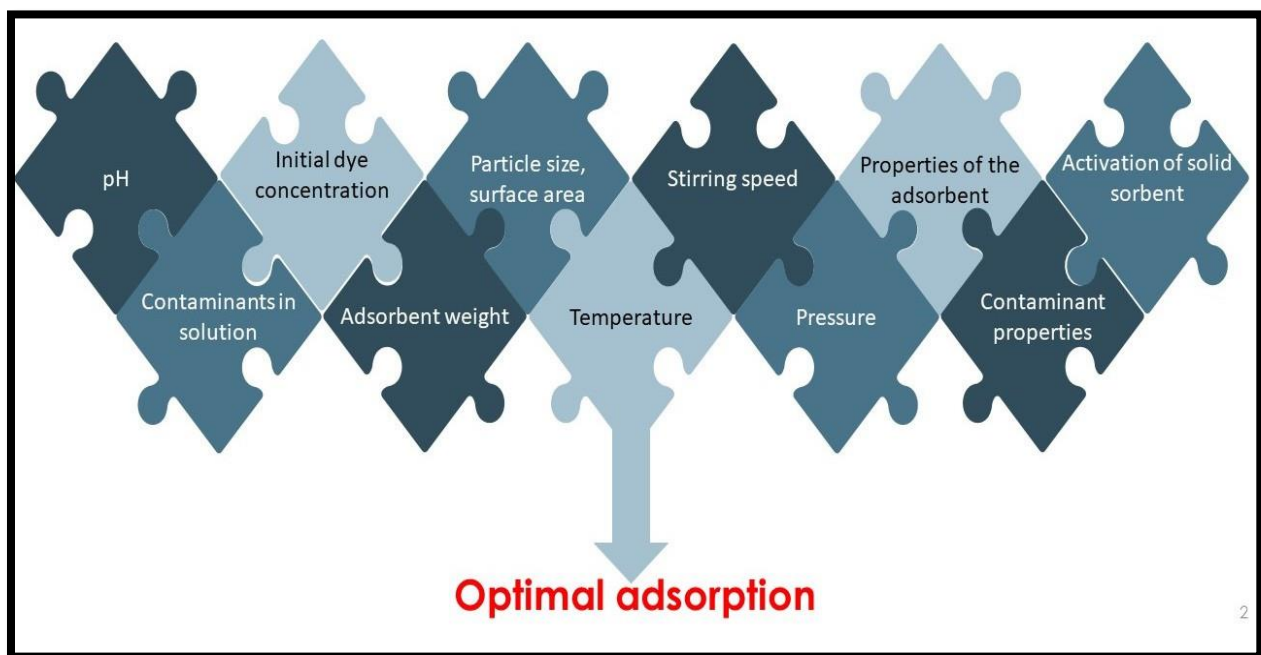


Figure.I.7. Factors affecting adsorption process [44].

1.2.4. Equilibrium of adsorption

On solid adsorbents, liquid-phase adsorption takes place through equilibrium or dynamic processes. As was previously explained in brief, both batch and column methods can be used to carry out an adsorption procedure. The batch approach will be the main topic of this discussion [45].

Some advantages of batch investigations at equilibrium include simple access to sorption sites inside the adsorbent. This approach involves adding the solid adsorbents to the solution phase, which is made up of the solvent medium, the adsorbate species, and the adsorbate/solvent where the ensemble and the adsorbent surface interact until the bound and unbound sites of the adsorbent reach equilibrium. A plot of sorption capacity (q_e) vs. equilibrium or total concentration able to be applied to graphically calculate the highest possible adsorption level (q_{\max}) at equilibrium. This plot can then be examined using an appropriate isotherm model[46]. For the process of liquid-phase adsorption, the function q_e depends on the solute's mole fraction in relation to the

adsorbent's specific area of surface. Considering the perfect dilute the solution condition governs the adsorption procedure, Considerations for mass balance (mg/g) can be used to estimate q_e , the dye's starting and equilibrium concentrations (mg/L) are denoted by the letters C_0 and C_e , respectively. According to Equation (I.1), V is the volume (L) of the dye solution, W is the total amount of adsorbent (g) [47].

$$q_e = \frac{(C_0 - C_e)V}{W} \quad (I.1)$$

Within these kinds of systems for water purification, the dye's effectiveness adsorbed elimination, R (%) was established by employing Equation (I.2) [48]:

$$R(\%) = \frac{(C_0 - C_e)}{C_0} \times 100 \quad (I.2)$$

1.2.5 Different models of adsorption isotherms applicability to adsorption of dyes

The isotherm of adsorption is important because it provides insight into the type of interaction between the adsorbate and adsorbent as well as shows the amount of adsorption. They are essential for understanding how the adsorption mechanism works. The surface phase can be conceptualized as either a multilayer or monolayer.

Many isotherms' models are presented in the literature [49]. The most popular models for explaining the phenomenon of adsorption are the Temkin, Freundlich and Langmuir models. As per Eqs. (I.3) through (I.5), the forms of the not linear Freundlich [50], Temkin [51, 52] and Langmuir [53] are expressed. As follows:

$$\frac{C_e}{q_e} = \frac{q_{max} K_a C_e}{1 + K_a C_e} \quad (I.3)$$

$$q_e = K_F C_e^{\frac{1}{n}} \quad (I.4)$$

$$q_e = \frac{RT}{b_T} (\ln K_T C_e) \quad (I.5)$$

Where the maximum capacity for adsorption (mg/g) is denoted by q_{\max} . where K_a represents the L/mg isotherms constants, the constant Freundlich = K_F (mg/g) $^{1/n} \times$ (L/mg), The constant n , which is dimensionless represents the intensity of adsorption Temperature is represented by T (K), the Temkin constant K_T (L/mg). The universal gas constant is denoted by R , which is (8.314 J/mol), Adsorption intensity and heat of adsorption are represented by b_T (J/mol), respectively.

1.2.6 Dye adsorption kinetic-study

To determine the adsorption mechanism, investigating the kinetics is essential of thermodynamics and adsorption. The adsorption kinetics models of cationic and anionic dye onto various adsorbent substances, such as for this purpose, the pseudo first order was employed, the intraparticle diffusion models and pseudo second order models are commonly applied to the adsorption systems. The pseudo first order [54] kinetic models' non-linear equations, Equations (I.6–I.8) express PSO [55] and intraparticle diffusion models [56], respectively.

$$q_t = q_e (1 - \exp^{-k_1 t}) \quad (I.6)$$

$$q_t = \frac{q_e^2 k_2 t}{1 + q_e k_2 t} \quad (I.7)$$

$$q_t = K_{id} (t^{0.5}) \quad (I.8)$$

Where: The speed constant of the diffusion of intraparticle is K_{id} (mg/g \times min $^{0.5}$), k_1 (1/min) is PFO's speed constant, the speed constant of PSO is k_2 (g/mg \times min), the amount of compound adsorbed to the adsorbent during time t (min) is expressed as q_t (mg/g).

1.2.7 Adsorption Thermodynamics

Adsorption thermodynamic parameters are conducted in order to look into the spontaneity, feasibility also the dye adsorption procedure onto the surface of the adsorbent, not only does it compute the degree of randomness at the dye-adsorbent surface interface. The parameters of thermodynamics for adsorption, the energy-free change of Gibbs, ΔG° (kJ/mol) is included, [57, 58].

$$\Delta G^\circ = -RT \ln K_d \quad (I.9)$$

$$K_d = \frac{q_e}{C_e} \quad (I.10)$$

$$\ln K_d = \frac{\Delta S^\circ}{R} - \frac{\Delta H^\circ}{RT} \quad (I.11)$$

1.2.8 Adsorption Mechanis

Adsorbate molecules or particles build up within the adsorbent layer due to a variety of interactions and forces involved in the adsorption process. The following are the primary mechanisms of adsorption:

The forces of Van der Waals: All molecules are attracted to one another despite being weak, whether polar or nonpolar. An important factor in adsorption is the force of van der Waals, particularly in physical adsorption, or physisorption.

- Electrostatic Forces: In some cases, electrostatic interactions between charged species in the adsorbate and adsorbent contribute to adsorption. This is common in chemisorption (chemical adsorption).
- Hydrogen Bonding: When hydrogen atoms in the adsorbate form hydrogen bonds with atoms in the adsorbent, this can lead to adsorption.
- Dipole-Dipole Interactions: If the adsorbate molecules have a permanent dipole moment, adsorption may result from their interaction with the adsorbent's dipole moments.

I.3 Clay and clay minerals

The discipline of clay studies in science has recently received a great deal of attention. Because of their adaptability in meeting market demands across various industrial and environmental sectors [59]. This field is interdisciplinary, including physics, geotechnology, chemistry, crystallography, mineralogy, and geology [60]. Throughout history, civilizations have highly valued clays for construction, pottery, brick making, ceramics, and more. Today, clays not only enhance performance in these traditional applications but also play crucial roles in paints, plastics, rubber, construction, cosmetics, and pharmaceuticals [61,62].

I.3.1. Clay Definition

Agricola originally codified the meaning behind «clay» in 1546. Many revisions have been made since then, while the principles of hardening, particle size, and plasticity [63]. The reader is referred to Mackenzie at the (1963) for a comprehensive history of definition history up to that year [64]. Weaver (1989) [65] pointed out one more difficulty: The conceptual challenge of integrating mineralogy and the particle size requirements of clay constituents. The definition of a mineral group cannot be based on particle size in order the word "mineral" has a specific definition that excludes particle size. The CMS and AIPEA nomenclature committees started defining clay at the same time and concluded that working together would produce a more acceptable result.

More broadly, hydrated aluminosilicates that are members of the phyllo-silicate family are what clays and clay minerals are, made up of infinite two dimensional sheets[66]. The term in Greek "argilos" (which means white) is where the word "clay" first appeared. It describes materials that are primarily made up of tiny grains, or smaller than two microns. These minerals harden when dried or burned, and they become plastic at specific water contents[67].

Depending on the discipline, the term "clay mineral" can refer to a number of different concepts. These concepts have to do with discipline, physical characteristics, and crystallographic structure. Every mineral has tiny particles are categorized as minerals made of clay (between two and four μm) by geologists and soil scientists. The proportion of minerals within a specific fraction of clay is what draws civil engineers in, since this behavior of the minerals affects all properties, encompassing physical, thermal and chemical characteristics. The clay minerals' ability to change their properties when exposed to water is of interest to ceramists [68].

1.3.2. Composition and Clay mineral structure

At the microscopic level, clay is an ordered material; at the macroscopic level, it is disordered. From a microscopic perspective, the phyllosilicate family of clay minerals, using a framework made of two sheets dimensional stacked atop one another [69]. Covalent connections bind such sheets together, which allow for apical oxygen sharing, and can be either octahedral or tetrahedral [70]. Where the three basal oxygens that bind the superposition of elementary tetrahedrons together form the tetrahedral sheet of coordinate four. (Fig.5.a), and the sequence of basic octahedra that make up the octahedral sheet of coordination six are connected by sharing edges. (**Figure. I.8.b**) [71].

Additionally, a layer is created when two or three sheets are joined. Hydrogen bonds hold these layered structures together, which are formed between the atoms of oxygen in the layer's tetrahedral sheet next to it, the octahedral sheet's groups of hydroxyls, or by the forces of Vander Waals, producing a crystallite. Inter-layer space is the area between two parallel layers; depending on the charge of the sheets, it can be either empty or occupied. The interlayer space and layer combination is referred to as "structural unit", The clay particles are formed by the arrangement of these units between them [72].

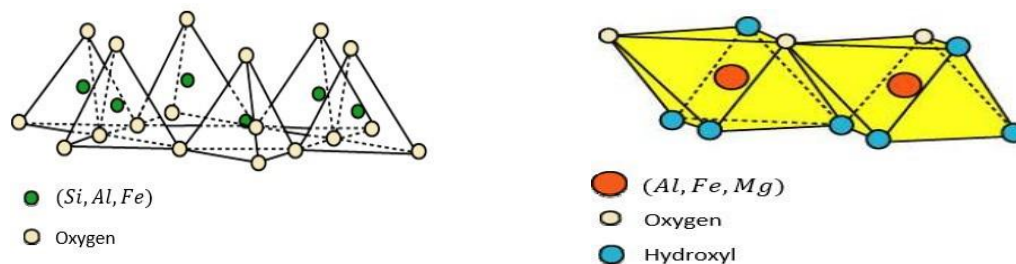


Figure. I .8. Representation of Tetrahedrons (a) and Octahedra Sheet (b)[73].

I.3.3. Clay mineral classification

Numerous clay minerals exist, and they differ in terms of their chemical makeup and molecular crystal structure. In fact, the primary classification criteria for these minerals are determined by a number of variables, such as the number of tetrahedral in addition octahedral sheets that make up the layer, the octahedron and tetrahedron's chemical makeup, the layers' distance apart, and the kind of cations they contain, the species' characteristics in the interlayer space and the sheet's charge. These primary factors lead to a number of classifications, but the most traditional one is determined by the arrangement of the sheets, which enables the differentiation of minerals of types 1:1, 2:1, and 2:1:1. However, classification shows seven groups of clay minerals (table 1), including the kaolinites group, which includes serpentine, halloysite, and kaolinite.

However, another classification based solely on color is unreliable due to significant variations caused by factors like impurities, mineral composition, weathering, and geological conditions.

1.3.3.1. Classification based on Structure

In light of the structure, there are four distinct groups for the minerals found in clay. The minerals in the 1:1 family are the first category, whose structure is made up of two octahedral and one tetrahedral sheet interacting (**Figure. I .9.a**). The tetrahedral sheet's atoms of oxygen and the octahedral sheet's groups of hydroxyls form a hydrogen bond, offers this structure a great deal of stability. Thus, a low basal distance of roughly 7 Å is obtained. We can list dickite, halloysite, kaolinite, and other clay minerals as examples of this group.

Conversely, while two sheets that are tetrahedral encircle a sheet octahedral To form the elementary layer, (**Figure. I .9 .b**) identifies the 2:1 category. The interlayer space contains various elements that affect the distance at the base, which vary from nine to fifteen Å. The layer has a thickness of about 10 Å. The sheets that are T<octahedral and/or tetrahedral isomorphic substitutions show a negative charge in the elementary layer. The majority significant minerals within this group include vermiculites, illites, micas and smectites.

The final category is known as 2:1:1 and it consists of minerals with interstratification, which is a roughly regular arrangement in different kinds of sheets (**Figure. I .9 .c**). This arrangement is a particular instance of the 2:1 arrangement, with the exception that an octahedral layer occupies the interlayer space, giving rise to a basal space of roughly 14 Å. This category's sheet has a variable thickness. Among the inter-stratified, corrensite (chlorite-smectite), a regular inter-stratified, can be mentioned. In contrast, vermiculite-smectite, chlorite-chlorite, and kaolinite-smectite are part of the asymmetrical inter-layered clusters; allevardite and rectorite (illite-vermiculite) are not.

Table.I.2. Clay Mineral Classification [74].

Group	Mineral Clay	Type	Chemical Formula	CEC (meq/100 mg)	SSA (m ² /g)	Ref
Serpentine-Kaolinite	Kaolinite	1: 1	$Al_4Si_4O_{10}(OH)_8$	1-15	10-20	[47]
	Halloysite		$Al_2Si_2O_5(OH)_4 \cdot nH_2O$	5-10	-	[47]
	Nacrite		$Al_2SiO_5(OH)_4$	-	-	-
	Dickite		$Al_2SiO_5(OH)_4$	-	-	-
	Lizardite		$Mg_3(Si_2O_5)(OH)_4$	-	-	-
	Antigorite		$Mg_3(Si_2O_5)(OH)_4$	-	-	-
Talc	Talc	2: 1	$Mg_3Si_4O_{10}(OH)_2$	-	-	[47]
	Pyrophyllite		$Al_2Si_4O_{10}(OH)_2$	-	-	-
	Serpentine		$Mg_3Si_2O_5(OH)_4$	-	-	-
Smectite	Mmt	2: 1	$(Na, Ca)_{0.33}(Al, Mg)_2(Si_4O_{10})(OH)_2 \cdot nH_2O$	10-40	50-100	[47]
	Bentonite		$(Na, Ca)_{0.33}(Al, Mg)_2Si_4O_{10}(OH)_2 \cdot nH_2O$	-	-	[47]
	Beidellite		$H_2OAl_{1.67}(Fe^{2+}, Mg^{2+})$	-	-	[47]
	Nontronite		$Na_{0.3}Fe^{+++}2(Si, Al)_4O_{10}(OH)_2 \cdot n(H_2O)$	-	-	
	Saponite		$(Ca/2, Na)_{0.3}(Mg, Fe^{++})_3(Si, Al)_4O_{10}(OH)_2 \cdot 4(H_2O)$	86.6	-	-

	Hectorite		$(\text{Na}_{0.3}\text{Mg}_{2.7}\text{Li}_{0.3}\text{Si}_4\text{O}_{10}(\text{OH})_2)$	80-130	-	-
	Sauconite		$\text{Na}_{0.3}\text{Zn}_3\text{Si}_3\text{AlO}_{10}(\text{OH})_2 \cdot 4(\text{H}_2\text{O})$	-	-	-
Micas	Illite	2: 1	$(\text{K.H}_3\text{O}) \text{Al}_2(\text{Si}_3\text{Al}) \text{O}_{10}(\text{H}_2\text{O.OH})_2$	10-40	50-100	[47]
	Muscovite		$\text{KAl}_2(\text{Si}_3\text{Al}) \text{O}_{10}(\text{OH})_2$	Up to 5	-	[47]
	Phengite		$\text{K}(\text{AlMg})_2(\text{OH})_2(\text{SiAl})_4\text{O}_{10}$	-	-	-
	Biote		$\text{KMg}_3(\text{Si})_3\text{O}_{10}(\text{OH})_2$	Up to 5	-	-
	Phlogopite		$\text{KMg}_3(\text{AlSi}_3\text{O}_{10}) (\text{OH})_2$	-	-	-
Chlorite	Chlorite Diocta	2: 1 :1	$\text{Al}_4(\text{Si}, \text{Al})_4\text{O}_{10}(\text{OH})_8$	10-40	10-20	[47]
	Chlorite Triocta		$(\text{Mg}, \text{Fe})_6(\text{Si}, \text{Al})_4\text{O}_{10}(\text{OH})_8$	10-40	10-20	-
Vermiculite			$(\text{Al.Fe. Mg})_2(\text{Si}, \text{Al})_4\text{O}_{10}(\text{OH})_2$	100-150	10-800	[47]
Fibrous Minerals	Palygorskit e	2: 1 :1	$((\text{Mg. Al})_5(\text{Si. Al})_8\text{O}_{20}(\text{OH})_28\text{H}_2\text{O})$	5-30	150-900	[47]
	Sepiolite		$\text{Mg}_8(\text{H}_2\text{O}) (\text{Si}_6\text{O}_{15})_2(\text{OH})_48\text{H}_2\text{O}$	10-45	150-900	[47]

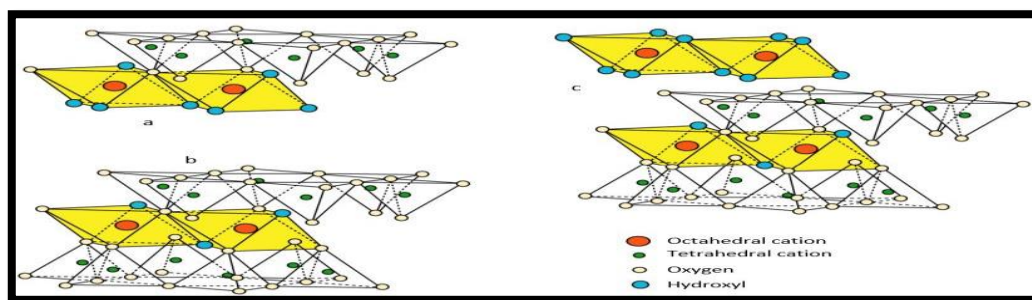


Figure. I .9. Clay Mineral Types, (a,b,c) [75].

1.3.3.2. Categorization based on Color

The existence of specific ions (Mg, Fe), this includes little quantities, affects the minerals in clay that determine their color. There are clays that are yellow, blue, red, pink, white, green and so on. With each hue, the clay mineral can be valued for use in more specialized applications. [76]. The white clays are the most widely used. (Free of any coloring agents, including smectites and kaolinite), the clays that are green (low iron oxide content minerals, like montmorillonite and illites and smectites), regarding the red clays that are abundant in iron oxides, these are typically iron oxides. Other minerals with high iron oxide and magnesium content turn yellow [77, 78].

1.3.4. Methods of Modification of Clay Minerals

Modification can enhance clay minerals' surface area, thereby boosting adsorption capabilities [79]. Clay minerals' chemical composition varies with origin, impacting the capacity for cation exchange and layer charge, morphology, and adsorption. These elements are crucial for modifying natural clay [80].

The term "activation" describes the physical and chemical processes used to increase clays' adsorption capabilities. [81]. There are several ways to change the minerals found in clay, such as heat treatment, bases, salts, and acid activation, pillaring by various polyhydroxy cations, grafting organic compounds, and modified clay - polymer [82].

1.3.4.1. Pillared Clays

Pillared clays (PILC), also called pillared interlayered clays or layered materials, undergo a process known as pillaring to enhance Clay minerals' mechanical and thermal stability, porosity, a specific section of the surface, and the catalyst's activity [83]. Several pillaring agents are used in the pillaring process, including metal hydroxo complexes, metal cluster complexes, metal chelates, and positively charged colloids [84]. This approach has gained traction recently for boosting the clay's mineral

adsorption capacity in wastewater treatment. Numerous studies explore the application of PILCs in the treatment of wastewater [85, 86].

1.3.4.2. Organoclays

Organoclays are a clay mineral pre-treatment step to create clay- polymer nanocomposites. Clay that is natural has no capacity for reaction with hydrophilous polymers [87]. Accordingly, to convert naturally hydrophilic clay into an organophilic surface, polymers are intercalated. Generally speaking, tertiary, quaternary, secondary and primary alkylphosphonium and alkylammonium cations are the primary the surfactants used in this Procedure for polymer combination [88]. Surfactants are non-polar and polar organic compounds that fall into the cationic group, nonionic and anionic surfactants according to their behavior in water. Surfactants that are nonionic provide greater chemical stability than cationic ones, while, anionic surfactants are more cost-effective but are rarely employed in clay modification [89]. The most widely used surfactants that are cationic for example CTAB, ODTMA, DMHDA ,TMAB, HTBPB, HTPB and TPB have been extensively employed as the clay modification using agents because of their charge that is positive [90]. Anionic in nature a surfactant has been used recently by certain scientists to modify clay. [91, 92].

1.3.4.3. Thermal Activation

The study of thermal treatment was initiated in 1951[93]. Clay undergoes a physical process called thermal activation. which includes heating clay to a high temperature [94], and also thermal modifying based on changing clay structures micro and macro characteristics has been carried out. Heating the clay could alter its size, shape, amorphization of its porosity, and crystallization[95, 96]. Furthermore, Different clays undergo different changes in structure and composition when heated, which are mostly dependent on the heating regime and particle size [97]. An essential factor in the composition and structure of minerals found in clay is the heat schedule. The thermal activation occurs in three different temperature ranges: At first, during the stage of dehydration, the contaminants affixed to the clay particles are eliminated,

along with the adsorbed and hydrated water. The clay particles lose weight consequently; their surface area has increased and opening up more adsorption sites. [98]. Further heating and dihydroxylation are equivalent. The clay's structure and surface functional groups are changed if heating is prolonged past dihydroxylation. The bonds within the clay structure break, causing the structure to collapse and the surface area to decrease [99, 100]. The textile industry makes extensive use of thermally activated clays, to eliminate color and other contaminants, the sugar and oil industries.

1.3.4.4. Acid Activation

In line with Lamar's 1951 definition [101] as well as Gregg's 1958 definition [102], Clays can be made more adsorbent by a chemical or physical process called activation. The acid-active clays are made of clay that has been heated to a high temperature and treated with inorganic acids [103]. Usually, H_2SO_4 or HCl treatment is used to activate the clay's acid. The physical characteristics, like porosity and surface area, have improved as a consequence of the activation of acid, and chemical characteristics like acidity and CEC, consequently producing the desired qualities needed for an efficient adsorbent [104].

Numerous researchers have examined how acid concentration affects, temperature and contact time on clay structural modification [105]. By contrast, acids that are organic (including sulfonic and carboxylic acids) can offer a different, less harmful method of altering clay minerals. That being said, lately, Combining modifications with various functional groups is an intriguing way to lessen acid activation's harmful effects, additionally to strengthen interface properties for a variety of pollutant removal [106].

1.3.5. Clay with Polymer Modification

By adding polymers to the interlayer spaces of clay minerals for physical adsorption, clays can improve their adsorption properties ion exchange, or chemical grafting [107]. Clay that has been modified with polymers frequently uses polyacrylamide. Other polymers, including polypropylene, polyesters, chitosan, epoxy, polyurethanes, poly-styrene and cellulose, have also been utilized recently to prepare clay- polymer nanocomposite materials [108]. The physical and chemical properties of the individual clay , polymer constituents can be enhanced by the clay - polymer nanocomposite [109]. In order to create clay mineral natural polymer nanocomposites, clay mineral modification has become a cutting-edge method of treating water that is contaminated[110]. By encasing clay and maghemite nanoparticles in cross-linked chitosan, magnetic chitosan/clay particles were created, offering greater water treatment efficacy than single-modified clay[111].

1.4 Cellulose (Biopolymers)

Natural materials have been abundantly supplied by nature, and the scientific community is highly interested in biobased natural polymers due to their potential applications. But the majority of these affordable and environmentally friendly biomaterials are left unused, typically allowed to break down naturally or through artificial means, resulting in the problems associated with environmental pollution [112].

The biomass of agricultural waste includes cellulose, lignin, proteins, hemicellulose, oils, waxes, and starch, among other materials. containing active functional groups such as ether, carbonyl, carboxylic acids, phenols, and alcohols [113]. Because of the existence of dynamic groups of functions, the biomaterials in question are modifiable for more effective and varied low-cost uses. Cellulose is a widely used biopolymer among the various components of biomaterials, used to make paper, cardboard,

fabrics, and cellophane membranes, binders, adhesives, other products that dissolve in water. Apart from these typical conventional uses, additionally, this biopolymer is able to use directly, grafted and modified to absorb a variety of ions of heavy metals. [114], the sorption of hazardous, toxic dye into the water.

The French chemist Anselme Payen discovered cellulose as the main element found in plant wall cells in 1838. Actually, it's primarily isolated from higher plants, but it is also isolated from marine animals and plants like tunicates and algae, and sources that are bacterial (like *Acetobacter xylinum*)[115].

The biopolymer that is producing the most frequently on Earth is cellulose. All plant cells have it in their cell walls. The cell walls of other species, such as bacteria and algae, also contain cellulose. Cotton has a cellulose content of about 98%, making it the purest form of the material. Moreover, wood that is harvested from trees also contains cellulose. Even though animal cells lack a cell wall, certain animal species do contain cellulose. It can be found in the shells of tunicates, which are marine invertebrate organisms[116].

1.4.1 Lignocellulosic material

Lignocellulosic material consists of three main components: hemicelluloses, lignin and cellulose. It represents the vast majority of biomass. On average, lignocellulosic material contains approximately twenty to forty percent hemicellulose, between ten and twenty lignin, and forty to sixty percent cellulose. It is estimated that the quantity of biomass synthesized each year is of the order of 300 billion-tonnes. The plant walls are made up of cellulose fibers whose network is inserted into a hemicellulosic matrix. Lignin serves as a cement between cellulose and hemicelluloses, giving strength to the plant wall. Cellulose is therefore intimately linked to the two other constituents of lignocellulosic biomass[117].

1.4.1.1. Structure and Characteristics of Lignin and Lignocellulosic Fibers

The globe's largest a renewable bioresource's source is fibers made of lignocellulosic material. Materials lignocellulosic usually consist of 35 to 55 percentage of cellulose by weight, Weight percentage of lignin: 10 to 25, and between 20 and 40 weight percent hemicellulose, together with extracts (for example, pectin, waxes, and resins.), minerals, and ash. In certain biomasses that are lignocellulosic, Table 1 displays the hemicellulose, cellulose and lignin contents[118].

1.4.1.2. Some lignocellulosic fibers' chemical makeup

Plant cell walls are primarily made up of lignocellulosic fibers and are made of hemicellulose, cellulose and lignin. The exact composition can vary depending on the plant source. In addition to these primary components, lignocellulosic fibers may also contain other minor constituents, including pectins, proteins, and ash, depending on the plant source and the degree of processing[119].

The makeup of lignocellulosic fibers can differ dramatically based on the plant species. Each source has its own unique composition, which can impact their suitability for various applications such as papermaking, biofuel production, and the manufacture of composite materials.

Table .I.3.Some lignocellulosic fibers' chemical makeup[120].

The fiber	Hemicellulose percentage (wt %)	Cellulose percentage (wt %)	Lignin percentage (wt %)	
Bamboo	30.0		26-43	21.0-31.0
Bagasse	16.8		55.2	25.3
Corn stalk	23.6		42.7	17.5
Birch branches	23.4		33	20.8

Kenaf	20.3	72.0	9.0
Flax	18.6-20.6	71.0	2.2
Jute	21-24	41-48.0	18.0-22.0
Hemp	15.0	68.0	10.0
Rice rusk	19.0-25.0	35.0-45.0	20.0
Wheat straw	15.0-31.0	38.0-45.0	12.0-20.0
Pine branches	32	32	21.5
Oil palm	-	65.0	29.0
Spruce branches	30	29	22.8
Sisal	12.0	65.0	9.9
Switchgrass	27.0	34.0	17.0

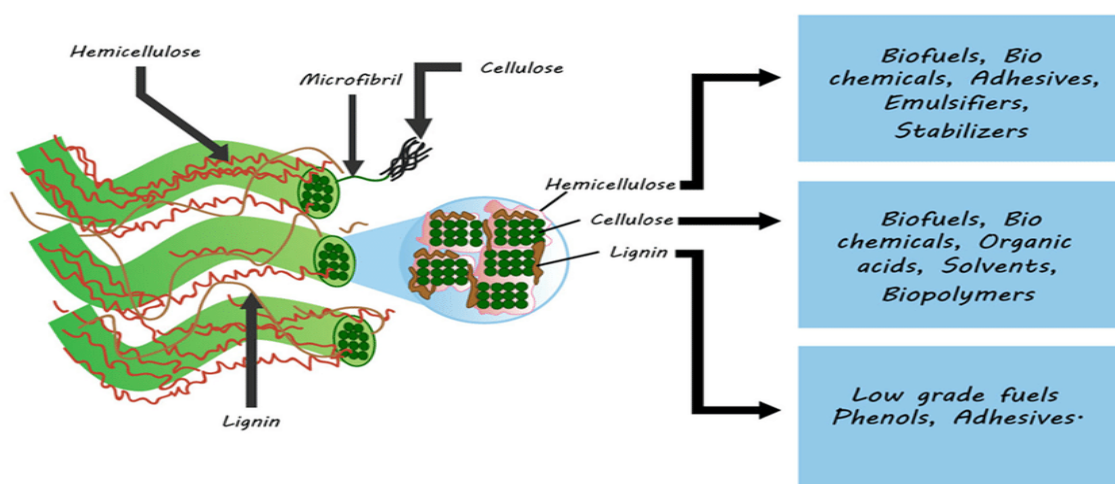


Figure. I. 10. Lignocellulose fiber components[121].

I.4.2. Cellulose

One organic material that is a member of the polysaccharide class is cellulose. Comprising glucose subunits, it is a polymer. Richly distributed in bacteria and plants both have cell walls; it can be found there. Plant strength and structure are significantly influenced by cellulose. In the industry, it is likewise highly valued[122].

Cellulose, with the chemical formula $C_6H_{10}O_5$, is the most prevalent organic substance on the planet. A complex carbohydrate made up of hydrogen, carbon, and oxygen is

called cellulose. It has no smell, is tasteless, and is chiral. In 1838, Anselme Payen, a French scientist, made the initial discovery of cellulose. This organic substance is biodegradable and soluble in water. It was employed in 1890 to create celluloid, the first thermoplastic. Ninety percent of cotton contains cellulose. 40–45% of the cellulose in wood and 57% of the cellulose in dry hemp, respectively.

A biopolymer that is linear, cellulose is made up of 7000–15,000 monomers of D-glucose joined by 1,4-glycosidic links. Hydrogen bonds within the microfibrils and van der Waals forces between cellulose chains. Microfibril arrangements vary between the various cell walls. To create cellulose fiber, microfibrils are merged. Crystallinity is one way that crystalline cellulose manifests itself [123]. The polymerization degree of cellulose ranges between fifteen hundred and five thousand, which makes it more crystalline. Additionally, disorganized and amorphous cellulose produces only a minimal amount. Compared to amorphous cellulose, the resistance of crystalline cellulose to enzyme degradation is higher.

1.4.2.1. Structure of Cellulose

Two thousand D-glucose subunits make up one gram of cellulose. Glycosidic linkages ranging from beta 1 through 4 relate glucose subunits within cellulose. In cellulose, glucose molecules are oriented in the opposite direction than in other polysaccharides. The hydroxyl group of the anomeric carbon, or carbon number one, is oriented above the plane of the glucose ring in their beta orientation.

In cellulose, glucose molecules are oriented in the opposite direction than in other polysaccharides. For the anomeric carbon, the group hydroxyl is used, or the first carbon, is oriented above the glucose ring's plane in their beta orientation. Below the ring plane are the carbon atoms' remaining hydroxyl groups. In cellulose, each alternating glucose molecule is reversed to form beta 1-4 glycosidic linkages. Carbon 1's hydroxyl group points upward, while carbon 4's is pointing downward. Now; one of these molecules needs to be inverted such that both hydroxyl groups are in the same

plane in order to form a Glycosidic beta 1-4 bond. This explains why each alternative in cellulose, the glucose molecule is flipped.

The molecule cellulose is unbranched. Glucose polymeric chains are organized in a linear fashion. These chains don't coil, form helices, or branch like those found in starch or glycogen. Instead, these chains are set up in a parallel fashion. These chains are tightly held together by hydrogen atoms and hydroxyl groups, which establish hydrogen bonds between them. Firm and robust cellulose microfibrils are formed as a result of this. Plant cells include microfibrils, which are composed of cellulose. A polysaccharide or cellulose matrix is created by these microfibrils working together. Later in this article, we will go over more specifics regarding the polysaccharide matrix[124].

The chains of cellulose are exported from the cell. And inside the cellular wall throughout the synthesis process, as we previously studied. This is where the hydrogen bonds between the parallel cellulose strands are formed. Cellulose microfibrils are produced because of this. When these cellulose microfibrils combine with other sugar molecules, a polysaccharide matrix is created. Arabinoxylans and Glucans are the principal constituents of the matrix of polysaccharides found in plants' principal cell walls.

The cellulose microfibrils are connected to one another by these polysaccharides through their interactions. The creation of cross-links fortifies this network. When residues of arabinoxylan interact with acids such as the two types of ferulic acid are DFA and FA, these cross-links are created. This leads to the additional claim that acidic polysaccharides comprise the polysaccharide matrix. Cross-linking polysaccharides are present in the main cell wall besides the polysaccharide matrix and microfibrils of cellulose. A complex network is formed by the cross-linking of cellulose microfibrils by these polysaccharides. Among these polysaccharides that cross-link, hemicellulose is the most significant.

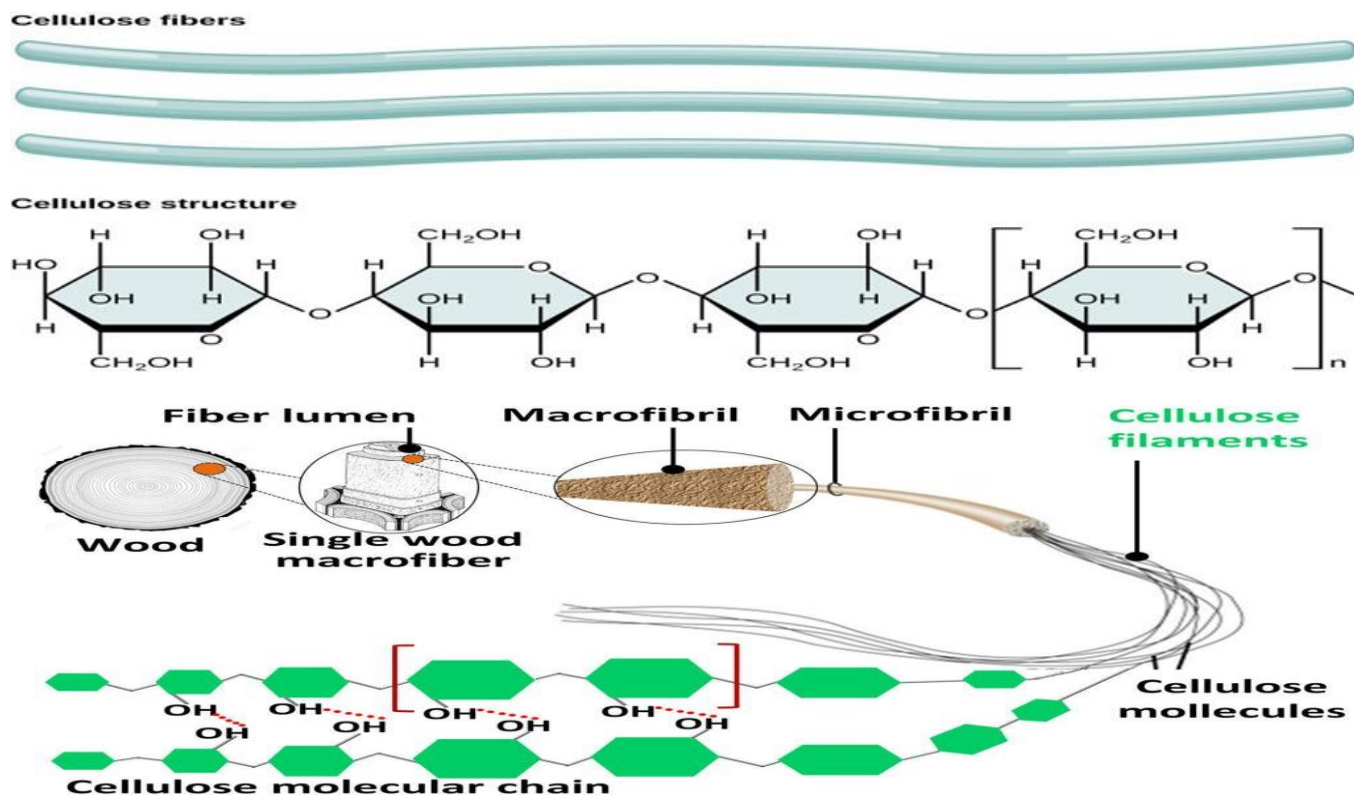


Figure.I.11. Cellulose structure[125].

I.4.2.2. Properties of cellulose

The characteristics of cellulose set it apart from the other polysaccharides. Its distinct structure gives cellulose its special qualities. Additionally, they depend upon the quantity of subunits of glucose cellulose contains. It possesses the subsequent qualities[126]:

- ✓ The most prevalent type of carbohydrates found in nature is cellulose.
- ✓ In water, it does not dissolve.
- ✓ Cellulose is a crystalline solid that resembles white powder.

- ✓ Because the individual chains of cellulose microfibrils are held together by strong hydrogen bonds, its tensile strength is quite high. Steel and cellulose microfibrils have comparable tensile strengths.
- ✓ The exceptional tensile power of cellulose is also a result of the glucose molecules' alternative configuration.
- ✓ In organic solvents, it is soluble.

1.4.3 Hemicellulose

Hemicellulose, which consists primarily of d-mannose, d-glucose, l-arabinose, d-galactose, and d-xylose, is a polymer of meaningless and hexoses that is amorphous and heterogeneously branched. With 500–3000 added sugar monomers. The primary bonds between sugars are -1,4- and sometimes -1, 3-glycosidic bonds. The figure illustrates the typical hemicellulose structure.

Compared to cellulose, hemicellulose has a reduced molecular mass between 50 and 200 degrees of polymerization, hemicellulose is easily hydrolysable and amorphous. Hemicellulose does not agglomerate when co-crystallized with cellulose[127].

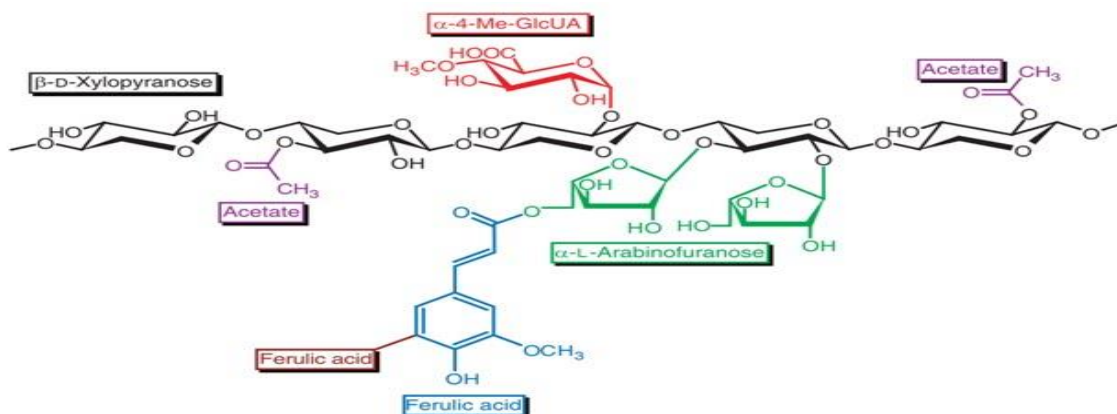


Figure. I .12. Hemicellulose structure[128].

I.4.4. Lignin

Since lignin has aromatic rings instead of lengthy molecular chains, it differs from cellulose and hemicellulose. Lignin has a variety of chemical structures that vary based on the kind of plant and the extraction method. The primary differences between the lignin fragments are their functional group, linkage type, and monomer content. The polyphenolic macromolecule known as Three phenylpropane monomeric units make up lignin: alcohol sinapyl (S), Alcohol p-hydroxyphenyl (H), alcohol coniferyl (G). Softwoods are dominated by the coniferyl alcohol structure.

Hardwood lignin frequently has both coniferyl and sinapyl alcohol structures, with the former being more prevalent than the latter. In contrast, lignin from grasses is primarily composed of p-hydroxyphenyl alcohol structures. Different lignin subunits form different kinds of both carbon-oxygen and carbon-carbon (Aryl-ether) bonds. The carbon-oxygen bonds from the p-hydroxy moiety to the propenyl group's -end (O-4) are the majority common type of linkages.

Lignin macromolecule is polarized by varying amounts of chemical groups, including methoxyl, hydroxyl, carbonyl, carboxyl, and others, in its structure. Phenolic groups are the most common chemical groups or hydroxyl groups aliphatic [129].

The most common type of lignin is resistant substance within lignocellulosic fibers, making it highly resistant to both chemical and enzyme effects. With the exception of alkalis. Acids, hot water and other solvents do not cause lignin to dissolve.

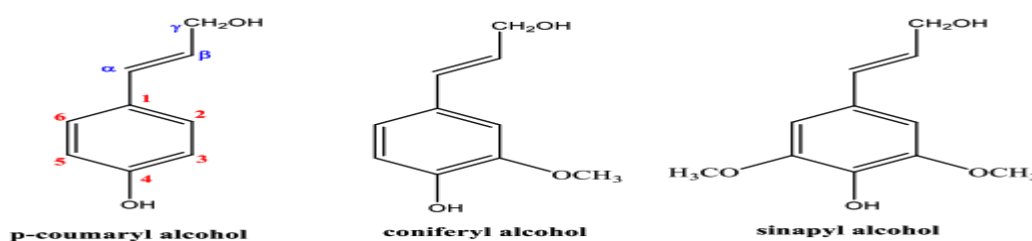


Figure.I.13. Lignin structure[130].

I.5 Methods of optimization

Instruments like as experiment design and optimization are utilized to methodically investigate the range of potential problems. Therefore it is apparent that if trials are carried out at random, the outcomes will also be selected at random.

As a result, the trials must be set up to ensure that interesting data is collected. .

See how the experiments are optimized and designed in the following section to give the researcher the necessary theoretical framework and practical tools for the actual experimental environment.

1.5.1. Experimental design

A set of procedures known as experimental design is used to gather, statistically evaluate, and draw conclusions from data or information that can be applied generally. With the goal of minimizing experimental error, these experiments enable the application of statistical methods in scientific research and the use of available resources to build the most suitable experimental designs on a solid scientific basis . Estimating and minimizing experimental error as well as carrying out the essential tests and estimations needed for research are the main goals of experimental design. We used Design-Expert 13 software for the design, analysis, and modeling of our experiments.

This branch of science includes new and unfamiliar terms, which is why we decided to present them for general benefit [131]:

- a. Design: Design refers to the research plan or framework that outlines how a specific experiment will be conducted. It involves defining the experimental parameters, conditions, and objectives with the aim of collecting data that can be analyzed to reach a specific conclusion.
- b. Unit of sampling: The subject of an experiment's measurement the sampling unit, as it is known. From the experimental unit, this might differ.
- c. Analysis: Analysis involves the process of collecting, organizing, and summarizing data obtained from the experiment. It also includes the

application of specific statistical tests to make informed decisions about the research objectives set for the experiment.

- d. Experiment: An experiment is a systematic procedure or method used to test a hypothesis and reveal relationships between variables. It is a controlled process designed to generate empirical data and draw conclusions based on observations.
- e. Treatments: Treatments are the specific conditions or parameters applied to experimental units as part of the experiment. These treatments are designed to achieve certain levels or outcomes, and they are typically applied in a controlled and randomized manner.
- f. Factor or Variable Level: In experimental design, factors or variables often have multiple levels or settings. These levels represent the range or field of change in the factor's coefficient. They are typically defined as two extremes, often symbolized as (-1) and (+1), to aid in determining the factor's impact about the variable of response.

The (RSM) is among the most significant techniques employed in this field[132].

1.5.2. Response Surface Methodology

A collection of statistical methods known as RSM, or response surface methodology, mathematical methods useful Created in the year 1950 to ascertain the best operating conditions for chemical industry applications. The RSM is a specialized type of experimental design commonly used for modeling and optimizing complex systems. It is particularly useful when you want to understand The link between multiple input factors as well as any output replies (usually quality or performance metrics) in a systematic way and efficient [133].

1.5.2.1. Principle of RSM

The RSM based on designing different experiments, where the values of different variables are systematically and systematically changed in each experiment, and the

response is measured each time. After collecting the data, it is examined through a variety of statistical methods, random regression and regression analyses, for example. These techniques estimate The relation between the response and the variables and figure out the ideal values for the variables that lead to the intended response [134].

I.5.2.2. Phases of modeling with the RSM

a. RSM experimental layout

To obtain excellent experimental planning, it is desirable to lessen the quantity of experiments in the same proportion as possible to reduce the computing needs, delays and costs of the experiment, which allows for the reduction of the variance of the parameters of the mathematical model used, which will make the obtained response surfaces more accurate. We must determine the most appropriate experimental design to obtain the desired experiences. The layouts used in the RSM study are quadratic layouts like Central Composite Design or Box-Behnken Design [135].

b. RSM modeling

RSM is primarily applied in scenarios where a process's quality characteristic or performance measure can be affected by a number of input variables. In this context, we refer to measure of performance or quality characteristic as the "response." It's common to refer to the input variables as "independent variables," and scientists or engineers have the authority to control them [136].

$$Y = f_{\beta}(X_1, X_2, \dots, X_k) \quad (\text{I.12})$$

Because the actual response's format function f_{β} it is unidentified, we have to estimate it. Utilizing RSM successfully depends on the experimenter's aptitude to create an appropriate f_{β} approximation.

Typically, In RSM, two key models are frequently employed. These represent exceptional instances of models (1.12) and include the **first-order model**.

$$Y = \sum_{i=1}^k \beta_i X_i + \beta_0 + \varepsilon \quad (\text{I.13})$$

And the model of second order which is extensively employed in RSM

$$Y = \sum_{i=1}^k \beta_i X_i + \sum_{i=1}^k \sum_{j=1}^k \beta_{ij} X_i X_j + \sum_{i=1}^k \beta_{ii} X_i^2 + \beta_0 + \varepsilon \quad (\text{I.14})$$

which: Y is the optimization goal of the predicted response, k represents the number of factors, i and j represent variable index numbers, β_0 coefficient constant, β_i coefficient - linear, β_{ii} coefficient square, β_{ij} interaction represents random error, x_j and x_i represents the process variable Y (-1,0, +1) response. An equation with a positive sign indicates that the variables work together; on the contrary, an antagonistic relationship between the variables is indicated by a negative sign.

The quantity of testing was computed in the manner described below:

$$N = k + c_p + k^2 \quad (\text{I.15})$$

In this case, c_p represents the central point's replicate number [137].

c. Variance Analysis

ANOVA, or variance analysis, is a statistical method employed to assess the impact of various factors on the variability observed in a particular variable of response. Regarding the analysis of regression, ANOVA serves the principle of analysis of variance to partition the total variance into a factor component that relates to the regression equation or model used and the component. The remaining factor components are represented mathematically by mean squares, i.e. variances. The advantage of variance analysis is the ability to assess the impact of variables on variations in a specific response [138].

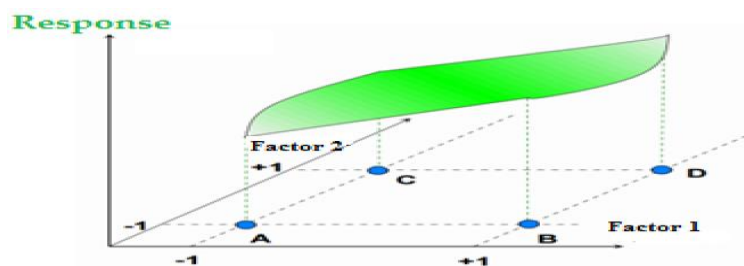


Figure. I.14. Response surface model plot[139].

1.5.3. Types of designs

Response Surface Methodology (RSM) employs various experimental designs to efficiently explore the connections between variables that are independent and the response variable. The design choice based on variables like the quantity of variables that are independent, the expected nature of the response surface, and the available research resources. Each design has its strengths and limitations, and selecting the most appropriate one is crucial for the success of an RSM study[140]. Some common types of designs used in RSM include:

1.5.3.1. Creating a Central Composite

The Central Composite's (CCD) Design is a significant and widely used experimental design in RSM. Box and Wilson introduced it in 1951, and it has since undergone various modifications and adaptations due to its versatility and effectiveness in building response surface of the second order models. This combines factorial, axial, and centre points to make a design that works well for fitting response surface models of second order. It allows for both estimating variables' quadratic and linear effects and evaluating the curvature of the response surface [141].

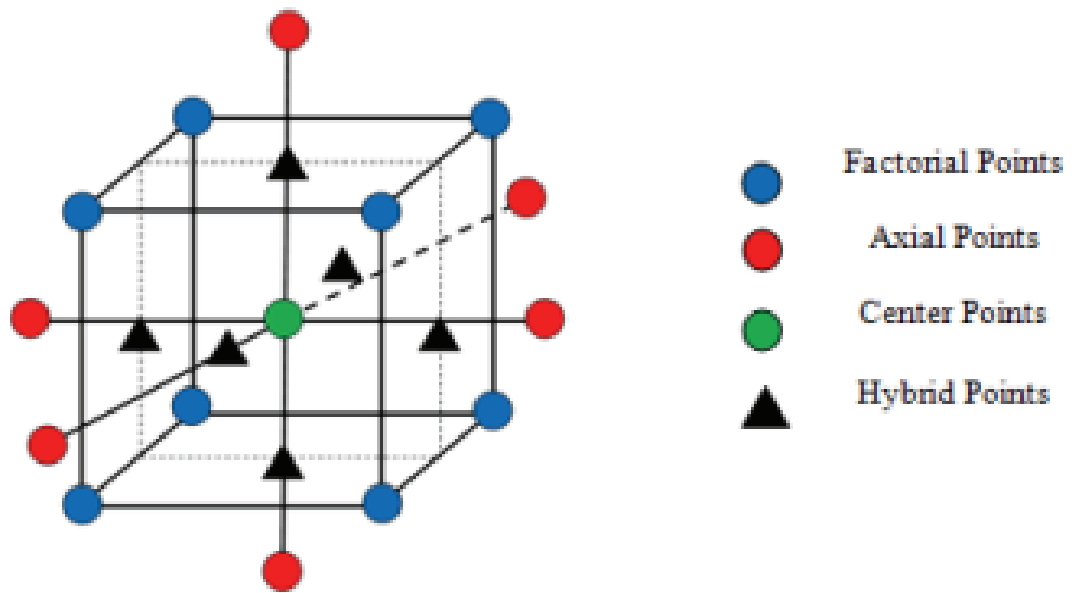


Figure. I.15. Central Composite Design augmented with hybrid points[142].

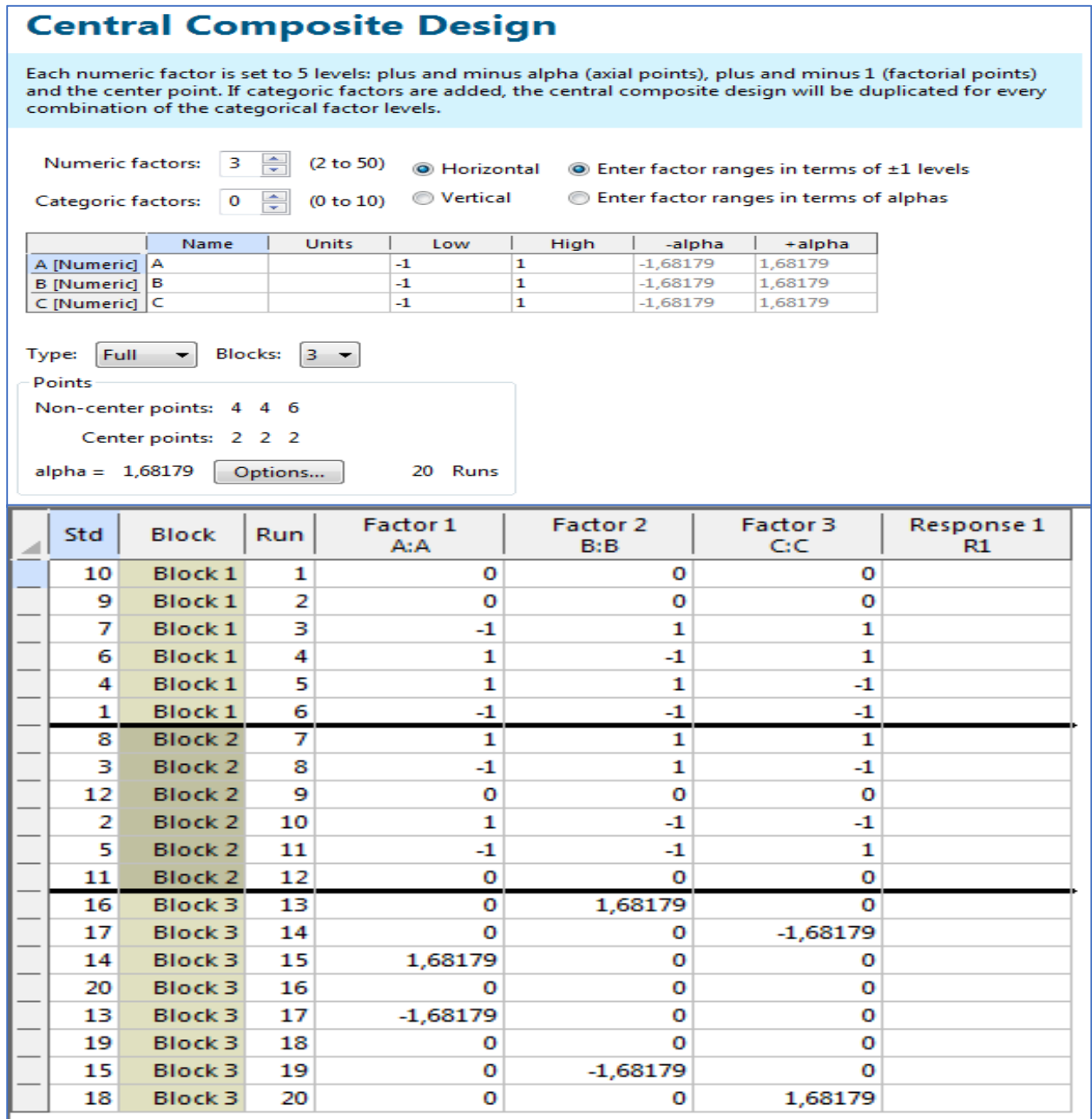


Figure . I.16 Composite Design provided by (Design-Expert 13)

I.5.3.2. Box-Behnken Design (BBD):

This arrangement is useful when the factors are moderate, as suggested by Dringroswick in 1980. Box and Behnken developed a standard model for handling multiple responses with a desirability function (D). This model provides for each variable three possible values (+1, 0, -1) with equal intervals; its purpose is to minimize the number of trials allowing approximation of quadratic and linear effects. It contains the set of points within the hypercube, excluding the center.

This model is valuable and practical, especially in general chemistry and improving chromatographic conditions [143]. The advantages of the design are that it covers a significant experimental area with experimental points (fewer trials) compared to (full factorial design), and this is because it does not include points in the corners and centers. The faces of the outer faces of the cube are similar to the structure of the central compound, but it differs from it in other features and does not have extended crossing points, so three-plane factors are used. This design allows researchers to better understand the perturbations or effects that allow the model to be built. This is the model we rely on in this study [144].

Box-Behnken Design

Each numeric factor is set to 3 levels. If categoric factors are added, the Box-Behnken design will be duplicated for every combination of the categoric factor levels. These designs have fewer runs than 3-Level Factorials.

Numeric factors: (3 to 21) Horizontal

Categoric factors: (0 to 10) Vertical

	Name	Units	Low	High
A [Numeric]	A		-1	1
B [Numeric]	B		-1	1
C [Numeric]	C		-1	1

Blocks:

Center points per block: (0 to 1000) 15 Runs

Figure.I.17.Box-BehnkenDesign for three variables by (Design-Expert 13).

BBD and CCD respectively in RSM are employed to optimize processes also understand factor-response relationships. Here's a comparison[145]:

- **Number of Experimental Runs:** BBD needs fewer runs and is cost-effective with limited resources. CCD demands more runs, potentially resource-intensive.
- **Design Space Coverage:** BBD efficiently explores but lacks the centre point. CCD assesses comprehensively, including centre and pivot points.
- **Levels of Factors:** BBD uses three levels ($\pm 1, 0$) for simpler models. CCD accommodates more levels, aiding detailed factor analysis.
- **Point Arrangement:** BBD simplifies with a hypercube arrangement. CCD includes axial and centre points for interactions.
- **Resource Efficiency:** BBD conserves resources, ideal for budget constraints. CCD is resource-intensive, offering in-depth understanding.
- **Model Complexity:** BBD suits simpler models (linear, quadratic). CCD handles complexity, capturing higher-order interactions.
- **Application Areas:** BBD is common in chemistry, moderate factor studies. CCD spans various fields and diverse designs.

Available Response Surface Designs (with Number of Runs)

Design		Factors								
		2	3	4	5	6	7	8	9	10
Central Composite full	unblocked	13	20	31	52	90	152			
	blocked	14	20	30	54	90	160			
Central Composite half	unblocked				32	53	88	154		
	blocked				33	54	90	160		
Central composite quarter	unblocked							90	156	
	blocked							90	160	
Central Composite eighth	unblocked									158
	blocked									160
Box-Behnken	unblocked		15	27	46	54	62		130	170
	blocked			27	46	54	62		130	170

Figure .I.18. Box-Behnken Design for three variables by (Design-Expert 13).

The BBD is a popular experimental design used in RSM for optimizing processes and studying the relationships between factors and responses. Like any design, it has its own set of advantages and disadvantages[146]:

a. Advantages of Box-Behnken Design (BBD):

- ***Efficiency in Number of Experimental Runs:*** BBD requires fewer experimental runs than a complete factorial design or other designs like CCD. This makes it cost-effective and time-efficient, especially when resources are limited.
- ***Exploration of Second-Order Effects:*** BBD is well suited for estimating linear and quadratic effects of factors. It offers important details regarding the response surface's curvature, allowing for the modelling of second-order relationships.
- ***Simplicity:*** BBD is relatively straightforward to set up and execute. It involves fewer experimental runs than other designs, simplifying data collection and analysis.
- ***Space-Filling Design:*** BBD covers a significant portion of the experimental space without including points at the corners and centre, providing a good balance between exploration and efficiency.
- ***Resource Conservation:*** When resources are limited, BBD can be a practical choice as it minimizes the number of experiments while yielding valuable insights into the surface of response.

b. Drawbacks of the BBD:

- ***Lack of Higher-Order Effects:*** BBD is not designed to capture higher-order effects beyond quadratic. If the response surface has significant higher-order interactions, BBD may not provide accurate models.
- ***Limited Factor Levels:*** BBD typically uses three levels for each factor, which may not be sufficient for some complex systems requiring more nuanced factor settings.
- ***Loss of Information:*** By excluding points at the corners and center of the design space, BBD sacrifices some information, which may be critical for certain applications.

- *Limited Applicability*: BBD is most effective when the number of factors is moderate and when the response is relatively well-behaved within the design space. In more complex scenarios, other designs like CCD may be more appropriate.

CHAPTER II
METHODOLOGY

II.1. Introduction

The three primary laboratories where all of the experiments for this research project were carried out were University of Ouargla's Laboratory of Pollution and Waste Treatment, Scientific and Technical Research Center in Physico-chemical Analysis (CRAPC) Ouargla, The University of Mersin's (Turkey) Department of Environmental Engineering laboratory.

There are four main sections of this chapter, that the following can be used to summarize. The initial step involves pretreating the raw clay (the source of the raw kaolinite) from Aougrout, Adrar, Southwest Algeria, in order to separate cellulose from red bean peels (RBPS), the RBPs were purchased from a nearby farm in El-Oued Southeast Algeria. The production of the biocomposites, which are based on Kaol-Cel-25 and Kaol-Cel-50, is shown in the second section. First, we used eight Different dyes cationic and anionic (Basic Red 18, Safranin O, Rhodamine B, Reactive Orange 16, Reactive Red 180, Acid Red18, Crystal Violet, Methyl Orange) to select high-performance dyes to continue with them for the rest of the study using Kaolinite clay .After the we use the Kaol/Cel Composite for removing contaminants from water bodies, such as synthetic dyes like crystal violet (CV) and the anionic dye methyl orange (MO). About the third section, it briefly explains the instruments: The techniques used in this work include pH_{pzc} , potentiometric titration, BET, FTIR, XRD, SEM, and others. The fourth section provides an illustration of how to use the Box Behnken design to find the ideal adsorption operation parameters.

II.2 Chemical Solvents and Materials Used

Analytical reagent (A.R.) grade chemicals were all that were used. Glassware was initially soaked in dilute HNO_3 (10 % v/v) and washed with distilled water before use. Hydrogen peroxide (H_2O_2) and Kompass provided high purity degree sodium hexametaphosphate (NaPO_3)₆. In deionized water, a stock solution of sodiumhexa-

metaphosphate (NaPO_3)₆ was made. 25% ammonia, HCl (hydrochloric acid), Thiourea $\text{SC}(\text{NH}_2)_2$, sodium hydroxide (NaOH), silver nitrate (AgNO_3), sodium acetate ($\text{C}_2\text{H}_3\text{NaO}_2$), sodium hypochlorite (NaOCl), and Aldrich supplied acetic acid (80%) of a high purity grade which was used without further purification. Similarly, Methyl orange, Crystal Violet, Basic Red 18, Safranin O, Rhodamine B, Reactive Orange 16, Reactive Red 180, Acid Red 18, and other supplies were bought from Sigma-Aldrich. Table (II.1) lists a few of these two dyes' distinctive qualities [147].

II.3 Sampling of Raw Clay

Aougrou District is a district of Timimoun Province where tertiary sedimentary rocks are exposed. Administratively speaking, Adrar serves as the provincial capital, Algeria's second-largest province. The commune is located near an oasis in the Algerian Sahara Desert's Touat region. Northeast of the Arder wilaya, at 28° 45' 0" North, 0° 15' 0" East, is where you will find Aougrou. Various clay sample beds were taken from the Aougrou quarry's face.

II.4. Pre-treatment of clay production

The technique used in this study to separate portions of the clay samples is a summary of multiple procedures previously used in other studies [148].

- ✓ To achieve particle sizes of less than 5 μm , preliminary pre-sieving was done on the raw clay using a cascade of sieves.
- ✓ Subsequently, it was coarsely ground into a powder and washed with 40 mL of 6% w/v H_2O_2 to eliminate any remaining organic substances.
- ✓ The final solution was then moved to an Erlenmeyer (1000 mL) and mixed with an 80 mL pH 4.8 buffer solution (16 g sodium acetate and 10 mL acetic acid).
- ✓ The final mixture was then put into a graduated tube and given a dispersible ingredient, sodium hexametaphosphate (NaPO_3)₆, and following a 7-hour and 45-minute decant period for the floating layer, ten centimeters below the

surface, the particles smaller than two meters were extracted. The purchased granules underwent centrifugation and repeated treatments with deionized water.

- ✓ Ultimately, one glass slide was used as the control and received no treatment, while the other slide was heated to a temperature of 105 °C for two hours in order to select the appropriate clay (Figure II.1).

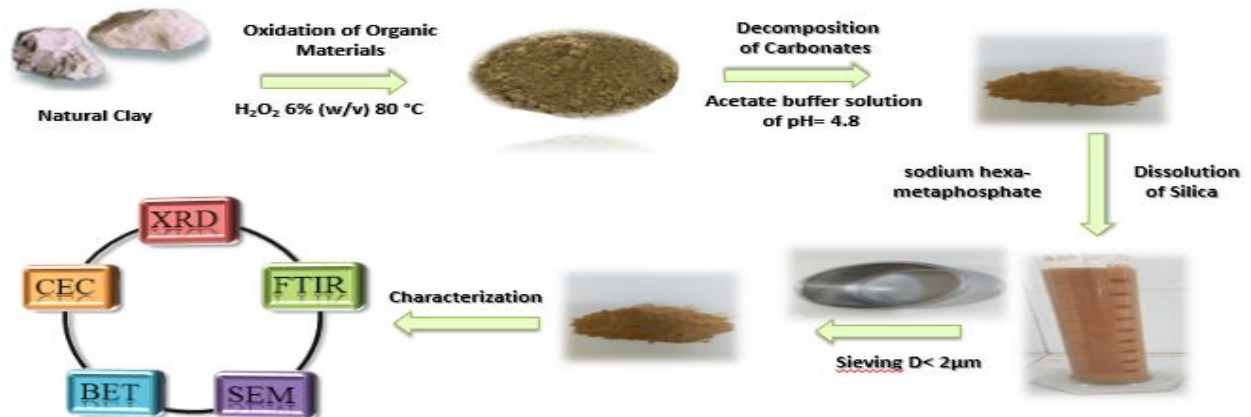


Figure II.1.Diagrammatic demonstration of preparation and analysis utilizing a clay sample.

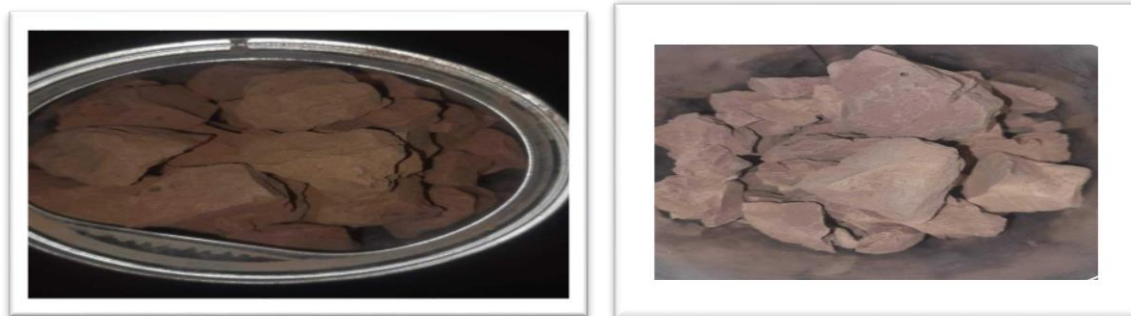


Figure II.2. Sample of raw clay.

II.5. Extracting Cellulose from Red Bean Peels (RBPs)

RBPs were bought from a neighboring farm in El-Oued, Southeast Algeria. To extract cellulose from the RBP powder, proceed as indicated in Figure II.3, The process, which has been discussed in several publications [149]. First, 100 g of dried RBP powder had to be simmered for 15 to 25 minutes in 3 L of hot, pH-balanced water

before being filtered. The resultant mass was repeatedly mixed with a 500 mL 1 M HCl solution and heated to 80–90 °C for 60 minutes in order to pretreat it with acid (HCl), After filtering, the residue was gathered. For the pretreatment of alkali (NaOH), There were three instances of the residue being stirred next for 60 minutes at 80–90 °C, the resulting filtrate was bleached twice using a 4% (w/v) NaOCl solution (at pH = 5 adjusted with 10% (v/v) CH₃COOH), providing cellulose with a white color. To bring the pH of the filtrate down, hot deionized water was used to rinse the cellulose several times. After being freeze-dried for seven hours, the cellulose was ground into a fine powder using a mixer grinder. Following that, it was kept for further study at room temperature [150].



Figure II.3.Diagram showing the steps involved in extracting cellulose from red bean peels.

II.6. Making the Kaol/Cel Composite

To make Kaol/Cel composite, the scientists adhered to a particular protocol[151]. First, 20 g of the pretreated kaolinite are dissolved in 200 mL of sulfuric acid (H₂SO₄) (15% W) in the beaker glass and the mixture is stirred for 4 hours at 80 °C.

The mixture of 10 g of activated kaolinite and 16 mL of 46% W NaOH in ice water was then shaken magnetically for six hours. The team added various ratios of Cel to the modified Kaol and then dissolved it in 0.6 M NaOH and 1 M thiourea solutions to optimize the process in accordance with BBD. After an intense four hours of stirring at 80 °C, the final mixture was oven-dried for an entire night at 60 °C.

II.7. Instrumentation

The physical characteristics of cellulose and clay have been ascertained through conventional techniques. The X-ray fluorescence measurement instrument (BTX-716) was utilized to determine the oxide content of different clays. Functional groups were the source. Using an infrared spectrophotometer, or Fourier transform, recognizable spectrophotometer, Cary 600 series), though the surface morphology was ascertained using scanning electron microscopy, additionally, we estimate the clay surface using BET. With multiple minerals subjected to XRD analysis. The compounds made for this investigation were characterized using a number of analytical techniques, which included the following:

II.7.1. Infrared spectroscopy using the Fourier Transform

Using an FTIR spectrometer (Spectrum RX I, Perkin-Elmer), The primary functional groups of the samples were identified, The mixture of the sample and potassium bromide was formed into a thin, transparent pellet, following milling and compression, respectively, using a hydraulic press and a mortar and pestle. Following that, it is put into the cell holder and put into the FTIR spectrophotometer for analysis.

II.7.2. Scanning Electron Microscopy

One of the most fascinating analytical techniques for capturing images of the compound's surface topography is scanning electron microscopy (SEM). A Polaron SC 515 sputter coater is used to apply a gold coating to the samples, the technique creates electrical conductivity in those samples by dispersing an electron beam within them.

This collision produces a large number of signals, which are then processed to create images.

It is important to mention that the samples were analyzed using an energy-dispersive X-ray analyzer and a scanning electron microscope (Hitachi, SEM-EDX, Tabletop Microscope, Japan, TM3030Plus).

II.7.3. X-Ray Diffraction

Making use of X-ray diffraction, it is possible to distinguish between phase and structural clay. The various crystalline phases were classified through the processing of XRD data. X'Pert-Pro's automated (PAN analytical), Diffractometer apparatus featuring a $\text{CuK}\alpha 1$ radiation source with a wavelength of 1.540598 \AA , at a step size angle of 0.02° , and a scan range from 5.053° to 120.046° , the X-ray, however, was produced at 20 mA and 30 kV.

II.7.4. Isotherm for the adsorption/desorption of nitrogen (BET)

The BET technique measures the total surface area inside or on top of micropores, macropores, mesopores, through the adsorption of flat surfaces and chemically inactive gases. The multi-point BET method was utilized to ascertain the specific surface area (SSA) of this unique clay. A thin layer of each of the resultant powders, weighing about 0.202 g, was applied to the bottom of a glass dish. For relative vapor pressures (P/P_0) of 0.29, nitrogen vapor adsorption data (77 K) were obtained. It was assumed that the cross-sectional area of a nitrogen molecule was 0.162 \AA^2 .

II.8. Zero-point charge

Jeon and Holl technique are one of the analysis methods that determines the type of surface charge of samples (positive, negative, or zero). About the mode of operation as follows: One hundred milliliters of NaCl solution (0.01N) were transferred into a sequence of conical flasks with pH values ranging

from two to twelve, following correction with an aqueous solution of 0.01 N HCl or 0.01 N NaOH using a pH metre (Metrohm, 827pH lab), the initial pH values were noted in this regard. After that, 100 mg of each adsorbent was combined with these solutions, and the mixture was stirred at 100 rpm for 24 hours in a shaker bath incubator to determine the final pH. Plotting ΔpH vs. pH revealed that the pH_{pzc} point is the point where the pH straight line and curve intersect.

II.9. Preliminary experiments of dyes with clay

Firstly, a pre-treatment study was carried out to determine which types of dyes the Kaolinite clay was effective on. Optimization studies were then carried out on the dye with the highest removal among eight different cationic and anionic dyes under the same adsorption conditions. In optimization studies, parameters such as pH, adsorbent dose, and temperature and contact time were carried out with experimental sets created with the help of RSM, and their effects on dye removal were evaluated for each parameter. After the adsorption procedure, we activated the Kaolinite clay to finally rescue it. First, we used eight Different dyes cationic and anionic (Basic Red 18, Safranin O, Rhodamine B, Reactive Orange 16, Reactive Red 180, Acid Red18, Crystal Violet, Methyl Orange) to select high-performance dyes to continue with them for the rest of the study. We conducted experiments on paint. Adsorption experiment sets were set up for each dye prepared at 25 ppm concentrations. In adsorption experiments, 1 g/L Kaolinite was added and mixed continuously on an orbital shaker at 250 rpm for 1 h contact time. Following the adsorption experiments, the influent and effluent concentrations of all after experiments were measured with a spectrophotometer and the removal efficiencies were calculated.

As a result of preliminary studies in adsorption experiments, higher removal efficiency was obtained for Kaolinite Crystal Violet and Methyl Orange dyes compared to the other dyes used in our study. Therefore; these two dyes were chosen for optimization experiments of adsorption conditions.

Table II.1: Percentage of dye removal by brown clay.

Dye	Dye Removal (%)
Basic Red 18	89.06
Safranin O	95.17
Rhodamine B	49.14
Reactive Orange 16	3.60
Reactive Red 180	1.94
Acid Red 18	6.29
Crystal Violet	98.01
Methyl orange	96.76

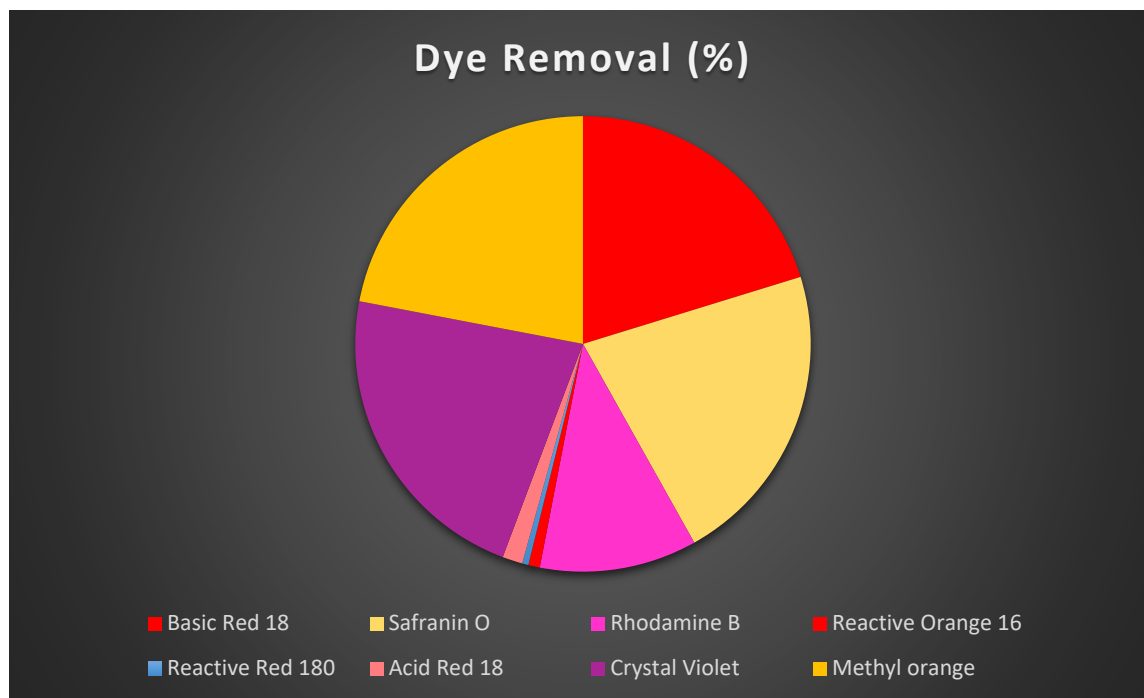


Figure II.4.Percentage of dye removal by Kaolinite clay.

II.10 Design Experiments on Kaol/Cel Composite (Crystal Violet and Methyl Orange dyes)

Process optimization can be achieved with BBD since it follows a quadratic surface. It was consequently incorporated into the experiment's general design. The BBD and statistical data were assessed using a program called Stat-Ease Design-Expert. 13.0 is the version. There was a second-order polynomial model employed, containing every square term, every linear term, and every interaction item that is linear by linear, the definition of the quadratic response model is as follows:

$$Y = \beta_0 + \sum_{i=1}^k \beta_i X_i + \sum_{i=1}^k \beta_{ii} X_i^2 + \sum_{i=1}^k \sum_{j=1}^k \beta_{ij} X_i X_j + \varepsilon \quad (\text{II.1})$$

When Y stands for the response optimization goal, whereas k indicates how many variables are being taken into account. To represent the variable numbers, utilize the indices j, and I the constant coefficient is denoted by β_0 , while the linear and quadratic coefficients are represented by β_i and β_{ii} , respectively. The interaction coefficient is

referred to as β_{ij} , and ε is a random error. The coded values for the independent factors (-1, 0 and +1) and the response of the removal of the MO and CV dyes are represented by the values X_i and X_j . Using Equation (II.1), When the variables are positive, it suggests that they work in concert, and when they are negative, it suggests that they work against each other[152].

A total of forty-six distinct tests were conducted in order to ascertain how the five primary independent factors will impact the removal of CV and MO. To determine the ideal parameters and specify the experimental domain, preliminary experiments were conducted. These investigations were centered around the following elements.

The injection of adsorbent (B), the pH (C), the residence time (D), the temperature (E), and the loading of Cel into Kaol (A). The codes for the different experimental levels of independent variables are listed in Table (II.3).

Table II.2. CV, MO independent factor experimental levels using Box-Behnken design codes.

	Levels		
	Low (-1)	Medium (0)	High (+1)
A : Loading (%)	0	25	50
B : Adsorbent dose (g)	0.02	0.035	0.05
C :pH	4	7	10
D : Temperature (°C)	30	45	60
E : Contact time (min)	5	17.5	30

The researchers looked at the coefficients using Analysis of Variance (ANOVA) to assess the model's precision. ANOVA yielded multiple parameters, such as the determination coefficient (R^2), F-value, and p-value. The adjusted determination coefficient (R^2_{adj}), the projected determination coefficient (R^2_{pred}), acceptable

standard deviation (SD), degree of freedom, and precision. These parameters were applied in order to assess the experimental data and model precision. A trustworthy second-order quadratic model equation was employed by the researchers to forecast the ideal value and explain how the elements interacted. We solved the regression equation to find the factors' optimal values, assessed the counter-response surface map and established restrictions for the different levels. In order to determine the extreme values of the variables, preliminary tests have been run.

II.11. Adsorption Studies in Batch on Kaol/Cel Composite (Crystal Violet and Methyl Orange dyes)

To find out how well Kaol/Cel can adsorb and remove MO and CV dye, using 100 mL of dye solution at concentrations of 50–300 mg/L and different volumes (0–50%) of the adsorbent, a BBD experiment was conducted. The experiments were conducted at different pH ranges (4–10) and temperatures (30–60 °C), with adjustments made using 0.1 N HCl and NaOH solutions at different times (5–120 min). Use of a Cary Series UV-vis spectrophotometer at $\lambda_{\max} = 590$ nm (CV dye) and $\lambda_{\max} = 465$ nm (MO dye) allowed for the determination of residual concentrations after the adsorption trials. After samples were spun for ten minutes at 3400 rpm. Equations (II.2) and (II.3) were used to determine the adsorption capacity of Kaol/Cel for the removal of MO and CV dyes (q_e ; mg/g) and the percentage of dye removal (R %). While the initial and equilibrium CV and MO dye concentrations are, respectively, C_e (mg/L), C_0 (mg/L), W is the weight of Kaol/Cel in grams (g), and V (L) is the volume of the dye solution.

$$R(\%) = \frac{C_0 - C_e}{C_0} * 100 \quad (\text{II. 2})$$

$$q_e = \frac{V}{W} (C_0 - C_e) \quad (\text{II. 3})$$

In order to examine the equilibrium data, the adsorption isotherms have been assessed. Evaluating the kinetic data using pseudo-first order and pseudo-second

order kinetic models allowed for the analysis of the impact of contact time on the adsorption of dyes.

II.12. Isotherms of Adsorption

The equilibrium relationship between the concentrations in the liquid and adsorbent phases in the adsorbent particles at a specific temperature is known as the adsorption isotherm. The adsorption of dye on clay is described by means of an analysis of the experimental data using adsorption isotherms. The data in this study were analyzed using the Freundlich, Langmuir models and Temkin, which are frequently employed in solid-liquid adsorption systems.

II.12.1. The Isotherm of Langmuir

The Langmuir adsorption the earliest kinetic group on the theory of adsorption was examined by Langmuir in 1918 and is known as the isotherm. The Langmuir adsorption isotherm is predicated on the idea that the adsorbate molecules adhere to the adsorbent's surface in a monolayer.

Adjacent adsorbed molecules don't communicate with one another. Regardless of whether the nearby sites are adsorbed or not, the adsorbate at a given location will still adsorb. The commonly used Langmuir isotherm can be shown as [153]:

$$q_e = Q_m \left[\frac{K_L C_e}{1 + K_L C_e} \right] \quad (\text{II.4})$$

Were

C_e : Solute concentration at equilibrium (mg/L)

K_L : Constant of Langmuir equilibrium

q_m : Maximum amount of adsorption possible (mg/g)

q_e : Capacity of adsorption at equilibrium (mg/g)

According to Freundlich's adsorption isotherm, the concentration of the solution at

equilibrium determines how much solute is adsorbed per specific mass of an adsorbent (q_e).

II.12.2. The Isotherm of Freundlich

Freundlich Isotherms can be applied to heterogeneous systems and involve the creation of multiple layers, The Freundlich isotherm can be shown as follows:

$$Q_e = K_F C_e^{\frac{1}{n}} \quad (II.5)$$

Where, the Freundlich constants are represented by K_F and $1/n$. representative of the adsorption capacity and intensity[154].

II.12.3. The Isotherm of Temkin

Temkin Isotherm includes a component that specifically accounts for interactions between the adsorbent and the adsorbate. Ignoring the concentrations' incredibly low and huge values. The model predicts that, rather of decreasing logarithmically with coverage, the heat of adsorption (a function of temperature) of each molecule in the layer will fall linearly. Its derivation, which is indicated by the equation, is characterized by a uniform distribution of binding energies (up to a maximum binding energy).

The amount sorbed q_e was plotted against $\ln C_e$, and the slope and intercept were used to get the constants. The equation that follows provides the model[155].

$$q_e = B \ln A_T + B \ln C_e \quad (II.6)$$

II.13. Kinetics of Adsorption

It has been determined how quickly CV and MO adsorb on both raw and modified Kaolinite. First-order pseudo-kinetics was used to analyze the experimental data, to comprehend the dynamics of the adsorption process, adopt pseudo-second-order kinetics.

II.13.1. Model of pseudo-first order

To comprehend the kinetic behavior of the system, many people use the pseudo-first-order kinetic model, commonly referred to as the Lagergren kinetic equation. The following equation provides it:

$$q_t = q_e(1 - \exp^{-k_1 t}) \quad (\text{II.7})$$

The amounts of dye adsorbed at equilibrium (mg. g⁻¹) are denoted by q_e and q_t , respectively, and the pseudo first-order rate constant (min⁻¹) is represented by k_1 .

II.13.2. Model of pseudo-second order

Equation: gives the pseudo-second-order kinetic model.

$$q_t = \frac{q_e^2 k_2 t}{1 + q_e k_2 t} \quad (\text{II.8})$$

Where K_2 is the final equilibrium constant for the rate of the pseudo-second-order model (g.mg⁻¹.min⁻¹), q_t and q_e are respectively the amounts of dye adsorbed at equilibrium and at time t . The pseudo second order model is **Lethal dose for 50 % of the population** predicated on the idea that chemisorption, which entails an electron exchange or valence forces through sharing between the adsorbent and the adsorbate, could be the rate-limiting step.

CHAPTER III

RESULTS AND DISCUSSION

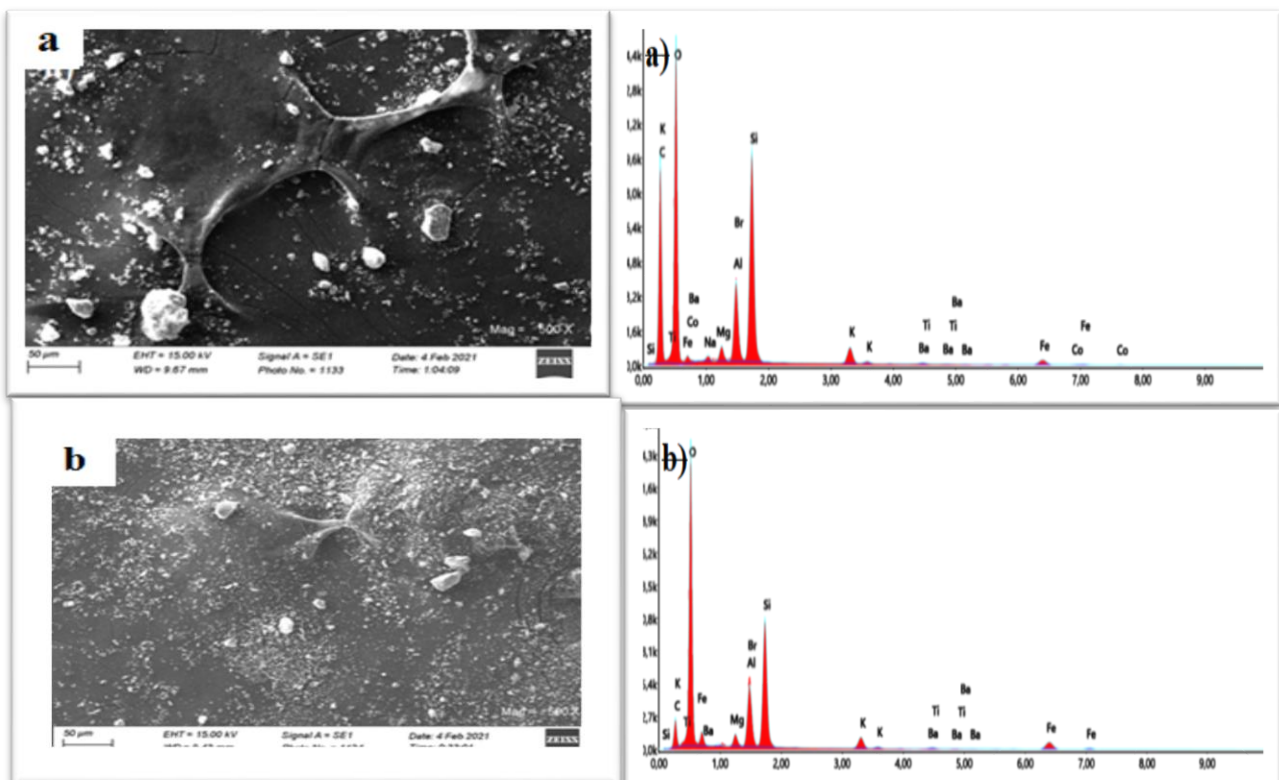
In this chapter, we analyze and discuss the results obtained. We first studied the properties of the pre-treated clay, and then we studied the properties of the adsorbents (Kaol/Cel Composite) after the adsorption of both the dyes crystal violet and methyl orange.

III. Results and Discussion

III.1. Characterization of Kaolinite

III.1.1. SEM-EDX analysis

These fissures mark the surface. Its EDX spectrum (Figure III.1) indicates that pre-treated clay contains O, Al, Si, K, Fe, and Ti. These elements are present in many different types of minerals. Such as quartz, kaolinite, and additional clay components.



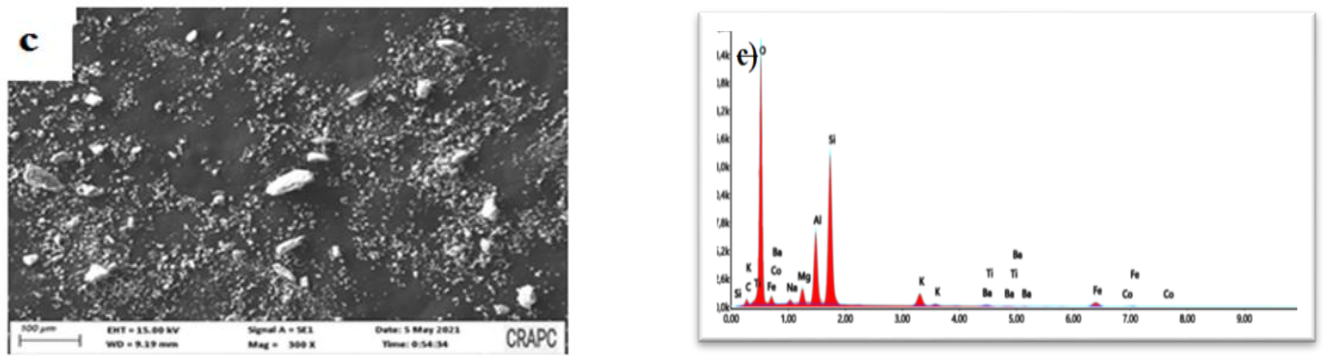


Figure III.1. SEM and EDX a) brown clay minerals, b) green clay minerals, c) red clay minerals.

III.1.2. Surface Area

Initially, we collected three raw clay samples in the colors green, red, and brown from the same distinct area. We analyzed the three samples of clay (The Brunauer-Emmett-Teller method BET); through analysis, we selected brown clay in our study because it has a large surface area compared to red and green clay.

Table. III.1. Surface Area of three different samples of clay minerals.

Type of clay	Brown Clay (Kaolinite)	Green Clay (Chlorite)	Red Clay (Muscovite)
BET Surface Area	110.786 m ² /g	96.7743 m ² /g	106.7085 m ² /g
Langmuir Surface Area	159.4214 m ² /g	145.3670 m ² /g	157.9767 m ² /g
Micropore area	13.0827 m ² /g	1.6862 m ² /g	11.0234 m ² /g

t-Plot external surface area	96.0166 m ² /g	93.8688 m ² /g	93.6259 m ² /g
-------------------------------------	------------------------------	---------------------------	---------------------------

Based on the previous results, we chose kaolinite clay to complete the study. The BET surface area of this clay is 110.786 m²/g.

III.2. Characterization of kaolinite mixed with cellulose (Kaol/Cel)

III.2.1.XRD analysis

Figure (III. 2. a–c) shows the XRD patterns. For the XRD pattern of kaolinite (a), the planes (110), (002), (020) and 021 were marked for the known diffraction peaks at 6.0°, 19.6°, 20.8°, 26.5° and 29.3°, all of which were acceptable due to the different unique orientations of the layers in the kaolinite (Kaol) crystal structure. The XRD pattern of cellulose (b) shows that the (101), (002), (110) planes account for the peaks observed at 2° at about 5.7°, 14, 1°, 20.8°, 27.0° and 29.0° in the cellulose structure, respectively. These spike sites indicate how the cellulose chains are arranged and arranged between the planes [156]. The peak intensity of the XRD pattern (c) of the kaolin/Cel-25 composite is significantly lower than that of the individual kaolin and cellulose patterns.

The integration of cellulose molecules into the clay body causes its density to decrease. In addition, this work provided further evidence that Kaol particles can be successfully produced using the Kaol/Cel-25 combination [157].

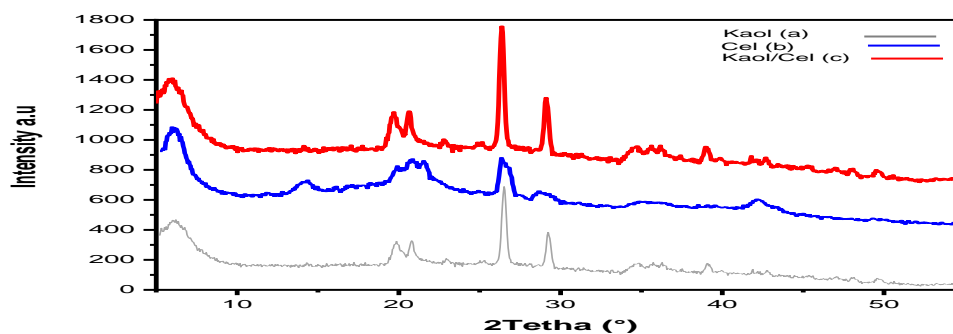


Figure III. 2. Patterns of X-ray diffraction for a) Kaol, b) Cel, and c) Kaol/Cel-25.

III.2.2. FT-IR analysis

The functional groups on the surface of Kaol/Cel-25 was compared using FT-IR analysis before and after CV adsorption, as shown in Figure III.3 (a, b), respectively. O-H stretching and coordinated water bending vibrations, respectively, will be recognized within the bands at 1633 cm^{-1} visible within the FT-IR spectra of Kaol/Cel-25 previous to CV adsorption (Figure III.3.a) [158]. The height at 803 cm^{-1} is because of the Si-O-Si stretching vibrations of quartz or kaolinite, even as the peaks at 3625 cm^{-1} are because of the Al-OH-Al and Fe-OH-Al deformation. Utilizing the applicable cellulose spectrum, one can learn about the amazing chemical properties of cellulose. along with glycosidic linkages at approximately 987 cm^{-1} , - C-H interactions at around 995 cm^{-1} and 2157 cm^{-1} , -C-O-C rings of pyranose at around 1630 cm^{-1} [159]. The bands within the FT-IR spectrum of Kaol/Cel-25 have been seen each earlier than and after CV dye adsorption (Figure III.3.b), with a small shift in a few bands, suggesting that Kaol's useful corporations are worried within the adsorption of CV dyes liable for the arrival of a brand-new band on the more or less 1744 cm^{-1} band. Aromatic C-C stretches are liable for the band at 1582 cm^{-1} , and the vibration of fragrant tertiary amine N-C is detected at 1366 cm^{-1} , proving that the crucial Kaol/Cel-25 practical organizations had been liable for the CV dye adsorption [160].

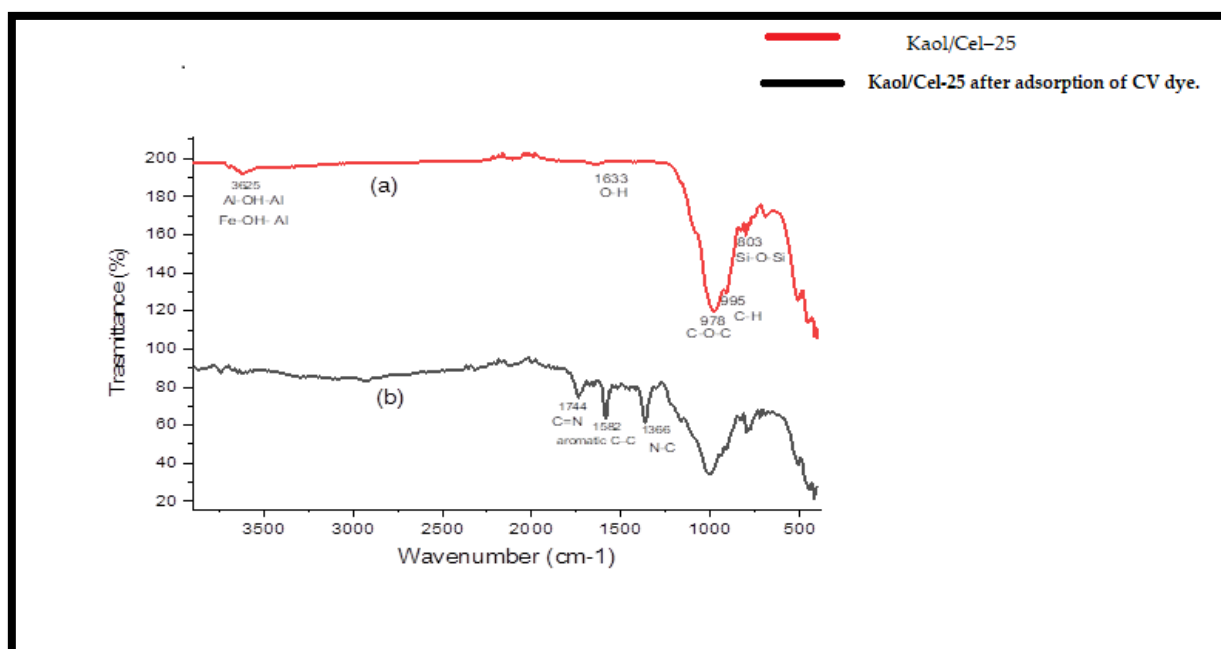


Figure III. 3. Fourier-transform spectra of the following: (a) Kaol/Cel-25 and (b) Kaol/Cel-25 following CV dye adsorption.

III.2.3.SEM-EDX analysis

Kaol's surface morphology is depicted in Figure (III.4.a), and it can be characterized as an uneven, heterogeneous surface crevice. One can see these cracks all the way across the surface. Kaol's EDX spectrum indicates the presence of O, Al, Si, K, Fe, and Ti. A wide range of minerals contain these materials, such as other clay constituents, as determined by XRD analysis, and kaolinite and quartz, in advance of dye adsorption. The SEM-EDX analysis result for Kaol/Cel is displayed in Figure (III.4.b). The surface morphology appears as a surface with numerous large spaces and fissures along with protrusions of different widths. The presence of the components O, C, Al, Si, K, Fe, and Ca is confirmed by the EDX analysis. This implies that the cellulose particles were successfully incorporated into the clay matrix. However, after the absorption of the CV dye, the morphological structure of Kaol/Cel-25 changed (Figure III.4.c), resulting in a reduced number of many tiny apertures and surface Nevertheless, the morphological structure of Kaol/Cel-25 altered following the absorption of the CV dye (Figure III.4.c). Slices in the substance. This observation shows that molecules of CV dye have been loaded onto the surface of Kaol/Cel-25. Additional evidence that the CV is

adhering to the Kaol/Cel-25 surface is provided by the EDX analysis, which also reveals an increase in the carbonation rate in the grelated EDX spectrum.

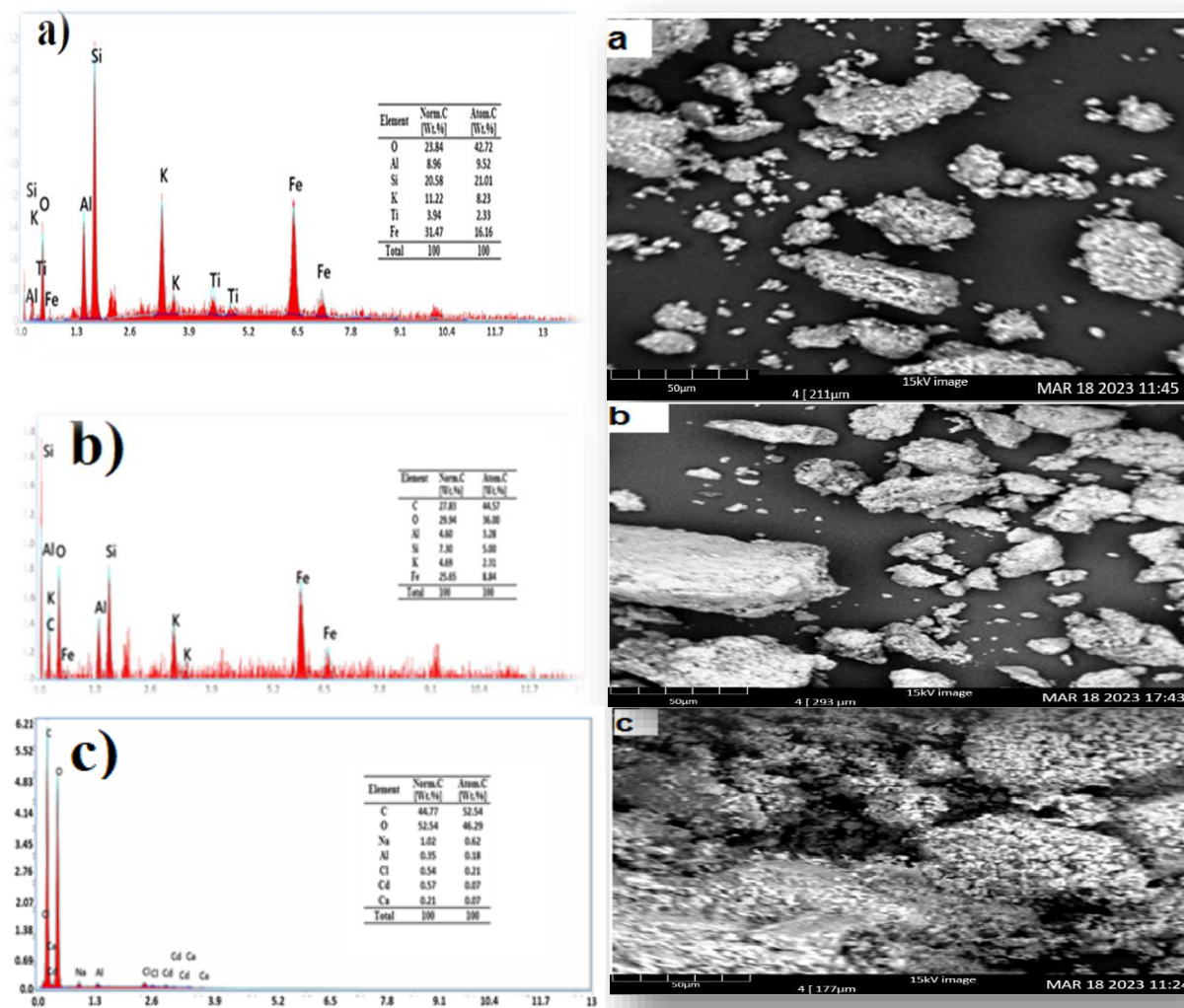


Figure.III.4. Energy-dispersive X-ray microscopy of (a) Kaol, (b) Kaol/Cel-25, and (c) Kaol/Cel-25 following CV dye adsorption.

III.2.4. Adsorbent Characterization of Kaol/Cel Composite after CV and MO dye adsorption

Tables III.2 and III.3 show that BBD planned 46 experiments (runs). The BBD approach was used to investigate the individual and interactive effects of the four examined factors on the CV and MO removal efficiency, respectively (as response). The examiners considered the Cel loading (A), adsorbent dose (B), solution pH (C), temperature (D), and Contact time (E) as independent process factors. It was discovered that in runs 23 and 13 respectively, the highest dye removal effectiveness (%) of CV and MO were 99.58% and 84.66 % (Table III.2, III.3).

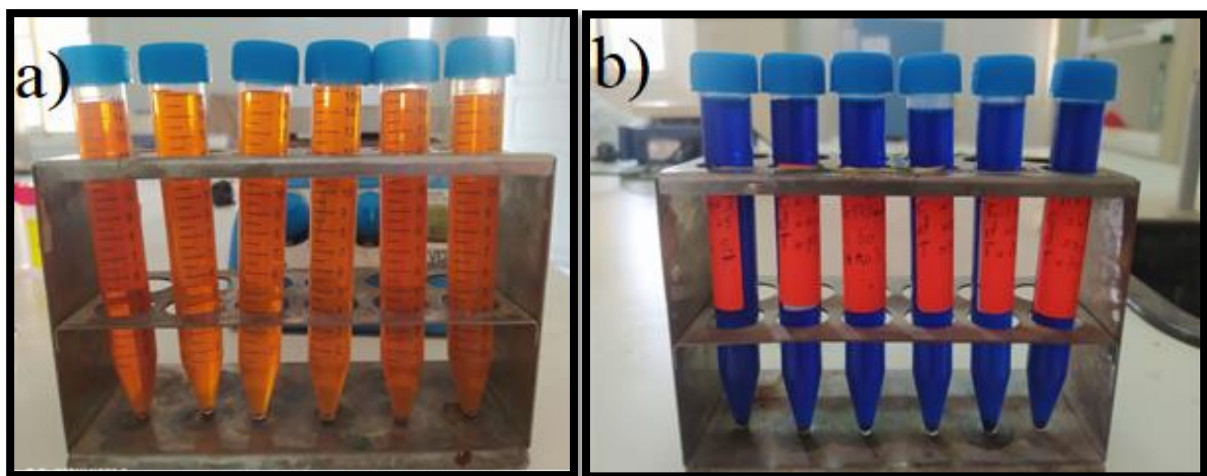


Figure III.5. The natural dyes decantation after adsorption onto Kaol/Cel for (a-MO , b-CV).

TableIII.2. Results of experiments for the crystal violet and the box-Behnken design matrix with five factors.

Run	A : Loading (%)	B : Adsorbent dose(g)	C : pH	D : Temperature (°C)	E : Contact time (min)	Dye Removal (%)
1	25	0.035	7	45	17.5	97.95
2	0	0.035	7	60	17.5	75.88
3	25	0.020	7	60	17.5	72.02
4	25	0.050	10	45	17.5	99.05
5	25	0.035	10	30	17.5	98.75
6	0	0.035	7	45	30	72.02
7	50	0.035	10	45	17.5	99.34
8	50	0.020	7	45	17.5	99.48
9	0	0.050	7	45	17.5	79.25
10	25	0.020	4	45	17.5	61.82
11	25	0.050	7	45	30	99.05
12	25	0.050	7	60	17.5	99.16
13	25	0.050	7	30	17.5	98.91
14	25	0.035	7	45	17.5	97.95
15	50	0.035	7	45	5	96.37
16	25	0.020	10	45	17.5	98.19
17	25	0.035	10	60	17.5	99.21
18	25	0.035	7	60	5	98.55
19	25	0.035	7	45	17.5	97.95
20	50	0.035	7	45	30	99.49
21	50	0.035	7	60	17.5	99.37
22	0	0.035	7	30	17.5	61.82
23	25	0.035	10	45	5	99.58
24	25	0.050	4	45	17.5	98.51
25	25	0.035	4	60	17.5	98.18
26	0	0.035	4	45	17.5	75.88
27	25	0.020	7	45	5	86.14
28	25	0.020	7	30	17.5	97.91
29	25	0.035	7	60	30	97.40
30	25	0.050	7	45	5	99.52
31	0	0.035	10	45	17.5	75.88

32	25	0.035	7	30	30	97.97
33	50	0.035	7	30	17.5	99.34
34	25	0.035	4	45	30	99.41
35	0	0.035	7	45	5	79.25
36	25	0.035	4	30	17.5	99.41
37	25	0.035	4	45	5	98.44
38	25	0.020	7	45	30	83.76
39	25	0.035	7	45	17.5	98.22
40	50	0.035	4	45	17.5	95.86
41	25	0.035	7	45	17.5	97.54
42	25	0.035	7	45	17.5	98.22
43	25	0.035	7	30	5	96.40
44	50	0.050	7	45	17.5	99.40
45	0	0.020	7	45	17.5	79.25
46	25	0.035	10	45	30	98.75

TableIII.3. Results of experiments for the methyl orange, the box-Behnken design matrix with five factors.

Run	A : Loading (%)	B : Adsorbent dose(g)	C : pH	D : Temperature(°C)	E : Contact time(min)	Dye Removal (%)
1	25	0.035	4	60	17.5	64.55
2	25	0.035	10	60	17.5	66.22
3	50	0.02	7	45	17.5	65.55
4	0	0.035	7	45	30	72.23
5	25	0.035	7	45	17.5	76.07
6	25	0.035	4	30	17.5	52.72
7	25	0.035	10	45	5	58.74
8	25	0.035	7	45	17.5	77.93
9	25	0.02	7	45	30	65.5
10	25	0.035	4	45	30	57.92
11	25	0.05	4	45	17.5	62.95
12	25	0.035	4	45	5	49.9
13	50	0.035	7	45	30	82.26

14	25	0.02	4	45	17.5	47.99
15	0	0.05	7	45	17.5	72.89
16	25	0.02	7	60	17.5	65.5
17	25	0.05	7	60	17.5	76.6
18	25	0.05	10	45	17.5	54.39
19	25	0.035	10	30	17.5	55.7
20	25	0.05	7	30	17.5	84.55
21	25	0.05	7	45	30	80.8
22	25	0.02	7	30	17.5	68.2
23	50	0.035	7	45	5	74.64
24	50	0.05	7	45	17.5	76.75
25	25	0.035	7	45	17.5	77.22
26	25	0.02	10	45	17.5	65.5
27	25	0.05	7	45	5	80.8
28	50	0.035	7	60	17.5	78.02
29	0	0.035	7	45	5	68.92
30	50	0.035	4	45	17.5	58.33
31	50	0.035	10	45	17.5	63.41
32	25	0.035	7	45	17.5	76.07
33	25	0.02	7	45	5	66.95
34	25	0.035	7	30	30	80.36
35	25	0.035	7	60	5	70.68
36	25	0.035	10	45	30	46.66
37	0	0.035	7	30	17.5	68.22
38	25	0.035	7	30	5	70.97
39	25	0.035	7	60	30	80.03
40	0	0.02	7	45	17.5	64.55
41	50	0.035	7	30	17.5	80.05
42	0	0.035	7	60	17.5	54.44
43	25	0.035	7	45	17.5	81.45
44	25	0.035	7	45	17.5	82.63
45	0	0.035	10	45	17.5	46.04
46	0	0.035	4	45	17.5	48.14

III.3. Results and Discussion of BBD model analysis for CV, MO dye

III.3. 1. Fitting the Process Models Kaol/Cel Composite following the adsorption of CV dye

Using the quadratic polynomial model, the mathematical relationship between the process's component elements and the result was established. Table III.4 displays the findings of the ANOVA's significance test for the response in the regression model. The model's p-value is less than 0.0001 and its F-value is 5.66, indicating the significance of the model terms. For the selected conditions, significance is defined as a p-value of less than 0.05. The main model terms used in the response were A, B, BC, BD, and A² for the elimination of CV. However, it was discovered that the residency period component (E) had no effect on the removal of the CV, most likely because the adsorption process was not very sensitive to changes in time. The quadratic regression model shown in Equation (III.1) expresses the empirical link between CV removal and the significant factors.

$$\text{CVremoval}(\%) = +97.97 + 11.83A + 5.89B - 8.95BC + 6.53BD - 9.66A^2 \quad (\text{III.1})$$

Table III.4. Analysis of variance of the crystal violet dye removal response surface quadratic model.

Source	Sum of Squares	<i>d_f</i>	Mean Square	F-value	p-value	Remarks
Model	4461.30	20	223.07	5.66	<0.0001	Significant
A: Cel loading	2242.11	1	2242.11	56.92	<0.0001	Significant
B: Adsorbent dose	555.69	1	555.69	14.11	0.0009	Significant
C-pH	106.31	1	106.31	2.70	0.1130	Insignificant
D-Temp.	7.19	1	7.19	0.1826	0.6728	Insignificant
E-Time	2.57	1	2.57	0.0652	0.8006	Insignificant
AB	0.0015	1	0.0015	0.0000	0.9951	Insignificant
AC	3.04	1	3.04	0.0772	0.7834	Insignificant
AD	49.21	1	49.21	1.25	0.2743	Insignificant
AE	26.74	1	26.74	0.6787	0.4178	Insignificant

BC	321.01	1	321.01	8.15	0.0085	Significant
BD	170.74	1	170.74	4.33	0.0477	Significant
BE	0.9046	1	0.9046	0.0230	0.8808	Insignificant
CD	0.7121	1	0.7121	0.0181	0.8941	Insignificant
CE	0.8080	1	0.8080	0.0205	0.8873	Insignificant
DE	1.85	1	1.85	0.0469	0.8303	Insignificant
A ²	814.98	1	814.98	20.69	0.0001	Significant
B ²	166.50	1	166.50	4.23	0.0504	Insignificant
C ²	3.48	1	3.48	0.0882	0.7689	Insignificant
D ²	11.12	1	11.12	0.2823	0.5999	Insignificant
E ²	0.1796	1	0.1796	0.0046	0.9467	Insignificant
Residual	984.81	25	39.39			
Cor Total	5446.11	45				

Equation (III.1) has positive and negative signs, corresponding to the synergistic and antagonistic effects of the various factors [161]. As can be seen the response factors R-squared (determination coefficient) is 0.97, a very high value that indicates an excellent correlation between the actual and projected values.

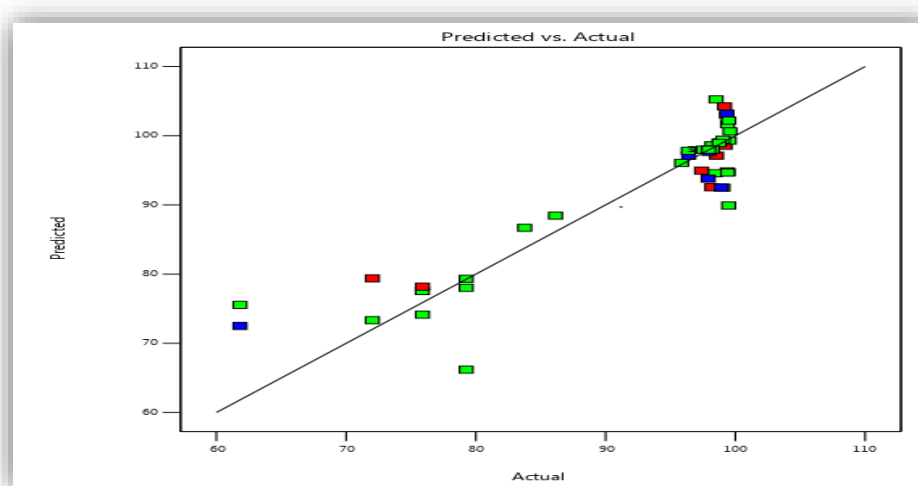


Figure III. 6. Linear correlation between predicted values vs. the observed values of CV adsorption on Kaol/Cel-25

III.3. 2. Fitting the Process Models Kaol/Cel Composite following the adsorption of MO dye

To test the significance of the adequacy of the model, the analysis of variance was used. The outcomes of the ANOVA statistics for MO adsorption is tabulated in Table III.5. The model's p-value is less than 0.0001 and its F-value is 8.18, indicating the significance of the model terms. For the selected conditions, significance is defined as a p-value of less than 0.05. The main model terms used in the response were A, B, BC, A² and C² for the elimination of MO. However, it was discovered that the residency temperature (D) and contact time (E) have not effect on the removal of the MO, most likely because the adsorption process was not very sensitive to changes in temperature and time. The quadratic regression model shown in Equation (III.2) expresses the empirical link between MO removal and the significant factors.

$$\text{MO removal (\%)} = +78.56 + 5.22A + 4.99B - 6.51 BC - 4.92 A^2 - 19.53 C^2 \quad (\text{III.2})$$

Table III.5. Analysis of variance of the MO dye removal response surface quadratic model.

Source	Sum of Squares	df	Mean Square	F-Value	P-Value	Remarks
Model	4773.73	20	238.69	8.18	< 0.0001	Significant
A : Cel loading	436.60	1	436.60	14.97	0.0007	Significant
B : Adsorbent	399.90	1	399.90	13.71	0.0011	Significant
C-pH	12.54	1	12.54	0.4297	0.5181	Insignificant
D-Temp	1.40	1	1.40	0.0479	0.8285	Insignificant
E-Time	36.48	1	36.48	1.25	0.2741	Insignificant
AB	2.04	1	2.04	0.0701	0.7934	Insignificant
AC	12.89	1	12.89	0.4418	0.5123	Insignificant
AD	34.52	1	34.52	1.18	0.2871	Insignificant

AE	4.64	1	4.64	0.1592	0.6933	Insignificant
BC	169.91	1	169.91	5.82	0.0235	Significant
BD	6.89	1	6.89	0.2362	0.6312	Insignificant
BE	0.5256	1	0.5256	0.0180	0.8943	Insignificant
CD	0.4277	1	0.4277	0.0147	0.9046	Insignificant
CE	101.00	1	101.00	3.46	0.0746	Insignificant
DE	0.0004	1	0.0004	0.0000	0.9971	Insignificant
A²	211.58	1	211.58	7.25	0.0125	Significant
B²	70.29	1	70.29	2.41	0.1332	Insignificant
C²	3328.86	1	3328.86	114.12	< 0.0001	Significant
D²	16.93	1	16.93	0.5804	0.4533	Insignificant
E²	41.49	1	41.49	1.42	0.2442	Insignificant
Residual	729.26	25	29.17			
Cor Total	5502.98	45				

BBD graphical ways can be utilized to analyze the relationship between the actual and expected values for the outcomes (MO removal). The statistical validation of the BBD model is supported by the proximity of the actual and expected values in Fig. III. 7, demonstrating a strong agreement between them.

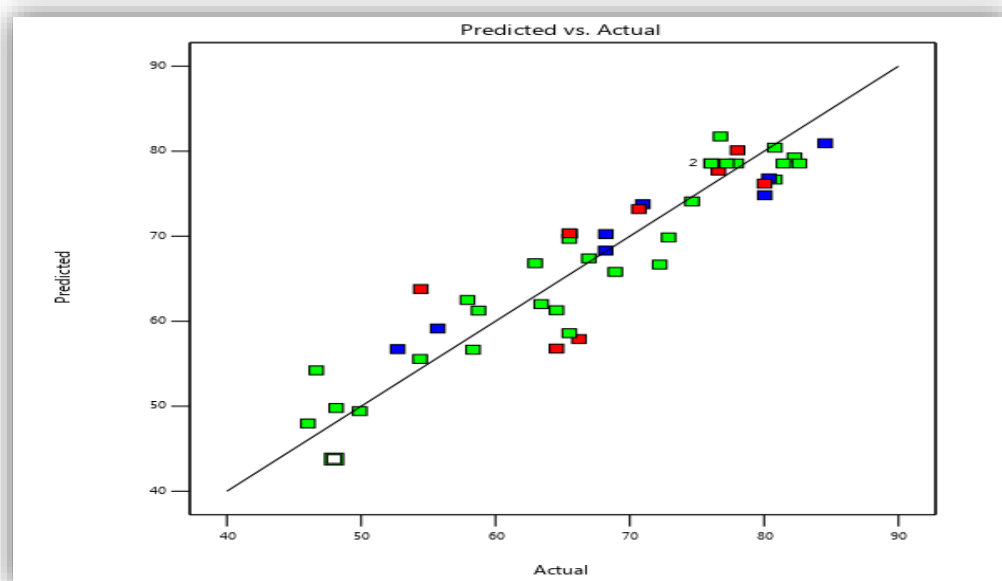


Figure III. 7. Linear correlation between predicted values vs. the observed values of MO adsorption on Kaol/Cel-25.

III.3.3. Interactions Significant for Crystal Violet (CV) Dye Removal

Adsorbent dosage (B) and solution pH (C) effects on CV elimination and efficacy demonstrate the remaining independent factors (i.e., 45° C temperature), The p-value of 0.0085 from Table III.5, which shows a significant interaction, was found between the five-minute residence time and the Cel loading (Kaol/Cel-25).The remaining uncorrelated independent variables (such as 45°C temperature, five minutes of residency, and Cel loading (Kaol/Cel-25) were kept constant throughout the trial

period. The 3D surface and 2D contour plots for the BC interaction are shown in Figures III.8 and III.9, respectively. These illustrate increasing the maximum adsorbent infusion from 0.02 g to 0.05 g.

By reducing the pH of the solution from 10 to 4, the effectiveness of CV removal was significantly increased from 61.82% to 99.86%. The highest CV removal efficiency was reached at pH 4, and dye removal gradually decreased as pH increased toward an alkaline environment. Additionally, figure (III.10) demonstrates that Kaol/Cel-25's pH_{pzc} was 8.71, proving that the material's surface starts to become positively charged at pH values lower than pH_{pzc} . On the other hand, Kaol/Cel-25's surface charge turns negative at pH values higher than pH_{pzc} , suggesting that Kaol/Cel-25 may adsorb cationic dyes. Stronger electrostatic interactions therefore form between the surface functional groups of negatively charged Kaol/Cel-25 and cationic CV dye, as shown in Equation (III.2).



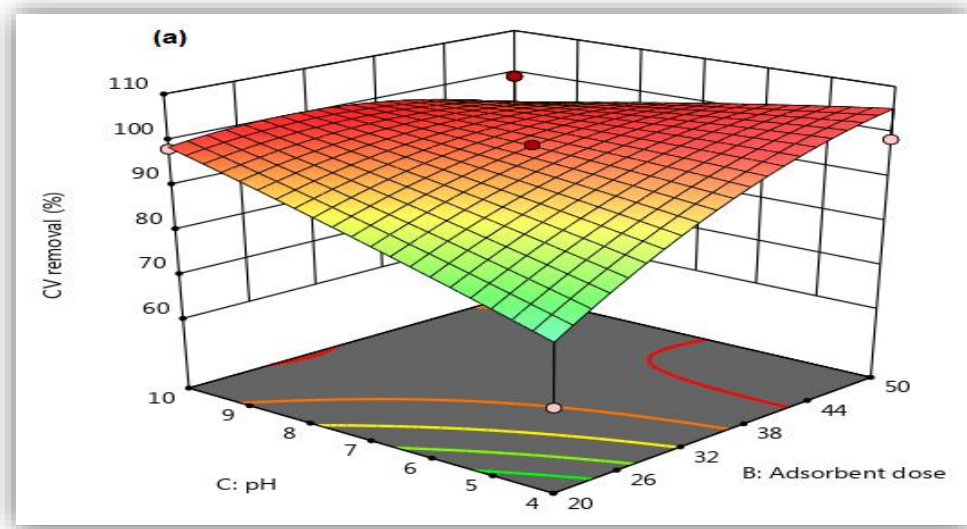


Figure . III.8. 3D surface plot of the influence of adsorbent dose and solution pH of CV adsorption on Kaol/Cel-25.

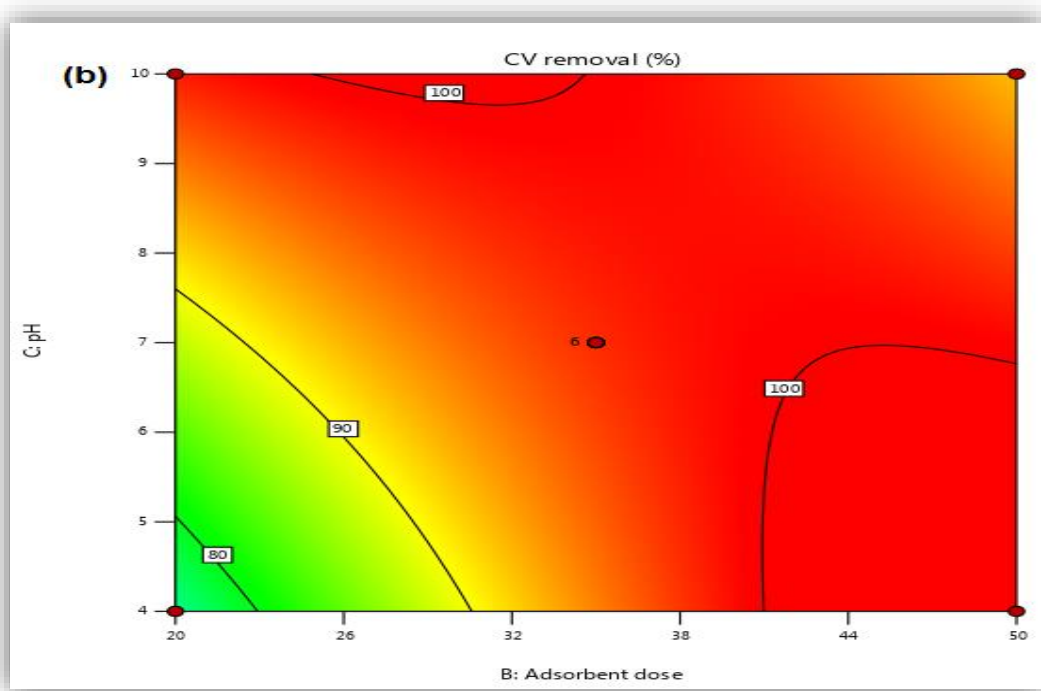


Figure III.9.2D contour plot of the influence of adsorbent dose and solution pH of CV adsorption on Kaol/Cel-25.

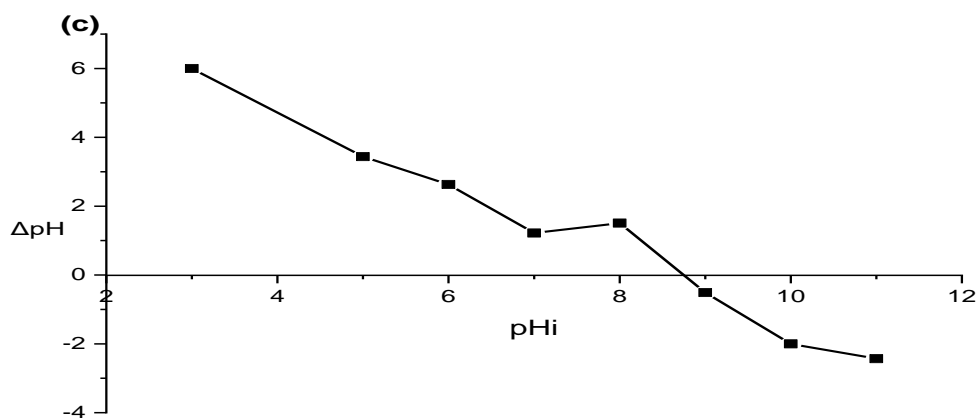


Figure III.10. The zero-point of charge (pH_{pzc}) of CV adsorption on Kaol/Cel-25.

The significance of the interactions between the independent variables was evaluated using (Table III.5). With a p-value of 0.0477, the findings demonstrated that the interaction influence between adsorbent dosage (B) and temperature (D) had a statistically significant effect on CV removal efficiency. The other factors were a pH of 10, a 25% Cel loading, and a 5-minute contact period, stayed unchanged in the course of the experiment. 3D and 2D response surface plots were used to further analyze the relationship between the temperature and the adsorbent dose, as shown in Figures (III.11, III.12), respectively. Plots showed that increasing the adsorbent dose from 0.02 g to 0.05 g resulted in a higher percentage of CV dye removal (%), which may have been caused by an increase in available surface area or active adsorption sites. However, there was no significant effect of temperature on the removal of CV dye, suggesting an exothermic adsorption process. These results will be covered in more detail in our discussion of adsorption thermodynamics.

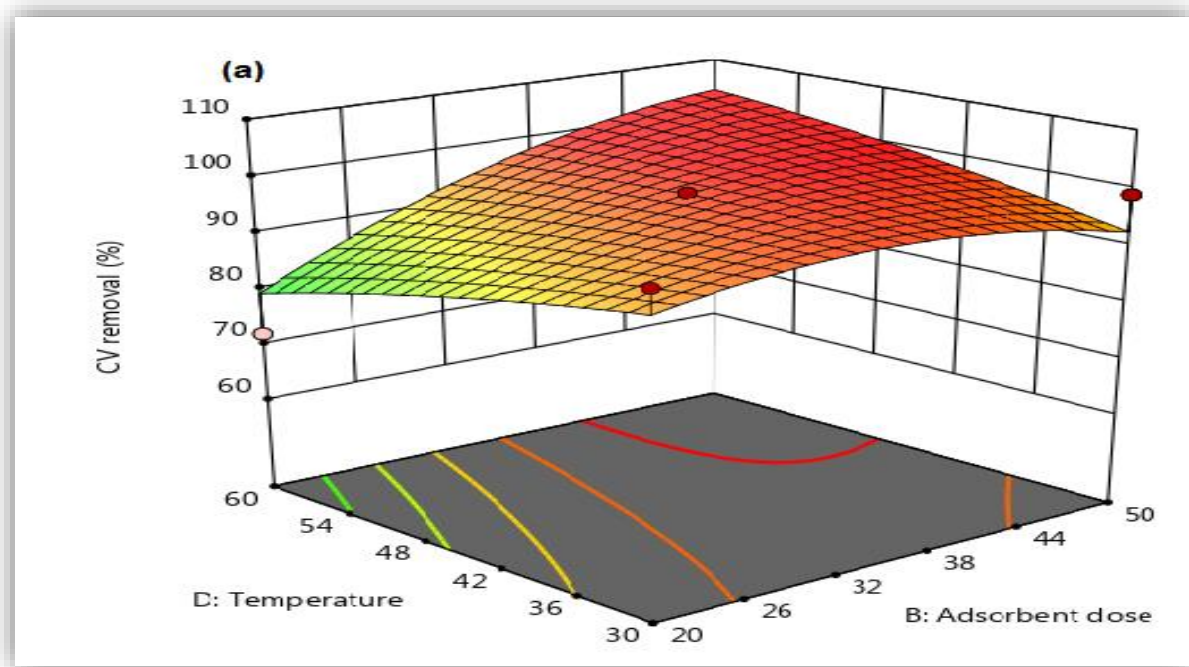


Figure III.11. 3D surfaceplot of the influence of adsorbent dose and temperature on Kaol/Cel-25 CV adsorption.

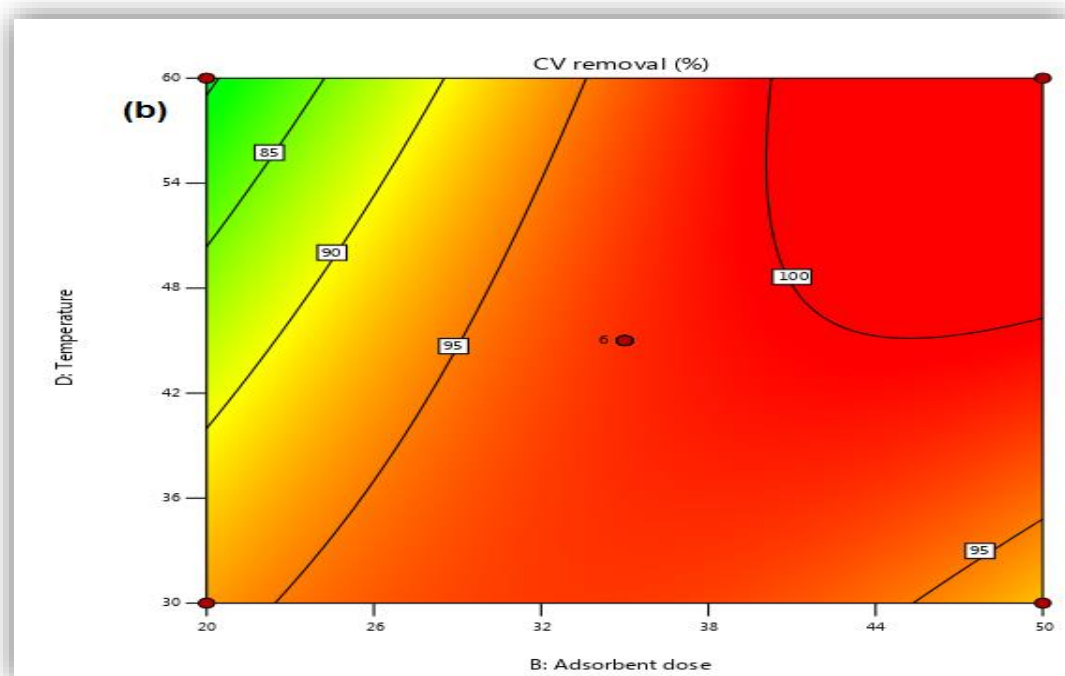


Figure III.12.2D contour plot of the influence of adsorbent dose and temperature on Kaol/Cel-25 CV adsorption.

For every pair of independent variables, the presence of a statistically significant interaction was ascertained. The findings showed that the temperature (D) and adsorbent dosage (B) interacted to significantly affect the efficiency of CV removal (p-value = 0.0477). The remaining independent variables, which were the 25% Cel

loading, the pH of the solution, and the 5-minute contact period, did not change during the trial. The response surface plots for the temperature and adsorbent injection interaction are shown in Figures III.11 and III.12. The results showed that a higher elimination of CV was obtained by increasing the adsorbent injection from 0.02 g to 0.05 g, an increase in surface area or active adsorption sites could be related to this. Furthermore, the results suggest that the dye molecules' adsorption onto the Kaol/Cel-25 surface was exothermic, as there was no discernible effect of temperature on the effectiveness of CV removal. A more comprehensive discussion of adsorption's thermodynamics.

III.3.4. Interactions Significant for Methyl orange (MO) Dye Removal

Graphical representations of three-dimensional (3D) response surface and two-dimensional (2D) contour plots using RSM can also enhance the understanding of the combined binary interaction of significant parameters such as Kaol/ Cel-25 dosage and pH as elucidated in Fig. III.13, III.14.

The combined effects of the Kaol/ Cel-25 dosage and solution pH for MO adsorption was found to be a significant factor, with temperature and time left unaltered. As the dosage of Kaol/ Cel-25 increases, the removal rate also increases. Specifically, the removal rate of MO increased from 46.04 % to 84.55 %. The remaining uncorrelated independent variables (such as 30°C temperature, 17.5 minutes of residency, and Cel loading (Kaol/Cel-25) were kept constant throughout the trial period. This logical remark can be attributed to the remarkable surface properties of Kaol/ Cel-25, which enhance the availability of active [163].

In this regard, the recorded pH_{pzc} value of this adsorbent was 8.71, as illustrated in Fig. III.10. The sorption rate of MO on adsorbent reached the highest yield in an acidic medium. This can be explained by the electrostatic forces between the anionic sulfonate (R- SO₃) and the protonated sites of adsorbent. It is worth noting that similar

findings regarding the uptake of MB dye by natural clay were previously reported by B. Abbou *et al* [164].

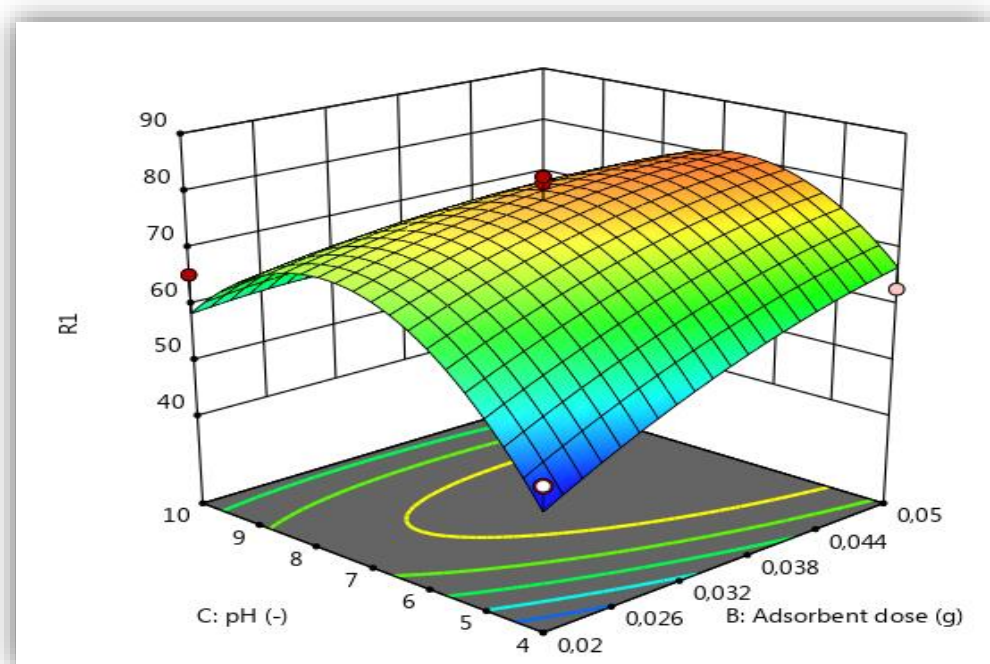


Figure III.13. 3D surface plot of the influence of adsorbent dose and solution pH of MO adsorption on Kaol/Cel-25.

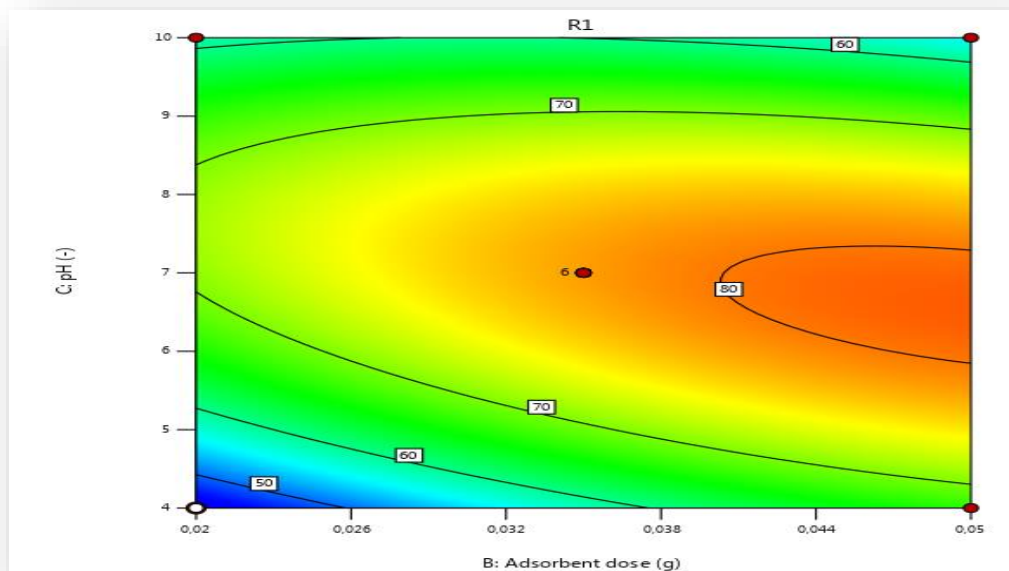


Figure III.14.2D contour plot of the influence of adsorbent dose and solution pH of MO adsorption on Kaol/Cel-25.

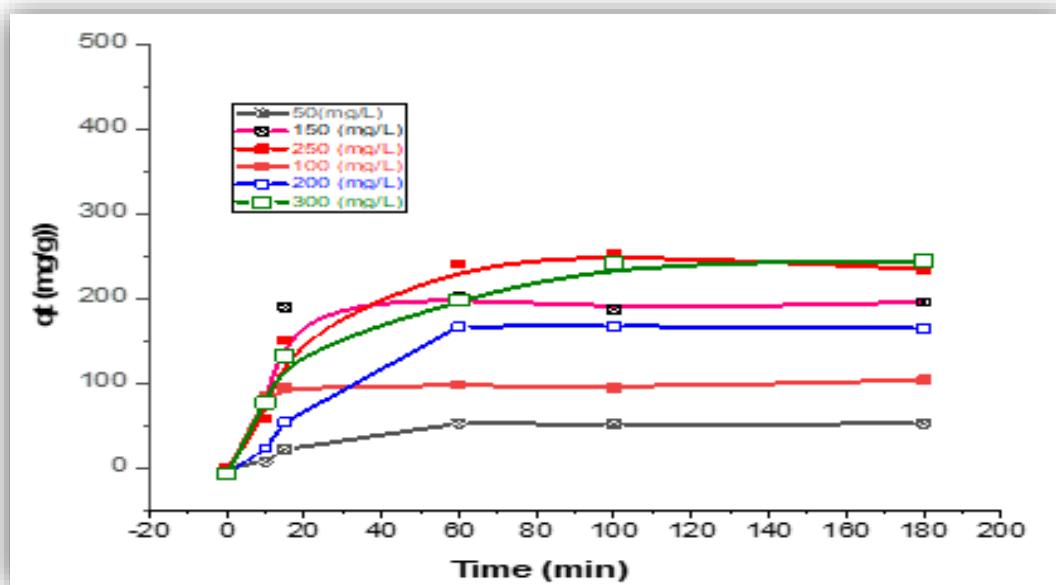
III.4. Result of adsorption experiments with Kaol/Cel Composite after CV and MO adsorption

This part examines the effects of residency time. Vs. initial CV (MO), level on Kaol/Cel-25's adsorption potential was investigated for a range of initial concentrations, from 50 to 300 mg/L. The experimental results are shown in Figure (III.15), and run 23 of Table (III.2) indicates that the best conditions for CV dye removal were found by analyzing the highest percentage of CV dye removal that was achieved

at 45 °C, pH 10, and a constant injection of Kaol/Cel-25 adsorbent (0.035 g). As shown in Figure (III.11), the equilibrium adsorption capacity increased from 51.7 to 297.7 mg/g as the initial CV level increased.

The best conditions for removing MO dye were found by maximizing the percentage of MO dye removed, which was observed at 30 °C, pH = 7, and a constant injection of 0.05 g of Kaol/Cel-25 adsorbent, as shown in run 20 of Table (III.3). The experimental results are shown in Figure (III.16). As shown in Figure, the equilibrium adsorption capacity increased from 40.05 to 132.89 mg/g as the initial MO level increased.

Due to the higher initial concentration of CV, MO, there is a higher collision rate between the dye and the Kaol/Cel-25 surface, which is the cause of this increase. Furthermore, the adsorption capacity was increased because the higher concentration gradient made it easier for dye molecules to diffuse into the adsorbent's internal pores and migrate toward the active adsorption sites [165].



FigureIII.15. Influence of initial concentrations versus CV adsorption contact time on Kaol/Cel-25.

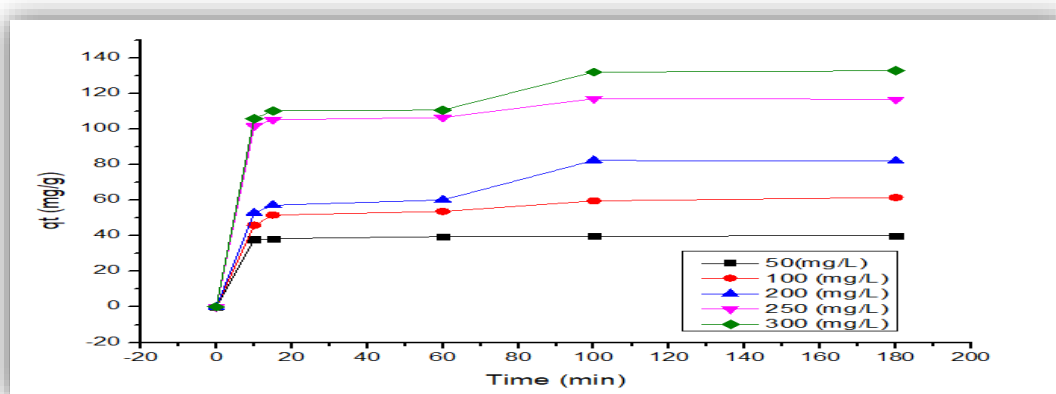


Figure.III.16. Effect of MO adsorption contact time on Kaol/Cel-25 versus initial concentrations.

III.5. Kinetic Modeling of adsorption experiments with Kaol/Cel Composite after CV and MO adsorption

Additional research was conducted, and it is important to understand the adsorption kinetics in order to understand how CV and MO adsorb and behave on the surface of kaolinite. In this case, pseudo-first-order (PFO) and pseudo-second-order (PSO) kinetic models were applied. Equation (III.3) for PFO and Equation (III.4) for PSO [166] represent these non-linear kinetic models:

$$q_t = q_e(1 - \exp^{-k_1 t}) \quad \text{(III.3)}$$

$$q_t = \frac{q_e^2 k_2 t}{1 + q_e k_2 t} \quad \text{(III.4)}$$

The symbol for designated is q_e (mg/g). For instance, the amount of dye adsorbed at a given time t is indicated by the value of q_t (mg/g). Additionally, the PFO's rate constant is represented by k_1 (1/min), and the PSO's rate constant is represented by k_2 (g/mg min).

More research was done in order to understand the adsorption pathway and behavior of CV and MO on the surface of Kaol/Cel-25. It is imperative to comprehend the adsorption kinetics. Here, two pseudo-first-order (PFO) and pseudo-second-order (PSO) kinetic models were applied. Equations (III.3) and (III.4) for PFO and PSO [167] respectively represent these non-linear kinetic models, expressed as q_e (mg/g). By contrast, q_t (mg/g) indicates the amount of MO and CV dye adsorbed at a given time t . Furthermore, k_1 (1/min) represents the rate constant of the PFO, and k_2 (g/mg min) represents the rate constant of the PSO.

The model parameters and correlation coefficients (R^2) for the PSO and PFO are shown in Table III.5. The PSO model fits the CV dye adsorption on the Kaol/Cel-25 surface better than the PFO model, as demonstrated by the kinetic adsorption data in Table III.5. This is supported by the fact that the PSO model had higher R^2 values than the PFO model. Additionally, compared to the q_e values computed using the PFO model, the q_e (i.e., q_e , cal) values estimated using the PSO model are closer to the experimental q_e (i.e., q_e , exp) values. These findings and FT-IR analyses indicate that the adsorption process depends critically on the chemical interaction between the CV dye and the active functional groups on the Kaol/Cel-25 surface. Therefore, the chemisorption process regulates the adsorption of CV dye on the Kaol/Cel-25 surface.

Table III.6. The optimal conditions for the CV sorption onto Kaol/Cel Composite in terms of the pseudo-first-order and pseudo-second-order kinetic parameters

Concentration (mg/L)	$q_{e\text{ exp}}$ (mg/g)	PFO			PSO		
		$q_{e\text{ cal}}$ (mg/g)	K_1 (1/min)	R^2	$q_{e\text{ cal}}$ (mg/g)	$K_1 10^{-2}$ (g/mg. min)	R^2
50	51.74	54.23	0.0459	0.963	59.52	0.074	0.994
100	131.5	130.53	0.0531	0.955	133.33	0.298	0.999
150	195.6	180.33	0.0277	0.994	198.33	0.042	1
200	203.2	182.66	0.0215	0.945	208.56	0.016	0.997
250	252.1	192.31	0.0318	0.938	294.12	0.014	0.995
300	297.7	274.82	0.0434	0.954	299.58	0.020	0.996

The model parameters and correlation coefficients (R^2) for the PSO and PFO are shown in Table III.6. The PFO model fits the MO dye adsorption on the Kaol/Cel-25 surface better than the PSO model, as demonstrated by the kinetic adsorption data in Table III.6. This is supported by the fact that the PSO model had higher R^2 values than the

PFO model. Additionally, compared to the q_e values computed using the PFO model, the q_e (i.e., q_e , cal) values estimated using the PSO model are closer to the experimental q_e (i.e., q_e , exp) values. Therefore, the chemisorption process regulates the adsorption of MO dye on the Kaol/Cel-25 surface.

Table III.7. The optimal conditions for the MO sorption onto Kaol/Cel Composite in terms of the pseudo-first-order and pseudo-second-order kinetic parameters

Conc (mg/L)	q_e _{exp} (mg/g)	PFO			PSO		
		$q_{e,cal}$ (mg/g)	K_1 (1/min)	R^2	$q_{e,cal}$ (mg/g)	$K_2 \cdot 10^{-2}$ (g/mg. min)	R^2
50	40.05	43.48	0.0318	0.9515	43.64	0.00153	1
100	61.61	56.57	0.045	0.8916	62.89	0.00301	0.9938
150	74.90	61.62	0.0228	0.9388	73.33	0.00047	0.9455
200	82.08	73.65	0.046	0.7668	86.96	0.00104	0.9884
250	116.81	114.11	0.0055	0.6257	119.05	0.00303	0.999
300	132.89	133.05	0.0617	0.9103	136.99	0.00131	0.9956

III.6. Isotherms of adsorption experiments with Kaol/Cel Composite after CV and MO adsorption

The understanding of the adsorption isotherm is crucial to understanding the interaction between the molecules of CV, MO dye, The most widely used isotherms are selected, namely Langmuir , Freundlich , and Temkin [168]. Are selected with the goal of examining the equilibrium adsorption data and determining Kaol/Cel Composite adsorption potential. The nonlinear formulations of the Freundlich, Temkin, and Langmuir equations are each reflected in the independent equations (III.5– III.7).

$$\frac{C_e}{q_e} = \frac{q_{\max}K_a C_e}{1 + K_a C_e} \quad (\text{III.5})$$

$$q_e = K_f C_e^{\frac{1}{n}} \quad (\text{III.6})$$

$$q_e = \frac{RT}{b_T} (\ln K_T C_e) \quad (\text{III.7})$$

When trying to explain the interaction between the molecules of CV and MO dye and Kaol/Cel-25, the adsorption isotherm is an essential piece of knowledge to have. As a result, the most commonly used isotherms are Langmuir, Freundlich, and Temkin [169]. These are selected with the goal of evaluating the equilibrium adsorption data and determining the adsorption potential of Kaol/Cel-25. The Langmuir, Freundlich, and Temkin equations' nonlinear forms are each individually reflected in the equations (III. 5–III.7).

The variables utilized in the analysis are as follows: q_{\max} (mg/g) indicates the maximum amount of MO and CV dye that can be adsorbed per unit mass of Kaol/Cel-25; q_e (mg/g) indicates the amount of dye absorbed per unit weight; and C_e (mg/L) indicates the equilibrium concentration of CV and MO dye. The heat of adsorption, temperature, and universal gas constant are represented by the dimensional less constant n for the adsorption intensity, the Langmuir (K_a), Freundlich (K_f), and Temkin (K_T) constants (L/mg), b_T (J/mol), T (K), and R (8.314 J/mol K), respectively. Table (III.7, III.9) demonstrates that the Langmuir adsorption isotherm model provides the greatest fit for the absorption of CV and MO dye by Kaol/Cel-25. Its R^2 (CV) =0.99 and R^2 (MO) =0.89 are greater than those of the Freundlich and Temkin models. This suggests that the dyes CV and MO form an energetically comparable monolayer covering on the adsorbent's homogenous surface [170].

Table III.8. Langmuir, Freundlich, and Temkin constants of CV dye adsorption onto Kaol/Cel Composite are presented.

Model	Parameters	Value
Langmuir	$q_{max}(\text{mg/g})$	294.12
	$K_a (\text{L/mg})$	0.03
	R^2	0.99
Freundlich	$K_f(\text{mg/g}) (\text{L/mg})^{1/n}$	38.37
	N	2.43
	R^2	0.98
Temkin	$K_T(\text{L/mg})$	0.07
	b_T	22.40
	R^2	0.91

Moreover, using the Langmuir model, we determined that 294.12 mg/g is the q_{max} for Kaol/Cel-25. Table (III.8) compares the q_{max} of CV dye adsorption onto Kaol/Cel-25 to that of other adsorbents that have been published for removing CV, highlighting that the cationic dye removal efficiency of Kaol/Cel-25 is highly effective and shows promise for further applications.

Table III.9. Comparison of the q_{max} (mg/g) values for CV dye adsorption to that of various adsorbents

Adsorbents	q_{max} (mg/g)	References
Palm kernel fiber	78.9	[113]
Rice husk NaOH-modified	44.87	[114]
Fly ash	74.6	[115]
cellulose-based from sugercane bagasse	107.5	[116]

Magnetite graphene oxide-doped super adsorbent hydrogel	88.78	[117]
Rubber seed pericarp treated with sulfuric acid	302.7	[118]
Microalgae	243.0	[119]
zeolite-montmorillonite	150.52	[120]
Durian seeds powder	158	[121]
Kaol/Cel-25	294.12	This study

Furthermore, the Langmuir isotherm model to be 113.64 mg/g estimated the maximum adsorption capacity q_{max} . Thus, the q_{max} of MO dye onto Kaol/Cel-25 was compared with other adsorbents reported in the literature for removing MO as listed in (Table III.10). This (Table III.10) reveals that Kaol/Cel-25 is a promising magnetic composite material for removal of an anionic dye (MO) from aqueous environment with very preferable adsorption capacity.

Table III.10. Langmuir, Freundlich, and Temkin constants of MO dye adsorption onto Kaol/Cel Composite are presented.

Model	Parameters	Value
Langmuir	$q_{max}(\text{mg/g})$	113.64
	$K_a (\text{L/mg})$	0.5087
	R^2	0.8892
Freundlich	$K_f(\text{mg/g}) (\text{L/mg})^{1/n}$	57.70
	N	5.53
	R^2	0.85
Temkin	$K_T(\text{L/mg})$	4.1916E-25
	b_T	42502.3457
	R^2	0.70

Table III.11. Comparison of the q_{\max} (mg/g) values for MO dye adsorption to that of various adsorbents

Adsorbents	q_{\max} (mg/g)	References
chitosan-glyoxal/TiO ₂	416.1	[82]
Chitosan/PVA/zeolite nanofiber	153	[43]
Chitosan-Montmorillonite	64.9	[49]
ZnO/chitosan coating layer	42.8	[49]
Chitosan Biomass	29	[47]
Maghemite/chitosan films	33	[42]
Kaol/Cel-25	113.64	This study

III.7. Thermodynamic Functions Results of adsorption experiments with Kaol/Cel Composite after CV and MO adsorption

Various adsorption thermodynamic characteristics were obtained in order to evaluate the viability and spontaneity of the MO and CV dye adsorption phenomenon onto the Kaol/Cel-25 surface and calculate the degree of unpredictability at the dye/surface interface. They are the entropy change (ΔS°) (kJ/mol. K), the enthalpy change (ΔH°) (kJ/mol), and the Gibbs free energy change (ΔG°) (kJ/mol). Equations (III.8) – (III.11) [171] were used to calculate these thermodynamic parameters:

$$\Delta G = -RT \ln K_d \quad \text{(III.8)}$$

$$K_d = \frac{q_e}{C_e} \quad \text{(III.9)}$$

$$\ln K_d = \frac{\Delta S^\circ}{R} - \frac{\Delta H^\circ}{RT^\circ} \quad \text{(III.10)}$$

The plot of $\ln K_d$ against $1/T$ is shown in Figures (III.17, III.18), from which the thermodynamic parameters (ΔH° and ΔS°) were derived. This plot's intercept is ΔS° , and its slope is ΔH° .

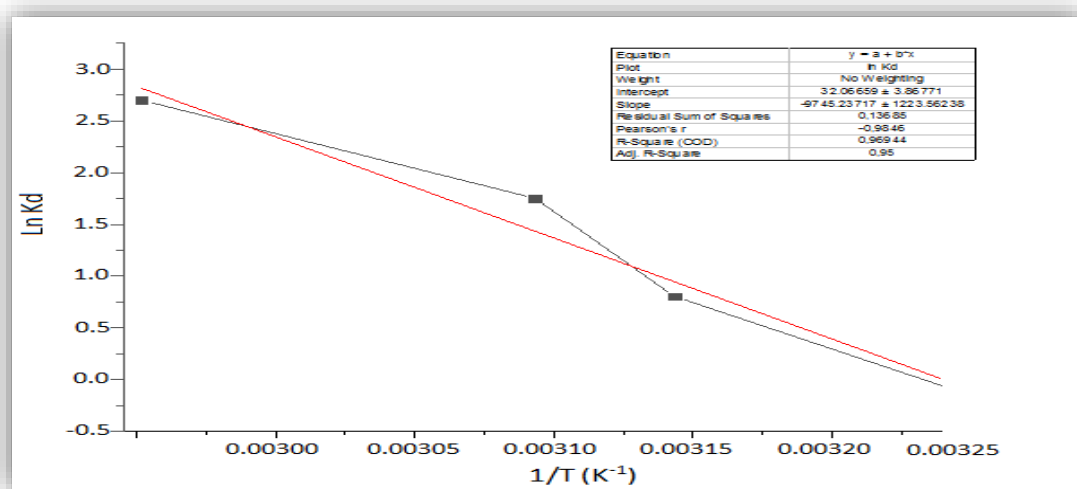


Figure III.17. Plot of Van't Hoff equation for CV adsorption onto Kaol/Cel-25.

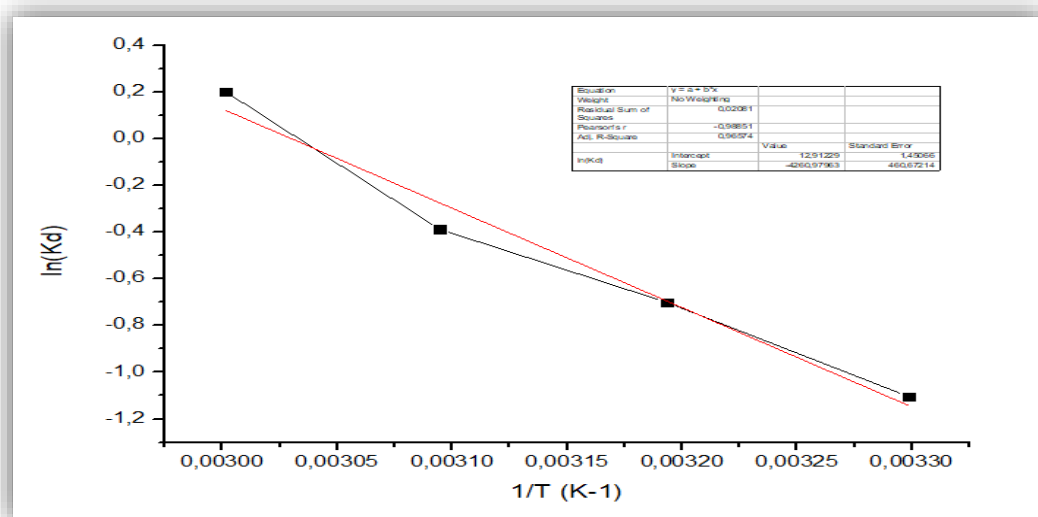


Figure III.18. Plot of Van't Hoff equation for MO adsorption onto Kaol/Cel-25.

The results presented in Tables (III.11) indicate that the Gibbs free energy shift (ΔG°) for the adsorption of CV dye on the Kaol/Cel-25 surface is negative, suggesting that the process is spontaneous and beneficial [172]. Moreover, the negative enthalpy values obtained for the adsorption process of CV by Kaol/Cel-25 indicate that the process is exothermic, aligning with the findings from the BBD parametric optimization shown in Figure 9. Moreover, the adsorption of CV on Kaol/Cel-25 results in increased disorder at the solid-solution interface, as seen by the negative entropy values [173].

Table III.12. Parameters thermodynamic of crystal violet dye adsorption onto Kaol/Cel-25

T (K)	Ln k_d	ΔG° (kJ/mol)	ΔH° (kJ/mol)	ΔS° (kJ/mol K)
303.15	0.0867	-0.22		
313.15	0.5931	-1.54		

323.15	1.5411	-4.07	- 78.65	0.108
333.15	2 .9099	-8.06		

The results presented in Table (III.12) show that the Gibbs free energy change (ΔG°) for the adsorption of MO dye onto the surface of Kaol/Cel-25 is negative, indicating that the process is spontaneous and favorable [174]. Furthermore, the negative enthalpy values obtained for the adsorption process of CV by Kaol/Cel-25 suggest that the process is exo-thermic, which is consistent with the results obtained from the BBD parametric optimization. Furthermore, the adsorption of CV onto Kaol/Cel-25 appears to cause a greater level of disorder at the interface between the solid and solution, as indicated by the negative entropy values [175].

Table III.13. Parameters thermodynamic of methyl orange dye adsorption onto Kaol/Cel-25.

T (K)	Ln k_a	ΔG° (kJ/mol)	ΔH° (kJ/mol)	ΔS° (Kj/mol K)
303,15	-1.104	- 2.78	35.43	0.108
313,15	-0.700	-1.82		
323,15	-0.387	-1.04		
333,15	0.202	-0.56		

III.8. Mechanisms of adsorption

Surface-active functional groups and the pH of the surrounding medium are critical variables that additionally regulate the adsorption process. Schematic representation of the dyes (cationic: CV; anionic: MO) elimination mechanisms by Kal/Cel-25 is

shown in Figure III. 10. The value of the pH_{pzc} for the Kal/Cel-25 is 8.71, as illustrated the results suggest that the Kal/Cel-25 surface has the potential to acquire a positive charge at $pH < pH_{pzc}$ and a negative charge at $pH > pH_{pzc}$. As a result, the surface of Kal/Cel-25 may transition from being positively charged at pH 4 to negatively charged at pH 10, indicating its ability to adsorb organic dyes containing cationic or anionic groups, such as CV and MO. As a result, there may be substantial electrostatic interactions between the cation/anion group of the CV and MO and the surface functional groups of the positively/negatively charged Kal/Cel-25. Notably, the most impactful interaction is an electrostatic attraction between the dyes molecules and the surface of the Kaol/Cel-25 adsorbents. Such an adsorption pathway encompasses the electrostatic interaction between CV dye cations and the negatively charged sites on the surface of Kaol/Cel-25. Additionally, there is the possibility of $n-\pi$ interaction, which typically occurs when the lone pair electrons on an O are spread out into the orbital of an aromatic ring of dye[176]. Two kinds of hydrogen bonding take place between the Kaol/Cel-25 and the molecular structure of CV. The first and more frequent kind is dipole-dipole hydrogen bonding interaction between present O on the surface of Kaol/Cel-25 with the O and N atoms existing in the CV molecular structure. This interaction is illustrated in Figure 11. The last kind is Yoshida H-bonding, which takes place between -OH groups on the surface of Kaol/Cel-25 and the CV aromatic ring [177]. This thereby leads to the conclusion that all these interactions empowered the Kaol/ Cel-25 to perform poly- tasks of CV and MO adsorption.

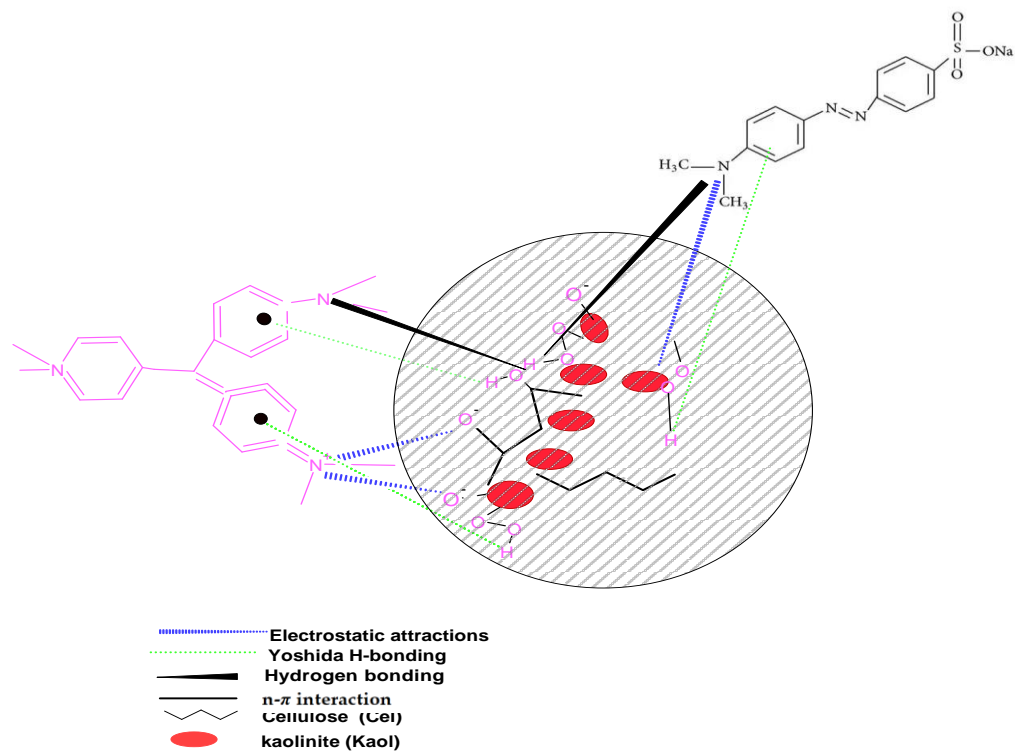


Figure III.19. Possible mechanism between Kaol/Cel-25 surface and dyes (Crystal Violet and Methyl Orange).

GENERAL CONCLUSION

GENERAL CONCLUSION

This research aimed to expand an environmentally friendly composite cloth known as kaolinite-cellulose (Kaol/Cel) to the usage of waste red bean peels (RBPs) as a cellulose source. First, we used eight Different dyes cationic and anionic (Basic Red 18, Safranin O, Rhodamine B, Reactive Orange 16, Reactive Red 180, Acid Red18, Crystal Violet, Methyl Orange) to choose high-overall performance dyes to hold with them for the rest of the study. Higher removal efficiency was obtained for kaolinite Crystal Violet and Methyl Orange dyes compared to the other dyes used in our study. In the have a look at we centered on crystal violet (CV) due to the fact it is miles extra poisonous to people and different dwelling organisms. A Box–Behnken design became employed to carry out the parametric optimization of the synthesis situations and adoptive overall performance of the Kaol/Cel composite to get rid of crystal violet (CV) and methyl orange (MO) dye.

- ✓ The composite polymeric matrix with uniform Cel distribution became determined to contribute to its increased absorptive conduct in the direction of CV. The fine parameters for CV elimination (99.58%) have been diagnosed as 25% cell loading, 0,035 g adsorbent dosage, pH 10, 45 °C temperature, and 5 min contact time.
- ✓ The best conditions for removing MO dye were found by maximizing the percentage of MO dye removed (84,55%), which was observed at 30 °C, pH 7, and a constant injection of 0.05 g of adsorbent and 17.5 min contact time.
- ✓ Furthermore, we discovered that the q_{\max} (CV) and q_{\max} (MO) for Kaol/Cel–25 is 294.12 mg/g and 113.64 mg/g, respectively, the use of the Langmuir model.
- ✓ The proposed adsorption mechanism proved highly plausible, considering various factors, with the nature of the medium being a crucial determinant.

The significant outcome of this study is the potential of Kaol/Cel–25 as a promising

GENERAL CONCLUSION

Future Recommendations

Based at the results from this observe the subsequent suggestions be done for any destiny work as continuation:

- ✓ Response surface methodology is taken into consideration very crucial to optimize adsorption procedure factors.
- ✓ Clays and their composites have lately emerged as powerful adsorbents for dye-containing water.
- ✓ Kaol/Cel nanocomposites are effective for disposing of organic pollution from wastewater and can be used for mineral contaminants.

BIBLIOGRAPHY

- [1] E. Rápó and S. Tonk, "Factors affecting synthetic dye adsorption; desorption studies: a review of results from the last five years (2017–2021)," *Molecules*, vol. 26, p. 5419, 2021.
- [2] E.-K. Hachem, M. Belghazdis, and A. Bendouch, "Adsorption of the Polymer on a Clay Matrix: Theoretical Study," *International Journal of Integrated Engineering*, vol. 14, pp. 21-32, 2022.
- [3] S. Benkhaya, S. M'rabet, and A. El Harfi, "A review on classifications, recent synthesis and applications of textile dyes," *Inorganic Chemistry Communications*, vol. 115, p. 107891, 2020.
- [4] R. J. Chudgar, "Azo dyes," *Kirk-Othmer Encyclopedia of Chemical Technology*, 2000.
- [5] A. Gürses, M. Açıkyıldız, K. Güneş, and M. S. Gürses, *Dyes and pigments*: Springer, 2016.
- [6] Y. Zhang, "Reduction of the water footprint in the textile dyeing process," *Universitat Politècnica de Catalunya*, 2022.
- [7] S. C. Druding, *Dye History from 2600 BC to the 20th Century*: Susan C. Druding, 1982.
- [8] P. Gregory, "Important chemical chromophores of dye classes," ed: Wiley-VCH: Federal Republic of Germany, 2003, pp. 35-39.
- [9] M. Elkady, A. M. Ibrahim, and M. Abd El-Latif, "Assessment of the adsorption kinetics, equilibrium and thermodynamic for the potential removal of reactive red dye using eggshell biocomposite beads," *Desalination*, vol. 278, pp. 412-423, 2011.
- [10] E. Forgacs, T. Cserhádi, and G. Oros, "Removal of synthetic dyes from wastewaters: a review," *Environment international*, vol. 30, pp. 953-971, 2004.
- [11] D. Bhardwaj and N. Bharadvaja, "Phycoremediation of effluents containing dyes and its prospects for value-added products: A review of opportunities," *Journal of Water Process Engineering*, vol. 41, p. 102080, 2021.
- [12] A. Gürses, M. Açıkyıldız, K. Güneş, M. S. Gürses, A. Gürses, M. Açıkyıldız, *et al.*, "Classification of dye and pigments," *Dyes and pigments*, pp. 31-45, 2016.
- [13] M. T. Yagub, T. K. Sen, S. Afroze, and H. M. Ang, "Dye and its removal from aqueous solution by adsorption: a review," *Advances in colloid and interface science*, vol. 209, pp. 172-184, 2014.
- [14] L. Tang, J. Yu, Y. Pang, G. Zeng, Y. Deng, J. Wang, *et al.*, "Sustainable efficient adsorbent: alkali-acid modified magnetic biochar derived from sewage sludge for aqueous organic contaminant removal," *Chemical Engineering Journal*, vol. 336, pp. 160-169, 2018.
- [15] A. Zobeidi and A. A. Bebba, "Seasonal variations of physical, chemical parameters in a wastewater treatment plant by aerated lagoons at Southern-East of Algeria," *Research Journal of Pharmaceutical, Biological and Chemical Sciences*, vol. 6, pp. 1097-1102, 2015.
- [16] M. Rafatullah, O. Sulaiman, R. Hashim, and A. Ahmad, "Adsorption of methylene blue on low-cost adsorbents: a review," *Journal of hazardous materials*, vol. 177, pp. 70-80, 2010.

- [17] M. A. M. Salleh, D. K. Mahmoud, W. A. W. A. Karim, and A. Idris, "Cationic and anionic dye adsorption by agricultural solid wastes: a comprehensive review," *Desalination*, vol. 280, pp. 1-13, 2011.
- [18] X. S. Wang, Y. Zhou, Y. Jiang, and C. Sun, "The removal of basic dyes from aqueous solutions using agricultural by-products," *Journal of Hazardous Materials*, vol. 157, pp. 374-385, 2008.
- [19] R. Penthal, M. Han, R. Manivannan, and Y.-A. Son, "Synthesis and spectral properties of novel cationic fazo dyes and calix [4] arene macromolecule: Application studies towards the cationic dyeing and dye effluent water purification technology," *Journal of Molecular Structure*, vol. 1286, p. 135645, 2023.
- [20] T. J. O'Brien, S. Ceryak, and S. R. Patierno, "Complexities of chromium carcinogenesis: role of cellular response, repair and recovery mechanisms," *Mutation Research/Fundamental and Molecular Mechanisms of Mutagenesis*, vol. 533, pp. 3-36, 2003.
- [21] C. R. Holkar, A. J. Jadhav, D. V. Pinjari, N. M. Mahamuni, and A. B. Pandit, "A critical review on textile wastewater treatments: possible approaches," *Journal of environmental management*, vol. 182, pp. 351-366, 2016.
- [22] M. Gallo, L. Ferrara, A. Calogero, D. Montesano, and D. Naviglio, "Relationships between food and diseases: What to know to ensure food safety," *Food Research International*, vol. 137, p. 109414, 2020.
- [23] C. O'Neill, A. Lopez, S. Esteves, F. Hawkes, D. Hawkes, and S. Wilcox, "Azo-dye degradation in an anaerobic-aerobic treatment system operating on simulated textile effluent," *Applied microbiology and biotechnology*, vol. 53, pp. 249-254, 2000.
- [24] R. R. Karri, G. Ravindran, and M. H. Dehghani, "Wastewater—sources, toxicity, and their consequences to human health," in *Soft computing techniques in solid waste and wastewater management*, ed: Elsevier, 2021, pp. 3-33.
- [25] O. Pourret, J.-C. Bollinger, A. Hursthouse, and E. D. van Hullebusch, "Sorption vs adsorption: The words they are a-changin', not the phenomena," *Science of the Total Environment*, vol. 838, p. 156545, 2022.
- [26] R. Kecili and C. M. Hussain, "Mechanism of adsorption on nanomaterials," in *Nanomaterials in chromatography*, ed: Elsevier, 2018, pp. 89-115.
- [27] S. Brunauer, P. H. Emmett, and E. Teller, "Adsorption of gases in multimolecular layers," *Journal of the American chemical society*, vol. 60, pp. 309-319, 1938.
- [28] D. M. Ruthven, *Principles of adsorption and adsorption processes*: John Wiley & Sons, 1984.
- [29] R. D. Noble and P. A. Terry, *Principles of chemical separations with environmental applications*: Cambridge University Press, 2004.

- [30] J. Serafin and B. Dziejarski, "Application of isotherms models and error functions in activated carbon CO₂ sorption processes," *Microporous and Mesoporous Materials*, vol. 354, p. 112513, 2023.
- [31] R. Bardestani, G. S. Patience, and S. Kaliaguine, "Experimental methods in chemical engineering: specific surface area and pore size distribution measurements—BET, BJH, and DFT," *The Canadian Journal of Chemical Engineering*, vol. 97, pp. 2781-2791, 2019.
- [32] M. Thommes, K. Kaneko, A. V. Neimark, J. P. Olivier, F. Rodriguez-Reinoso, J. Rouquerol, *et al.*, "Physisorption of gases, with special reference to the evaluation of surface area and pore size distribution (IUPAC Technical Report)," *Pure and applied chemistry*, vol. 87, pp. 1051-1069, 2015.
- [33] T. K. Sen, "Adsorptive Removal of Dye (Methylene Blue) Organic Pollutant from Water by Pine Tree Leaf Biomass Adsorbent," *Processes*, vol. 11, p. 1877, 2023.
- [34] C. D. Díaz-Marín, L. Zhang, Z. Lu, M. Alshrah, J. C. Grossman, and E. N. Wang, "Kinetics of sorption in hygroscopic hydrogels," *Nano Letters*, vol. 22, pp. 1100-1107, 2022.
- [35] R.-L. Tseng, H. N. Tran, and R.-S. Juang, "Revisiting temperature effect on the kinetics of liquid-phase adsorption by the Elovich equation: A simple tool for checking data reliability," *Journal of the Taiwan Institute of Chemical Engineers*, vol. 136, p. 104403, 2022.
- [36] H. R. Mahmoud, S. M. Ibrahim, and S. A. El-Molla, "Textile dye removal from aqueous solutions using cheap MgO nanomaterials: adsorption kinetics, isotherm studies and thermodynamics," *Advanced Powder Technology*, vol. 27, pp. 223-231, 2016.
- [37] I. A. Shabtai, L. M. Lynch, and Y. G. Mishael, "Designing clay-polymer nanocomposite sorbents for water treatment: A review and meta-analysis of the past decade," *Water Research*, vol. 188, p. 116571, 2021.
- [38] F. Bergaya and G. Lagaly, *Handbook of clay science*: Newnes, 2013.
- [39] P. B. Arab, T. P. Araújo, and O. J. Pejon, "Identification of clay minerals in mixtures subjected to differential thermal and thermogravimetry analyses and methylene blue adsorption tests," *Applied Clay Science*, vol. 114, pp. 133-140, 2015.
- [40] O. Gencil, E. Erdugmus, M. Sutcu, and O. H. Oren, "Effects of concrete waste on characteristics of structural fired clay bricks," *Construction and Building Materials*, vol. 255, p. 119362, 2020.
- [41] S. Guggenheim and R. Martin, "Definition of clay and clay mineral: joint report of the AIPEA nomenclature and CMS nomenclature committees," *Clays and clay minerals*, vol. 43, pp. 255-256, 1995.
- [42] R. Mackenzie, "De natura lutorum," *Clays and Clay Minerals*, vol. 11, pp. 11-28, 1962.
- [43] E.-K. Hachem, M. Belghazdis, and A. Bendouch, "Adsorption of the Polymer on a Clay Matrix: Theoretical Study," *International Journal of Integrated Engineering*, vol. 14, pp. 21-32, 2022.

- [44] M. Belghazdis and E.-K. Hachem, "Clay and clay minerals: a detailed review," *International Journal of Recent Technology and Applied Science (IJORTAS)*, vol. 4, pp. 54-75, 2022.
- [45] K. Jlassi, I. Krupa, and M. M. Chehimi, "Overview: clay preparation, properties, modification," *Clay-polymer nanocomposites*, pp. 1-28, 2017.
- [46] J. Madejová, "FTIR techniques in clay mineral studies," *Vibrational spectroscopy*, vol. 31, pp. 1-10, 2003.
- [47] M. Gautier, "Interactions entre argile ammoniée et molécules organiques dans le contexte du stockage des déchets. Cas de molécules à courtes chaînes," Université d'Orléans, 2008.
- [48] M. S. Alam, G. Sofi, and M. A. Ali, "Review of Therapeutic Clays Used in Reference to Unani System of Medicine," *J Young Pharm*, vol. 15, pp. 212-223, 2023.
- [49] G. Jozefaciuk and G. Bowanko, "Effect of acid and alkali treatments on surface areas and adsorption energies of selected minerals," *Clays and Clay minerals*, vol. 50, pp. 771-783, 2002.
- [50] A. Steudel, L. Batenburg, H. Fischer, P. Weidler, and K. Emmerich, "Alteration of swelling clay minerals by acid activation," *Applied Clay Science*, vol. 44, pp. 105-115, 2009.
- [51] R. Juang, F. Wu, and R. Tseng, "The ability of activated clay for the adsorption of dyes from aqueous solutions," *Environmental Technology*, vol. 18, pp. 525-531, 1997.
- [52] S. Barakan and V. Aghazadeh, "The advantages of clay mineral modification methods for enhancing adsorption efficiency in wastewater treatment: a review," *Environmental Science and Pollution Research*, vol. 28, pp. 2572-2599, 2021.
- [53] A. Gil, L. M. Gandia, and M. A. Vicente, "Recent advances in the synthesis and catalytic applications of pillared clays," *Catalysis Reviews*, vol. 42, pp. 145-212, 2000.
- [54] T. Mishra, "Transition metal oxide-pillared clay catalyst: synthesis to application," *Pillared Clays and Related Catalysts*, pp. 99-128, 2010.
- [55] Y. Dong, P. Zhang, and H. Lin, "A Review of Modified Clay Minerals for Thallium Absorption from Aqueous Environment: Preparation, Application, and Mechanism," *Water, Air, & Soil Pollution*, vol. 233, p. 532, 2022.
- [56] D. Karamanis and P. Assimakopoulos, "Efficiency of aluminum-pillared montmorillonite on the removal of cesium and copper from aqueous solutions," *Water Research*, vol. 41, pp. 1897-1906, 2007.
- [57] E. Ruiz-Hitzky and A. Van Meerbeek, "Clay mineral–and organoclay–polymer nanocomposite," *Developments in Clay Science*, vol. 1, pp. 583-621, 2006.
- [58] R. S. Sinha, *Clay-containing polymer nanocomposites: from fundamentals to real applications*: Newnes, 2013.
- [59] X. Yue and Y. Queneau, "5-Hydroxymethylfurfural and Furfural Chemistry Toward Biobased Surfactants," *ChemSusChem*, vol. 15, p. e202102660, 2022.

- [60] Z. Navratilova, P. Wojtowicz, L. Vaculikova, and V. Sugarkova, "Sorption of alkylammonium cations on montmorillonite," *Acta Geodynamica et Geomaterialia*, vol. 4, p. 59, 2007.
- [61] Y. Akbulut and C. S. Cardak, "Adaptive educational hypermedia accommodating learning styles: A content analysis of publications from 2000 to 2011," *Computers & Education*, vol. 58, pp. 835-842, 2012.
- [62] H. Noyan, M. Önal, and Y. Sarikaya, "The effect of heating on the surface area, porosity and surface acidity of a bentonite," *Clays and Clay Minerals*, vol. 54, pp. 375-381, 2006.
- [63] S. Al-Asheh, F. Banat, and L. Abu-Aitah, "Adsorption of phenol using different types of activated bentonites," *Separation and purification technology*, vol. 33, pp. 1-10, 2003.
- [64] F. Bergaya and G. Lagaly, "General introduction: clays, clay minerals, and clay science," *Developments in clay science*, vol. 1, pp. 1-18, 2006.
- [65] V. Vimonses, S. Lei, B. Jin, C. W. Chow, and C. Saint, "Kinetic study and equilibrium isotherm analysis of Congo Red adsorption by clay materials," *Chemical engineering journal*, vol. 148, pp. 354-364, 2009.
- [66] P. M. Patil, R. R. Ingavale, A. R. Matkar, R. Gurav, and M. J. Dhanavade, "An Innovative and Effective Industrial Wastewater Treatments to Reduce Water Pollution: A Brief History and Present Scenario," in *Advanced and Innovative Approaches of Environmental Biotechnology in Industrial Wastewater Treatment*, ed: Springer, 2023, pp. 191-220.
- [67] R. Lamar, "Bentonite activation," *California Journal of Mines*, vol. 49, pp. 297-302, 1951.
- [68] A. Riddiford, J. Danielli, and K. Pankhurst, *Surface Phenomena in Chemistry and Biology*: Pergamon Press, 1958.
- [69] H. Koyuncu, "Adsorption kinetics of 3-hydroxybenzaldehyde on native and activated bentonite," *Applied Clay Science*, vol. 38, pp. 279-287, 2008.
- [70] J. M. Yassin, Y. Shiferaw, and A. Tedla, "Application of acid activated natural clays for improving quality of Niger (*Guizotia abyssinica* Cass) oil," *Heliyon*, vol. 8, 2022.
- [71] B. Sajjadi, W.-Y. Chen, and N. O. Egiebor, "A comprehensive review on physical activation of biochar for energy and environmental applications," *Reviews in Chemical Engineering*, vol. 35, pp. 735-776, 2019.
- [72] P. Liu, "Polymer modified clay minerals: A review," *Applied Clay Science*, vol. 38, pp. 64-76, 2007.
- [73] Q. Cui and B. Chen, "Review of polymer-amended bentonite: Categories, mechanism, modification processes and application in barriers for isolating contaminants," *Applied Clay Science*, vol. 235, p. 106869, 2023.
- [74] M. Hnamte and A. K. Pulikkal, "Clay-polymer nanocomposites for water and wastewater treatment: A comprehensive," *Chemosphere*, p. 135869, 2022.

- [75] B. Bikbov, C. A. Purcell, A. S. Levey, M. Smith, A. Abdoli, M. Abebe, *et al.*, "Global, regional, and national burden of chronic kidney disease, 1990–2017: a systematic analysis for the Global Burden of Disease Study 2017," *The lancet*, vol. 395, pp. 709-733, 2020.
- [76] S. N. Monteiro, F. P. D. Lopes, A. P. Barbosa, A. B. Bevitori, I. L. A. D. Silva, and L. L. D. Costa, "Natural lignocellulosic fibers as engineering materials—An overview," *Metallurgical and Materials Transactions A*, vol. 42, pp. 2963-2974, 2011.
- [77] V. K. Thakur and M. K. Thakur, "Recent advances in green hydrogels from lignin: a review," *International journal of biological macromolecules*, vol. 72, pp. 834-847, 2015.
- [78] K. Shaker and Y. Nawab, "Lignocellulosic Fiber Structure," in *Lignocellulosic Fibers: Sustainable Biomaterials for Green Composites*, ed: Springer, 2022, pp. 11-19.
- [79] P. R. Lennartsson, C. Niklasson, and M. J. Taherzadeh, "A pilot study on lignocelluloses to ethanol and fish feed using NMMO pretreatment and cultivation with zygomycetes in an air-lift reactor," *Bioresource technology*, vol. 102, pp. 4425-4432, 2011.
- [80] S. Tadepalli, J. M. Slocik, M. K. Gupta, R. R. Naik, and S. Singamaneni, "Bio-optics and bio-inspired optical materials," *Chemical reviews*, vol. 117, pp. 12705-12763, 2017.
- [81] U. T. M. Sampath, Y. C. Ching, C. H. Chuah, R. Singh, and P.-C. Lin, "Preparation and characterization of nanocellulose reinforced semi-interpenetrating polymer network of chitosan hydrogel," *Cellulose*, vol. 24, pp. 2215-2228, 2017.
- [82] V. Rubenthaler, T. A. Ward, C. Y. Chee, P. Nair, E. Salami, and C. Fearday, "Effects of heat treatment on chitosan nanocomposite film reinforced with nanocrystalline cellulose and tannic acid," *Carbohydrate polymers*, vol. 140, pp. 202-208, 2016.
- [83] J. Pérez, J. Muñoz-Dorado, T. De la Rubia, and J. Martínez, "Biodegradation and biological treatments of cellulose, hemicellulose and lignin: an overview," *International microbiology*, vol. 5, pp. 53-63, 2002.
- [84] A. Duval, S. Molina-Boisseau, and C. Chirat, "Comparison of Kraft lignin and lignosulfonates addition to wheat gluten-based materials: Mechanical and thermal properties," *Industrial crops and products*, vol. 49, pp. 66-74, 2013.
- [85] J. Ralph, C. Lapierre, and W. Boerjan, "Lignin structure and its engineering," *Current opinion in biotechnology*, vol. 56, pp. 240-249, 2019.
- [86] W. Yang, E. Fortunati, F. Dominici, G. Giovanale, A. Mazzaglia, G. M. Balestra, *et al.*, "Effect of cellulose and lignin on disintegration, antimicrobial and antioxidant properties of PLA active films," *International Journal of Biological Macromolecules*, vol. 89, pp. 360-368, 2016.
- [87] R. L. Rardin and R. Uzsoy, "Experimental evaluation of heuristic optimization algorithms: A tutorial," *Journal of Heuristics*, vol. 7, pp. 261-304, 2001.

- [88] A. Simonofski, P. Handekyn, C. Vandennieuwenborg, Y. Wautelet, and M. Snoeck, "Smart mobility projects: Towards the formalization of a policy-making lifecycle," *Land Use Policy*, vol. 125, p. 106474, 2023.
- [89] A. P. Rovai, J. D. Baker, and M. K. Ponton, *Social science research design and statistics: A practitioner's guide to research methods and IBM SPSS*: Watertree Press LLC, 2013.
- [90] S. A. Siddiqui, O. Zannou, I. Karim, Kasmia, N. M. Awad, J. Gołaszewski, *et al.*, "Avoiding food neophobia and increasing consumer acceptance of new food trends—A decade of research," *Sustainability*, vol. 14, p. 10391, 2022.
- [91] B. M. Asenahabi, "Basics of research design: A guide to selecting appropriate research design," *International Journal of Contemporary Applied Researches*, vol. 6, pp. 76-89, 2019.
- [92] R. H. Myers, A. I. Khuri, and W. H. Carter, "Response surface methodology: 1966–1988," *Technometrics*, vol. 31, pp. 137-157, 1989.
- [93] Z. A. Sandhu, M. A. Raza, U. Farwa, S. Nasr, I. S. Yahia, S. Fatima, *et al.*, "Response Surface Methodology: A Powerful Tool for Optimizing the Synthesis of Metal Sulfide Nanoparticles for Dye Degradation," *Materials Advances*, 2023.
- [94] J. González-Reséndiz, K. C. Arredondo-Soto, A. Realyvásquez-Vargas, H. Híjar-Rivera, and T. Carrillo-Gutiérrez, "Integrating simulation-based optimization for lean logistics: a case study," *Applied sciences*, vol. 8, p. 2448, 2018.
- [95] A. I. Khuri and S. Mukhopadhyay, "Response surface methodology," *Wiley Interdisciplinary Reviews: Computational Statistics*, vol. 2, pp. 128-149, 2010.
- [96] S. Lamidi, N. Olaleye, Y. Bankole, A. Obalola, E. Aribike, and I. Adigun, "Applications of response surface methodology (RSM) in product design, development, and process optimization," *Response Surface Methodology-Research Advances and Applications*, 2022.
- [97] M. Kazemian, S. Gandjalikhan Nassab, and E. Jahanshahi Javaran, "Comparative study of Box–Behnken and central composite designs to investigate the effective parameters of ammonia–water absorption refrigerant system," *Proceedings of the Institution of Mechanical Engineers, Part C: Journal of Mechanical Engineering Science*, vol. 235, pp. 3095-3108, 2021.
- [98] R. Jeyapaul, P. Shahabudeen, and K. Krishnaiah, "Quality management research by considering multi-response problems in the Taguchi method—a review," *The International Journal of Advanced Manufacturing Technology*, vol. 26, pp. 1331-1337, 2005.
- [99] M. Kousha, E. Daneshvar, H. Dopeikar, D. Taghavi, and A. Bhatnagar, "Box–Behnken design optimization of Acid Black 1 dye biosorption by different brown macroalgae," *Chemical Engineering Journal*, vol. 179, pp. 158-168, 2012.
- [100] R. G. Shaw and T. Mitchell-Olds, "ANOVA for unbalanced data: an overview," *Ecology*, vol. 74, pp. 1638-1645, 1993.

- [101] R. Day and G. Quinn, "Comparisons of treatments after an analysis of variance in ecology," *Ecological monographs*, vol. 59, pp. 433-463, 1989.
- [102] C. N. Njoku and S. K. Otisi, "Application of Central Composite Design with Design Expert v13 in Process Optimization," 2023.
- [103] C. Manterola, M. Vial, V. Pineda, and A. Sanhueza, "Systematic Review of Literature with Different Types of Designs," *International Journal of Morphology*, vol. 27, 2009.
- [104] R. Ghelich, M. R. Jahannama, H. Abdizadeh, F. S. Torknik, and M. R. Vaezi, "Central composite design (CCD)-Response surface methodology (RSM) of effective electrospinning parameters on PVP-B-Hf hybrid nanofibrous composites for synthesis of HfB₂-based composite nanofibers," *Composites Part B: Engineering*, vol. 166, pp. 527-541, 2019.
- [105] N. R. Draper, "Introduction to Box and Wilson (1951) on the experimental attainment of optimum conditions," *Breakthroughs in Statistics: Methodology and Distribution*, pp. 267-269, 1992.
- [106] Shalabh, C. Heumann, S. H. Park, H. J. Kim, and J.-I. Cho, "Optimal central composite designs for fitting second order response surface linear regression models," *Recent Advances in Linear Models and Related Areas: Essays in Honour of Helge Toutenburg*, pp. 323-339, 2008.
- [107] M. Ozonoh, B. Oboirien, and M. Daramola, "Optimization of process variables during torrefaction of coal/biomass/waste tyre blends: Application of artificial neural network & response surface methodology," *Biomass and Bioenergy*, vol. 143, p. 105808, 2020.
- [108] S. Beg, S. Swain, M. Rahman, M. S. Hasnain, and S. S. Imam, "Application of design of experiments (DoE) in pharmaceutical product and process optimization," in *Pharmaceutical quality by design*, ed: Elsevier, 2019, pp. 43-64.
- [109] S. C. Ferreira, R. Bruns, H. S. Ferreira, G. D. Matos, J. David, G. Brandão, *et al.*, "Box-Behnken design: An alternative for the optimization of analytical methods," *Analytica chimica acta*, vol. 597, pp. 179-186, 2007.
- [110] K. Mathivanan, D. Thirumalaikumarasamy, M. Ashokkumar, S. Deepak, and M. Mathanbabu, "Optimization and prediction of AZ91D stellite-6 coated magnesium alloy using Box Behnken design and hybrid deep belief network," *Journal of Materials Research and Technology*, vol. 15, pp. 2953-2969, 2021.
- [111] A. Reghioua, D. Atia, A. Hamidi, A. H. Jawad, A. S. Abdulhameed, and H. M. Mbuvi, "Production of eco-friendly adsorbent of kaolin clay and cellulose extracted from peanut shells for removal of methylene blue and congo red removal dyes," *International journal of biological macromolecules*, p. 130304, 2024.
- [112] B. Abbou, I. Lebkiri, H. Ouaddari, A. El Amri, F. E. Achibat, L. Kadiri, *et al.*, "Improved removal of methyl orange dye by adsorption using modified clay: combined experimental study using

- surface response methodology," *Inorganic Chemistry Communications*, vol. 155, p. 111127, 2023.
- [113] G. O. El-Sayed, "Removal of methylene blue and crystal violet from aqueous solutions by palm kernel fiber," *Desalination*, vol. 272, pp. 225-232, 2011.
- [114] S. Chakraborty, S. Chowdhury, and P. D. Saha, "Adsorption of crystal violet from aqueous solution onto NaOH-modified rice husk," *Carbohydrate Polymers*, vol. 86, pp. 1533-1541, 2011.
- [115] S. Çoruh, F. Geyikçi, and O. N. Ergun, "ATINER's Conference Paper Series ENV2012-0057."
- [116] G. A. El Naeem, A. Abd-Elhamid, O. O. Farahat, A. A. El-Bardan, H. M. Soliman, and A. Nayl, "Adsorption of crystal violet and methylene blue dyes using a cellulose-based adsorbent from sugarcane bagasse: Characterization, kinetic and isotherm studies," *Journal of Materials Research and Technology*, vol. 19, pp. 3241-3254, 2022.
- [117] S. A. Khan, T. U. Rehman, L. A. Shah, and M. Ullah, "Magnetite graphene oxide-doped superadsorbent hydrogel for efficient removal of crystal violet from wastewater," *Chemical Papers*, pp. 1-11, 2023.
- [118] M. K. Uddin, N. N. Abd Malek, A. H. Jawad, and S. Sabar, "Pyrolysis of rubber seed pericarp biomass treated with sulfuric acid for the adsorption of crystal violet and methylene green dyes: an optimized process," *International Journal of Phytoremediation*, pp. 1-10, 2022.
- [119] A. S. Abdulhameed, A. H. Jawad, E. Kashi, K. A. Radzun, Z. A. ALOthman, and L. D. Wilson, "Insight into adsorption mechanism, modeling, and desirability function of crystal violet and methylene blue dyes by microalgae: Box-Behnken design application," *Algal Research*, vol. 67, p. 102864, 2022.
- [120] N. A. M. Hanafi, A. S. Abdulhameed, A. H. Jawad, Z. A. ALOthman, T. A. Yousef, O. Al Duaij, *et al.*, "Optimized removal process and tailored adsorption mechanism of crystal violet and methylene blue dyes by activated carbon derived from mixed orange peel and watermelon rind using microwave-induced ZnCl₂ activation," *Biomass Conversion and Biorefinery*, pp. 1-13, 2022.
- [121] N. A. Jani, L. Haddad, A. S. Abdulhameed, A. H. Jawad, Z. A. ALOthman, and Z. M. Yaseen, "Modeling and optimization of the adsorptive removal of crystal violet dye by durian (*Durio zibethinus*) seeds powder: insight into kinetic, isotherm, thermodynamic, and adsorption mechanism," *Biomass Conversion and Biorefinery*, pp. 1-14, 2022.
- [122] S. K. Singh and A. Das, "The $n \rightarrow \pi^*$ interaction: a rapidly emerging non-covalent interaction," *Physical Chemistry Chemical Physics*, vol. 17, pp. 9596-9612, 2015.
- [123] H. L. Parker, A. J. Hunt, V. L. Budarin, P. S. Shuttleworth, K. L. Miller, and J. H. Clark, "The importance of being porous: polysaccharide-derived mesoporous materials for use in dye adsorption," *RSC advances*, vol. 2, pp. 8992-8997, 2012.

- [124]Kurath, Hans. Middle English Dictionary: F. 4. University of Michigan Press, 1954.
- [125]I. Mazharul, "Difference between Dyes and Pigments," ed.
- [126]S. Benkhaya, S. M'rabet, and A. El Harfi, "A review on classifications, recent synthesis and applications of textile dyes," *Inorganic Chemistry Communications*, vol. 115, p. 107891, 2020.
- [127]E. Rápó and S. Tonk, "Factors affecting synthetic dye adsorption; desorption studies: a review of results from the last five years (2017–2021)," *Molecules*, vol. 26, p. 5419, 2021.
- [128]R. J. Chudgar, "Azo dyes," *Kirk-Othmer Encyclopedia of Chemical Technology*, 2000.
- [129]A. Gürses, M. Açıkyıldız, K. Güneş, and M. S. Gürses, *Dyes and pigments*: Springer, 2016.
- [130]S. C. Druding, *Dye History from 2600 BC to the 20th Century*: Susan C. Druding, 1982.
- [131]Y. Zhang, "Reduction of the water footprint in the textile dyeing process," *Universitat Politècnica de Catalunya*, 2022.
- [132]P. Gregory, "Important chemical chromophores of dye classes," ed: Wiley-VCH: Federal Republic of Germany, 2003, pp. 35-39.
- [133]M. Elkady, A. M. Ibrahim, and M. Abd El-Latif, "Assessment of the adsorption kinetics, equilibrium and thermodynamic for the potential removal of reactive red dye using eggshell biocomposite beads," *Desalination*, vol. 278, pp. 412-423, 2011.
- [134]E. Forgacs, T. Cserhádi, and G. Oros, "Removal of synthetic dyes from wastewaters: a review," *Environment international*, vol. 30, pp. 953-971, 2004.
- [135]D. Bhardwaj and N. Bharadvaja, "Phycoremediation of effluents containing dyes and its prospects for value-added products: A review of opportunities," *Journal of Water Process Engineering*, vol. 41, p. 102080, 2021.
- [136]A. Gürses, M. Açıkyıldız, K. Güneş, M. S. Gürses, A. Gürses, M. Açıkyıldız, et al., "Classification of dye and pigments," *Dyes and pigments*, pp. 31-45, 2016.
- [137]M. T. Yagub, T. K. Sen, S. Afroze, and H. M. Ang, "Dye and its removal from aqueous solution by adsorption: a review," *Advances in colloid and interface science*, vol. 209, pp. 172-184, 2014.
- [138]L. Tang, J. Yu, Y. Pang, G. Zeng, Y. Deng, J. Wang, et al., "Sustainable efficient adsorbent: alkali-acid modified magnetic biochar derived from sewage sludge for aqueous organic contaminant removal," *Chemical Engineering Journal*, vol. 336, pp. 160-169, 2018.
- [139]A. Zobeidi and A. A. Bebbi, "Seasonal variations of physical, chemical parameters in a wastewater treatment plant by aerated lagoons at Southern-East of Algeria," *Research Journal of Pharmaceutical, Biological and Chemical Sciences*, vol. 6, pp. 1097-1102, 2015.
- [140]M. Rafatullah, O. Sulaiman, R. Hashim, and A. Ahmad, "Adsorption of methylene blue on low-cost adsorbents: a review," *Journal of hazardous materials*, vol. 177, pp. 70-80, 2010.

- [141]M. A. M. Salleh, D. K. Mahmoud, W. A. W. A. Karim, and A. Idris, "Cationic and anionic dye adsorption by agricultural solid wastes: a comprehensive review," *Desalination*, vol. 280, pp. 1-13, 2011.
- [142]X. S. Wang, Y. Zhou, Y. Jiang, and C. Sun, "The removal of basic dyes from aqueous solutions using agricultural by-products," *Journal of Hazardous Materials*, vol. 157, pp. 374-385, 2008.
- [143]R. Penthala, M. Han, R. Manivannan, and Y.-A. Son, "Synthesis and spectral properties of novel cationic fazo dyes and calix [4] arene macromolecule: Application studies towards the cationic dyeing and dye effluent water purification technology," *Journal of Molecular Structure*, vol. 1286, p. 135645, 2023.
- [144]T. J. O'Brien, S. Ceryak, and S. R. Patierno, "Complexities of chromium carcinogenesis: role of cellular response, repair and recovery mechanisms," *Mutation Research/Fundamental and Molecular Mechanisms of Mutagenesis*, vol. 533, pp. 3-36, 2003.
- [145]C. R. Holkar, A. J. Jadhav, D. V. Pinjari, N. M. Mahamuni, and A. B. Pandit, "A critical review on textile wastewater treatments: possible approaches," *Journal of environmental management*, vol. 182, pp. 351-366, 2016.
- [146]M. Gallo, L. Ferrara, A. Calogero, D. Montesano, and D. Naviglio, "Relationships between food and diseases: What to know to ensure food safety," *Food Research International*, vol. 137, p. 109414, 2020.
- [147]C. O'Neill, A. Lopez, S. Esteves, F. Hawkes, D. Hawkes, and S. Wilcox, "Azo-dye degradation in an anaerobic-aerobic treatment system operating on simulated textile effluent," *Applied microbiology and biotechnology*, vol. 53, pp. 249-254, 2000.
- [148]R. R. Karri, G. Ravindran, and M. H. Dehghani, "Wastewater—sources, toxicity, and their consequences to human health," in *Soft computing techniques in solid waste and wastewater management*, ed: Elsevier, 2021, pp. 3-33.
- [149]O. Pourret, J.-C. Bollinger, A. Hursthouse, and E. D. van Hullebusch, "Sorption vs adsorption: The words they are a-changin', not the phenomena," *Science of the Total Environment*, vol. 838, p. 156545, 2022.
- [150]R. Kecili and C. M. Hussain, "Mechanism of adsorption on nanomaterials," in *Nanomaterials in chromatography*, ed: Elsevier, 2018, pp. 89-115.
- [151]S. Brunauer, P. H. Emmett, and E. Teller, "Adsorption of gases in multimolecular layers," *Journal of the American chemical society*, vol. 60, pp. 309-319, 1938.
- [153]D. M. Ruthven, *Principles of adsorption and adsorption processes*: John Wiley & Sons, 1984.
- [154]R. D. Noble and P. A. Terry, *Principles of chemical separations with environmental applications*: Cambridge University Press, 2004.

- [155]J. Serafin and B. Dziejarski, "Application of isotherms models and error functions in activated carbon CO₂ sorption processes," *Microporous and Mesoporous Materials*, vol. 354, p. 112513, 2023.
- [156]R. Bardestani, G. S. Patience, and S. Kaliaguine, "Experimental methods in chemical engineering: specific surface area and pore size distribution measurements—BET, BJH, and DFT," *The Canadian Journal of Chemical Engineering*, vol. 97, pp. 2781-2791, 2019.
- [157]M. Thommes, K. Kaneko, A. V. Neimark, J. P. Olivier, F. Rodriguez-Reinoso, J. Rouquerol, et al., "Physisorption of gases, with special reference to the evaluation of surface area and pore size distribution (IUPAC Technical Report)," *Pure and applied chemistry*, vol. 87, pp. 1051-1069, 2015.
- [158]T. K. Sen, "Adsorptive Removal of Dye (Methylene Blue) Organic Pollutant from Water by Pine Tree Leaf Biomass Adsorbent," *Processes*, vol. 11, p. 1877, 2023.
- [159]C. D. Díaz-Marín, L. Zhang, Z. Lu, M. Alshrah, J. C. Grossman, and E. N. Wang, "Kinetics of sorption in hygroscopic hydrogels," *Nano Letters*, vol. 22, pp. 1100-1107, 2022.
- [160]R.-L. Tseng, H. N. Tran, and R.-S. Juang, "Revisiting temperature effect on the kinetics of liquid-phase adsorption by the Elovich equation: A simple tool for checking data reliability," *Journal of the Taiwan Institute of Chemical Engineers*, vol. 136, p. 104403, 2022.
- [161]H. R. Mahmoud, S. M. Ibrahim, and S. A. El-Molla, "Textile dye removal from aqueous solutions using cheap MgO nanomaterials: adsorption kinetics, isotherm studies and thermodynamics," *Advanced Powder Technology*, vol. 27, pp. 223-231, 2016.
- [162]I. Langmuir, "The adsorption of gases on plane surfaces of glass, mica and platinum," *Journal of the American Chemical society*, vol. 40, pp. 1361-1403, 1918.
- [163]H. Freundlich, "Ueber die adsorption in loesungen," *Z Phys Chem*, vol. 57, pp. 385-470, 1907.
- [164]M. Temkin and V. Pyzhev, "Recent modifications to Langmuir isotherms," 1940.
- [165]M. Temkin, "Kinetics of ammonia synthesis on promoted iron catalysts," *Acta physiochim. URSS*, vol. 12, pp. 327-356, 1940.
- [166]S. Lagergren, "Zur theorie der sogenannten adsorption geloster stoffe," *Kungliga svenska vetenskapsakademiens. Handlingar*, vol. 24, pp. 1-39, 1898.
- [167]Y.-S. Ho and G. McKay, "Pseudo-second order model for sorption processes," *Process biochemistry*, vol. 34, pp. 451-465, 1999.
- [168]W. J. Weber Jr and J. C. Morris, "Kinetics of adsorption on carbon from solution," *Journal of the sanitary engineering division*, vol. 89, pp. 31-59, 1963.
- [169]R. Mecheri, A. Zobeidi, S. Atia, S. Neghmouche Nacer, A. A. Salih, M. Benaissa, et al., "Modeling and Optimizing the Crystal Violet Dye Adsorption on Kaolinite Mixed with Cellulose Waste Red

- Bean Peels: Insights into the Kinetic, Isothermal, Thermodynamic, and Mechanistic Study," *Materials*, vol. 16, p. 4082, 2023.
- [170]N. N. Abd Malek, A. H. Jawad, K. Ismail, R. Razuan, and Z. A. ALothman, "Fly ash modified magnetic chitosan-polyvinyl alcohol blend for reactive orange 16 dye removal: Adsorption parametric optimization," *International journal of biological macromolecules*, vol. 189, pp. 464-476, 2021.
- [171]I. A. Shabtai, L. M. Lynch, and Y. G. Mishael, "Designing clay-polymer nanocomposite sorbents for water treatment: A review and meta-analysis of the past decade," *Water Research*, vol. 188, p. 116571, 2021.
- [172]F. Bergaya and G. Lagaly, *Handbook of clay science*: Newnes, 2013.
- [173]P. B. Arab, T. P. Araújo, and O. J. Pejon, "Identification of clay minerals in mixtures subjected to differential thermal and thermogravimetry analyses and methylene blue adsorption tests," *Applied Clay Science*, vol. 114, pp. 133-140, 2015.
- [174]O. Gencil, E. Erdugmus, M. Sutcu, and O. H. Oren, "Effects of concrete waste on characteristics of structural fired clay bricks," *Construction and Building Materials*, vol. 255, p. 119362, 2020.
- [175]S. Guggenheim and R. Martin, "Definition of clay and clay mineral: joint report of the AIPEA nomenclature and CMS nomenclature committees," *Clays and clay minerals*, vol. 43, pp. 255-256, 1995.
- [176]R. Mackenzie, "De natura lutorum," *Clays and Clay Minerals*, vol. 11, pp. 11-28, 1962.
- [177]R. N. Aka, D. Mohotti, A. Nasir, E. Agyekum-Oduro, and S. X. Wu, "Evaluating a Liquid-Phase Plasma Discharge Process for Ammonia Oxidation in Wastewater," in *2023 ASABE Annual International Meeting*, 2023, p. 1.